2008

Thermal analysis of aluminum and copper rotor self excited induction generators

Gaurav Nanda
University of Windsor

THERMAL ANALYSIS OF ALUMINUM AND COPPER ROTOR SELF EXCITED INDUCTION GENERATORS

By

GAURAV NANDA

A Thesis

Submitted to the Faculty of Graduate Studies

through the Department of Electrical and Computer Engineering

in Partial Fulfillment of the Requirements for the

Degree of Master of Applied Science at the

University of Windsor

Windsor, Ontario, Canada

2008

Your file Votre référence
ISBN: 978-0-494-57614-4
Our file Notre référence
ISBN: 978-0-494-57614-4

Author's Declaration of Originality

I hereby certify that I am the sole author of this thesis and that no part of this thesis has been published or submitted for publication.

I certify that, to the best of my knowledge, my thesis does not infringe upon anyone's copyright nor violate any proprietary rights and that any ideas, techniques, quotations, or any other material from the work of other people included in my thesis, published or otherwise, are fully acknowledged in accordance with the standard referencing practices. Furthermore, to the extent that I have included copyrighted material that surpasses the bounds of fair dealing within the meaning of the Canada Copyright Act, I certify that I have obtained a written permission from the copyright owner(s) to include such material(s) in my thesis and have included copies of such copyright clearances to my appendix.

I declare that this is a true copy of my thesis, including any final revisions, as approved by my thesis committee and the Graduate Studies office, and that this thesis has not been submitted for a higher degree to any other University or Institution.

ABSTRACT

Wind energy is the one of the most abundantly available forms of renewable energy, and has emerged as a viable alternative to conventional non-renewable energy sources. The wind electrical generation system is the most competitive of all the environmentally clean and safe renewable energy sources. Electricity derived from wind power provides an alternative to conventional generation that could be used to achieve substantial reductions in fossil fuel use and industrial effluents like carbon dioxide. Current utilization of renewable energy systems in the form of wind, small hydro and bio-gas has led to the massive use of grid-connected and self-excited induction generators (SEIG). Besides being commonly used as drives in the industry, three-phase induction machines have earned much attention as wind generators because of the qualities such as ruggedness, fault tolerance and constructional simplicity, and constitute the biggest sector in the present wind power industry. This thesis consists of theory and background of self-excited induction generators (SEIGs), their dynamic and mathematical modeling, development of a laboratory experimental set-up, development of a thermal model and computational and experimental results of thermal modeling and aluminum-rotor and copper-rotor SEIGs and comparative analysis between the two kinds of SEIGs.

DEDICATION

This thesis is dedicated to my mother, who has nurtured me to be the person I am today and has always given me her unconditional support, inspiration and encouragement to lead a better life.

ACKNOWLEDGEMENT

An acknowledgement is not only a ritual but also an expression of indebtedness to all those who have helped me in the completion of this research work. First and foremost my sincere gratitude to my advisor Dr. Narayan Kar, who not only provided me with direction and guidance throughout the course of this work, but also showed confidence in my ideas and abilities. This work would not have been possible without his unending support and encouragement. He has always made sure that i strive for the best and it has been an honour working with him. I am also thankful to my thesis committee members, Dr. Jonathan Wu and Dr. Sreekanta Das for their invaluable suggestions and comments which have significantly enhanced this work.

Thanks are also due to our departmental technologists, Mr. Don Tersigni and Mr. Frank Cicchello for providing all the equipment and constant help, without which the experimental set-up would not have been completed.

I am also thankful to all my past and present friends in Windsor and at the Electric Machines and Drives Research Lab at the University. All of you have made my stay a truly memorable one.

And last but not the least, a special word of thanks for Mr. Khurshid Hafiz. He has not only been just a colleague, but a mentor and most importantly a very dear friend. Without his constant guidance this work would not have been the same.

TABLE OF CONTENTS

LIST OF TABLES

LIST OF FIGURES

NOMENCLATURE

v_{ds}, v_{qs}	: d- and q- axis stator voltages
v_{dr}, v_{qr}	: d- and q- axis rotor voltages
i_{ds}, i_{qs}	: d- and q- axis stator currents
i_{dr}, i_{qr}	: d- and q- axis rotor currents
λ_{ds}, λ_{qs}	: d- and q- axis stator flux linkages
λ_{dr}, λ_{qr}	: d- and q- axis rotor flux linkages
R_s, R_r	: Stator and rotor resistances
L_{ls}, L_{lr}	: Stator and rotor leakage inductances
L_m, i_m	: Magnetization inductance and current
R_l, L_l	: Load resistance and inductance
ω, ω_r	: Base and rotor speeds
i_{cd}, i_{cq}	: d- and q- axis capacitor currents
i_{ld}, i_{lq}	: d- and q- axis load currents
i_{dm}, i_{qm}	: d- and q- axis magnetizing currents
τ_{st}, τ_{max}	: Starting and maximum torque
s	: Slip
$P_{rotation}$	: Rotational loss
P_{core}	: Core loss
$P_{cu(stator)}$	: Copper loss in stator
$P_{cu(rotor)}$	: Copper loss in rotor

CHAPTER 1

INTRODUCTION

1.1 General

In the present scenario, most of the power generated in the world comes either from fossil fuels powered generating stations using fuels such as coal, oil and natural gas or through Nuclear power plants and large Hydro-electric generating stations. Majority of the countries still rely on fossil fuels as their main source of energy generation. The net effect being huge increase in pollutants emitted by these generating plants leading to deteriorating air quality and severe environmental and health hazards. Moreover, these fossil fuels have a finite supply and will eventually run out in years to come. The biggest dilemma facing the industrialized and developing nations at present is how to continue this massive growth and development without jeopardizing the environment. A Faster growth in economies is usually associated with increase in generation as well as consumption of power. The question then arises is as to how to keep a balance between economic growth and a clean and healthy environment. Renewable sources of energy such as Wind, Solar, Geo-thermal and Biomass provide an alternative for this predicament. These sources of energy are not only clean but also found in abundance in nature and if effectively harnessed can contribute a lot towards making our planet a better place to live. Rapid increase in Green House Gas (GHG) emissions has led to a far greater understanding and use of alternate and renewable sources of energy.

Electricity generated from wind provides an alternative to non-renewable sources of generation that could be used to achieve significant reductions in fossil fuel use and a subsequent reduction in emissions. Wind energy is the one of the most abundantly available forms of renewable energy, and has emerged as a viable alternative. The wind electrical generation system is the most competitive of all the environmentally clean and safe renewable energy sources. Electricity derived from wind power provides an alternative to conventional generation that could be used to achieve substantial reductions in fossil fuel use and industrial effluents like carbon dioxide, nitrous oxide, methane and other GHGs.

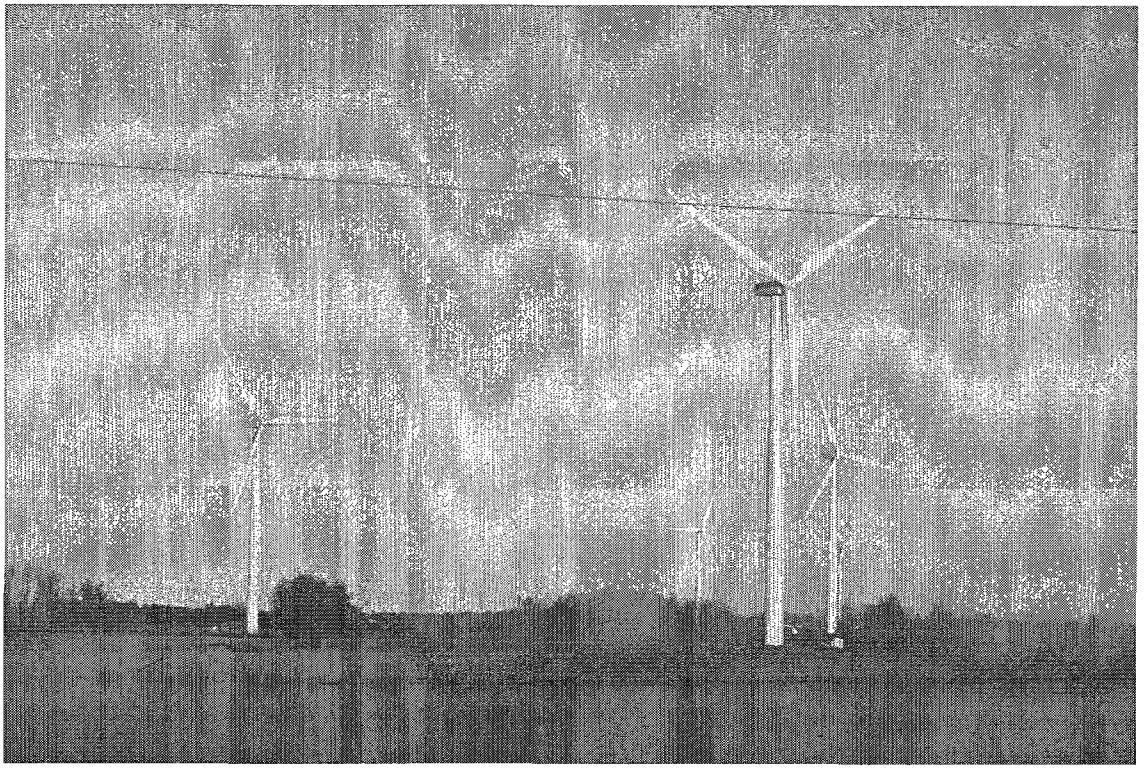

(a)

Fig. 1.1. Melanchton 1 Wind Farm in Shelburne, Ontario. (a) A set of turbines in the wind farm. (b) A view of the generator on the back side of the turbine.

Current utilization of renewable energy systems in the form of wind, small hydro and bio-gas has led to the massive use of grid-connected and self-excited induction generators (SEIG). Use of an induction machine as a generator is becoming more and more popular for the renewable sources. Induction generators have many advantages over synchronous generators, which make them ideally suited to be used in this kind of an application. A few of them are namely reduced cost and size, ruggedness, brushless, absence of separate dc source, ease of maintenance, self-protection against severe overloads and short circuits etc. Fig.1 shows an operational wind farm in south western Ontario.

Self-excitation phenomenon in induction machines although known for more than a half century is still a subject of considerable attention. The interest in this topic is primarily due to the application of SEIG in isolated power systems. The induction generator can work in two modes, grid connected and isolated mode. Self-excited induction generators are good candidates for wind powered electricity generation primarily in remote areas, because they do not need an external power supply to produce the excitation magnetic field. The main focus in this thesis is with respect to the stand alone mode of operation in induction generators.

Another aspect that this research covers is the analysis of SEIG having a copper rotor rather than the conventional aluminum rotor. A majority of the induction motors in different horsepower range of sizes are made with die-cast aluminum rotor cages. With the present day push for higher efficiency of energy usage, the possibility of improving efficiency in such motors has become enough of a priority to cause renewed interest in the use of copper in the squirrel cage.

1.2 Thesis Outline

This thesis work has been divided into 6 sections and 2 appendices. The thesis is an attempt to make the reader more comfortable with the research work related to self excited induction generators, basic theories regarding self excitation, the saturation characteristic of induction generators, mathematical modeling and analysis of the machines used in this research work, addition of the developed thermal model to the conventional model and comparison between an aluminum-rotor and copper-rotor induction machines.

Section 1.3 of this chapter reviews the previous work done through the ages in this area of research. The main purpose of reviewing this material is to give the reader sufficient knowledge to fully understand the concepts of induction generators, their uses and above all to lay open the vast amount of research work that has been done and which provides the direction, guidance and lays the background for all kinds of future work.

Chapter 2 of this thesis deals with the basic concepts of an induction generator. Starting off with the detailed theoretical and mathematical explanation of the process of self excitation in induction machines, the minimum capacitance required for self excitation and the saturation characteristics of the machines used in this research.

In Chapter 3 of this thesis, development of the complete mathematical model of induction generators used has been developed and explained. The fundamentals of induction machine modeling are also explained in this section. This also includes the conventional induction machine model, the model used in this research work and subsequently the addition of the thermal model to the existing model.

In chapter 4, the experimental set up used in this work has been explained. This includes details about the different tests done on the machines to obtain the machine parameters, physical descriptions of the machines used in the experiments and also a comparison between the aluminum-rotor and copper-rotor induction machine.

In chapter 5, the various results obtained during this research work, theoretical as well as experimental are compared and analyzed. These include the individual as well as comparative results for both thermal model and the conventional model and also for aluminum and copper rotor induction machine.

And finally in chapter 6, all the results from this work have been summarized and relevant conclusions drawn and this chapter also includes certain suggestions for any future works in this area.

1.3 Literature Review

This section gives the background and a review of previous works done in the area of induction generators.

1.3.1 Classification of Induction Generators

Basset and Potter reported in 1935 for the first time the concept of self-excitation of induction machines. They reported that the induction machine can be operated as an induction generator in isolated mode by using external capacitor. But there was a problem with the poor voltage regulation. Then in the year 1939, Wagner gave a method of analysis of self-excited induction generator by splitting if the real and reactive parts of the induction machine circuit. For this work the terminal voltage was determined by equating reactive VAR to zero, and slip by equating real power to zero. In 1954 Barkle and Ferguson presented the approximate model of both grid-connected and SIEG for studying the general aspects like power factor and short circuit behaviour.

On the basis of rotor construction, induction generators are two types (i.e., the wound rotor induction generator and squirrel cage induction generator). Depending upon the prime movers used (constant speed or variable speed) and their locations (near to the power network or at isolated places), generating schemes can be broadly classified as [1-4]

(i) Constant-speed constant-frequency

(ii) Variable-speed constant-frequency

(iii) Variable-speed variable-frequency

Constant-Speed Constant-Frequency

In this scheme, the prime mover speed is held constant by continuously adjusting the blade pitch and/or generator characteristics [5]. An induction generator can operate on an infinite bus bar at a slip of 1% to 5% above the synchronous speed. Induction generators are simpler than synchronous generators. They are easier to operate, control, and maintain, do not have any synchronization problems, and are economical.

Variable-Speed Constant-Frequency

The variable-speed operation of wind electric system yields higher output for both low and high wind speeds [6]-[9]. This results in higher annual energy yields per rated installed capacity. With variable prime mover speed, the performance of synchronous generators can be affected. For variable speed corresponding to the changing derived speed, SEIG can be conveniently used for resistive heating loads, which are essentially frequency insensitive. Both horizontal and vertical axis wind turbines exhibit this gain under variable-speed operation. Popular schemes to obtain constant frequency output from variable speed are

AC–DC–AC Link: With the advent of high-powered thyristors, the ac output of the three-phase alternator is rectified by using a bridge rectifier and then converted back to ac using line-commutated inverters. Since the frequency is automatically fixed by the power line, they are also known as synchronous inverters.

Double Output Induction Generator (DOIG): The DOIG consists of a three-phase wound rotor induction machine that is mechanically coupled to either a wind or hydro turbine, whose stator terminals are connected to a constant voltage constant frequency utility grid. One of the outstanding advantages of DOIG in wind energy conversion systems is that it is the only scheme in which the generated power is more than the rating of the machine. However, due to operational disadvantages, the DOIG scheme could not be used extensively. The maintenance requirements are high, the power factor is low, and reliability is poor under dusty and abnormal conditions. This scheme is not suitable for isolated power generations because it needs grid supply to maintain excitation.

Variable-Speed Variable-Frequency

With variable prime mover speed, the performance of synchronous generators can be affected. For variable speed corresponding to the changing derived speed, SEIG can be conveniently used for resistive heating loads, which are essentially frequency insensitive.

1.3.2 Modeling of Induction Generators

Various models and their applications [10],[11] have been presented to analyze the steady-state as well as transient performance of SEIG operating with either a regulated or unregulated prime mover . The following categories are the different models used.

D-Q Reference Model:

The *d-q* reference model was first proposed by Krause [12]. After a slight modification, many authors have formulated a reference model for a three-phase induction generator. Novotony [13] developed an analytical model of a system having an induction generator connected to a resistively loaded inverter using synchronously rotating *d-q* reference frame.

Impedance Based Model:

Murthy, Malik and Tandon studied the performance of the SEIG using an analytical model based on a conventional single-phase equivalent circuit with per-unit (p.u.) parameter. This model has been extended for the evaluation of various steady-state performance characteristics of stand-alone generators, such as the effect of shaft variation [14], [15], change in generator pole number [16], and parallel operation [17]. Potter [18] studied the effects of injected harmonic currents due to the electronic controller on generator losses in the steady-state model of SEIG. Rajakaruna *et al.* [19] have included the unregulated prime mover characteristic in the steady-state model of a three-phase-balanced induction generator.

Admittance Based Model:

Quazene *et al.* [20] developed an admittance-based model of SEIG using a single-phase equivalent circuit model with a balanced three-phase resistive load. For the determination of operating frequency and magnetizing reactance, real and imaginary parts of the sum of admittances of the rotor, magnetizing, and stator branches are equated to zero. This method gives an algebraic expression for magnetizing reactance in terms of generator frequency and other machines parameters and given speed. Ammasaigounden [21] also used an admittance-based model for a given output frequency, where the performance equation becomes quadratic in terms of speed and other machine parameters.

1.3.3 Steady-State Analysis of SEIG

A large number of articles have appeared on the steady-state analysis of the SEIG. In an isolated power system, both the terminal voltage and frequency are unknown and have to be computed for a given speed, capacitance, and load impedance. Steady-state analysis of SEIG is of interest, from both operation and design point of view.

Many articles been appeared on the steady-state analysis of the SEIG. Murthy *et al.* [22] developed a mathematical model to obtain the steady-state performance of SEIG using the equivalent circuit impedance of the machine. Two nonlinear equations, which are real and imaginary parts of the impedance, are solved for two unknowns. Jain [23] proposed a method in which the algebraic equation is solved for the initial value of and then the Secant method is used for the exact solution. Rahim [24] used a nodal admittance technique to obtain a nodal equation and then separated it into its real and imaginary parts so as to solve them first for the frequency f and then for the magnetizing reactance X_m. Chan [25] has proposed an iterative technique by assuming some initial value for and then solving for a new value considering a small increment until the result converges. Rajakaruna *et al.* [26] have used an iterative technique which uses an approximate equivalent circuit and a mathematical model for B-H curve and the solution is reduced to a nonlinear equation. Suitability of pole changing (4/6 pole) of SEIG for harnessing more wind energy under wide variation in wind speed is presented by, agarwal and singh [27] and chatterjee [28]. Sandhu *et al.* [29] have proposed an approach, which leads to a quadratic equation in slip making the steady-state analysis simple and comprehensive. Wang *et al.* [30], [31] have presented an eigenvalue-based approach to predict both minimum and maximum values of capacitance required for self-excitation of SEIG.

Steady-state analysis and performance of SEIG driven by regulated and unregulated turbines have been presented by Chan [32] and Alghuwainem [33]. Alghuwainem also has examined the steady-state analysis and performance characteristics of stand-alone SEIG when a transformer is connected to its terminals to supply the load at different voltage levels or to step up the terminal voltage. The transformer tends to saturate at higher speeds and, thus, absorbs the excess reactive power, limits the increase in the terminal voltage, and improves the voltage regulation. Kumarasen [34] compared the performance of wind-driven SEIG with load matching using the capacitor alone and with the combination of shunt and series capacitors. Alolah *et al.*

[35] have presented an optimization-based approach for the analysis of SEIG. The problem is formulated as a numerical optimization problem where no derivation of the analytical equation is needed.

1.3.4 Dynamic Analysis of SEIG

Many articles have appeared on the transient/dynamic analysis of SEIG and most of the transient studies of induction generators are related to voltage build-up due to self-excitation and load perturbation.

Shridhar *et al.* [36] present the transient performance of short-shunt SEIG. It is seen that it can sustain severe switching transients, has good overload capacity, and can re-excite over no load after loss of excitation. Tandon *et al.* [37] present the voltage buildup of SEIG due to switching of the three-phase capacitor bank at rated speed at no load. It is observed that depending on the machine parameters, the generator voltage builds up from small voltage due to residual magnetism to its rated value. Jha et al. investigated [38] the transient analysis of SEIG feeding an induction motor to analyze the suitability of the SEIG to sudden switching, such as starting of the IM. It is seen that reliable starting of an IM on SEIG is achievable with the value of capacitance determined through steady-state investigation; however, the capacitance should be applied in two steps: first to self-excite the generator, and second along with the motor or after switching on the motor.

Wang *et al.* [39] have presented the transient performance of stand-alone SEIG under the voltage buildup process, suddenly switching off one excitation capacitor and suddenly switching off two excitation capacitors. It is seen that when one of the three balanced excitation capacitors is switched off from the machine, SEIG can still maintain self-excitation and generates adequate voltage on other two phases. When two of the three balanced excitation capacitors are switched off from the machine, the generated voltage of the SEIG collapses and gradually reduces to zero. They have also presented a comparative study of long-shunt and short-shunt configurations on dynamic performance of an isolated SEIG feeding an induction motor load. Results show that the long shunt configurations may lead to unwanted oscillations while the short shunt provides the better voltage regulation. Levi [40] has presented an experimental study of the dynamic behaviour of SEIG. The emphasis is placed on the situation that leads to voltage collapse and the

total demagnetization of the machine and on the variable speed of the induction generator with a fixed capacitor bank. Jain et al. [41] presented the transient performance of three-phase SEIG during balanced and unbalanced faults, considering the effects of main and cross flux saturation for load perturbation, three-phase, and line-to-line short circuit, opening of one capacitor, two capacitors and a single line at the capacitor bank, opening of single-phase load, two-phase load, etc.

1.3.5 Voltage Regulation of SEIG

The need for reactive power support and poor voltage regulation are the two major drawbacks of induction generators. Induction generators and also load, which is generally inductive in nature, require the supply of reactive power. Unbalanced reactive power operation results in voltage variation. Malik *et al.* [42] have shown that the minimum capacitance requirement of SEIG is inversely proportional to the square of speed and maximum saturated magnetizing reactance. Sridhar *et al.* [43] have discussed a methodology to choose the appropriate value of capacitors for desired regulation of short-shunt SEIG. The short/long-shunt configurations of the SEIG give better performance in terms of voltage regulation than the simple shunt configuration, but the compensation used in these configurations causes the problem of sub-synchronous resonance while supplying power to inductive and/or dynamic loads.

A fixed capacitor alone, as presented in [44], cannot provide the adequate amount of reactive power needed by the induction generator at all possible speeds and loading conditions. Even if fixed capacitors are used to provide the average value, self-excitation may result in undue overvoltage. A fixed and switched capacitors scheme presented by Elsharkawi *et al.* [45] consists of two discrete groups of fixed and switched capacitors, which furnish enough reactive power for an induction generator throughout its desired operating region of speed. The number of switched capacitors is kept to a minimum to simplify the switching circuit, and yet provides adequate and varying reactive power compensation. The controller senses the reactive power drawn by the machine and accordingly provides the needed reactive power to improve the power factor to as close to unity as possible. This method has limited applications because it regulates a terminal voltage in discrete steps.

Wind is the main conventional energy source that fluctuates highly in nature, and power produced from the wind varies with the cube of the speed. Static var compensators (SVCs) have been used in conventional power systems and can also be used conveniently in isolated power systems where continuous and fast control of reactive power is required. SVC has fast response and continuous control of reactive power and offers a large number of advantages over conventional reactive power compensation schemes.

1.4 Thermal Effect

Due to their high reliability and their robust construction, induction machines with squirrel cage rotors are installed in many areas of industrial practice. The most important features of squirrel cage induction machine that enhances its suitability in hostile environment are ruggedness and robustness [46]. However, when the machine is continuously operated on load, it may be necessary to monitor the temperature of the various parts of the machine if the aforementioned important features are not to be compromised due to excessive heating. In the past decade, research in protection techniques and instrumentation technology has brought some new methods for the measurement of protection relevant variables [47]. Effective supervisory systems have two positive effects: the lifetime of the machine can be prolonged and the operating range of the machine and of the following process can be expanded.

Still, a critical variable for induction machines, in particular for those of high power, is the rotor temperature. Heat generated in the rotor and stator is dissipated by conduction, convection, and radiation. Anything that will obstruct the flow of air through or over the motor, or that will impede the radiation of heat from the motor parts, will cause an increase in winding temperatures. Therefore, it is important that the motor is kept clean inside and outside to assure that the flow of air is not restricted.

Thermal failures of induction machines occur primarily because of breakdown of the stator winding insulation or mechanical fatigue of the rotor conductors. For instance, modern induction machine protective devices are often expected to accommodate temporary running overloads which are used to boost the efficiency and versatility of a drive. Other irregular conditions such as low speed operation, inverter harmonics, temporary phase imbalances and repeated starts also contribute to the complexity of protecting induction machines. Generally,

when the thermal limit of an electrical machine is exceeded, the following undesirable effects result: Loss of dielectric property of the insulating material, thermal bending of the rotor and consequent loss of eccentricity, bearing wear and vibration, deterioration of bearing lubricants and thermal stresses and changes in geometry of the machine elements due to thermal expansion. Due to these undesirable effects, the temperatures in electrical machines must be properly monitored and specified within certain limits to reflect the mechanical, electrical and environmental conditions in which the machine will operate. The methods of heat transmission are conduction, convection and radiation. Heat is transmitted through the stator and rotor by conduction and from them to the air by a combined effect of conduction and convection, with the prevalence of the latter. Between the stator and rotor the transmission is carried out fundamentally by conduction through the airgap.

Maximini and Koglin [48] explained about the determination of absolute rotor temperature of squirrel cage induction motors. The study of transient thermal behaviour is useful to identify causes of failure in induction machines. Rajagopal *et al* [49] presented the transient thermal analysis of induction motors. This paper presented a two dimensional transient analysis of induction machines using the available heat transfer coefficients. Therefore, to have a better understanding of machine behaviour and performance it is of utmost importance that effect of temperature on machine performance is taken into account. Exact prediction of the temperature rise of all machine parts is an important design factor of a motor. Many publications only investigate the stationary heat transfer within a motor at rated conditions. The increasing demands on the reliability of motors, especially during switching operations with frequent reversing starts or run ups in automatic processes, require exact investigation of the thermal behaviour of a motor during transient conditions.

In order to predict the temperatures in electrical machines, thermal models are used. Thermal models of electrical machines vary in degree of complexities depending on areas of applications and the level of accuracy to which the models are expected to give when compared to the physical temperature measurements of the test machine. Knowledge of the rotor temperature of an induction motor enables motor surveillance, protection and operation based on the thermal limits of the actual machine. However, rotor temperature measurement is a difficult and expensive task. Therefore, the only appropriate way of temperature acquisition is the estimation based on machine models. Rotor temperature can be determined with the help of the

estimated resistance of the rotor cage. This task can he performed by evaluating the equations of the induction machine accordingly. Consequently, some of the machine parameters have to be determined in order to be able to compute the rotor resistance. The accuracy of the estimated rotor temperature is mainly determined by the accuracy of the employed model and the involved machine parameters.

1.5 Aluminum and Copper Rotor Induction Machines

Most of the induction motors in the fractional and integral horsepower range of sizes are made with die-cast alum rotor cages. This is due to the fact that the related die-cast aluminum-rotor technology is easy and less expensive in terms of manufacturing and material costs as compared to its copper counterpart [50]. Also the trend in price in the world market is higher in case of copper. Fig 1.2 shows the comparative trend in the price of aluminum and copper in the market. With the present day push for higher efficiency of energy usage, the possibility of improving efficiency in such motors has become enough of a priority to cause renewed interest in the use of copper in the squirrel cage because of its substantially higher electrical conductivity [51].

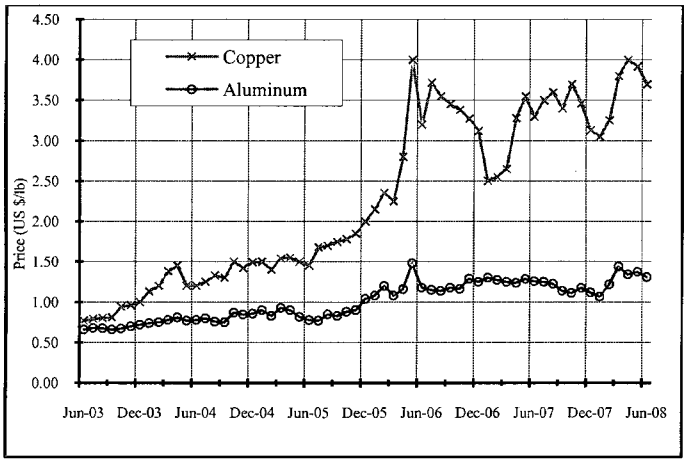

Fig. 1.2 Trend in the Price of Aluminum and Copper in World Market.

Electrically conductive parts of the squirrel cage rotor are either made of aluminum or copper. Rotor bars and end-rings are usually designed for different current densities. Therefore, losses in the bars and end-rings are different, too. Different rotor losses and cooling conditions lead thus to different temperatures in the bars and end-rings. The bars of aluminum (and copper) die casting rotors are not insulated. Due to shrinkage, a small gap between bars and iron teeth can be

expected. This additional gap slightly decreases thermal conductivity between bars and iron teeth. In squirrel cage rotors with fabricated bars, a greater gap between bars and iron teeth is needed to mount the bars, even if no additional insulation is used. This gives rise to an even higher decrease of the thermal conductivity. Fig 1.3 shows a cut section view of a Siemens high efficiency NEMA standard copper-rotor motor.

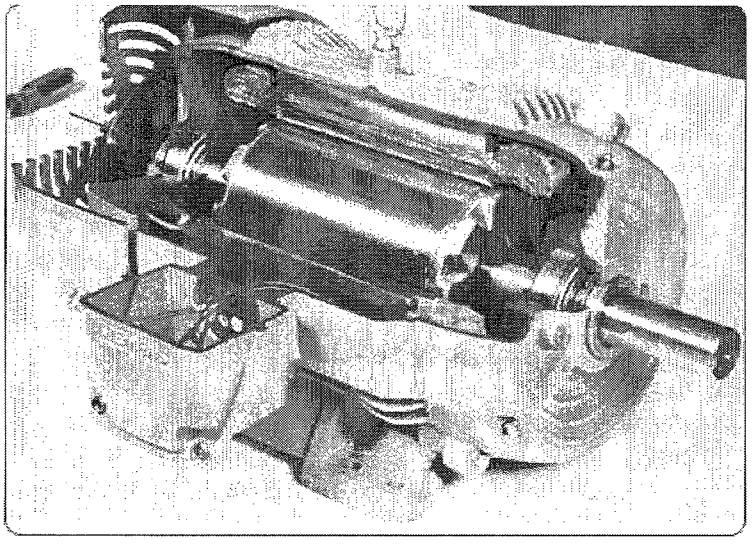

Fig. 1.3. Sectional View of Siemens Copper-Rotor Motor. (Picture courtesy Siemens)

Induction motors have been made with fabricated copper rotors since long. However, the high melting point of copper leads to difficulties in casting. Short die life resulting from high temperature has, in the past, made cast copper rotors uneconomical. The possibility of improving the efficiency in such motors has become enough of a priority to cause renewed interest in the use of copper in the squirrel cage. Induction machines fabricated and tested by several manufacturers have shown that machines with rotors using copper bars would achieve an overall loss reduction of 15% to 20%. Cowie and Peters [52] also presented the data on performance of motors incorporating the die-cast copper rotors and compares the performance with the aluminum cast ones.

Figs. 1.4 and 1.5 show the cross sectional view of the stator and rotor of the two 7.5 hp aluminum-rotor and copper-rotor induction machines used for experimental investigations.

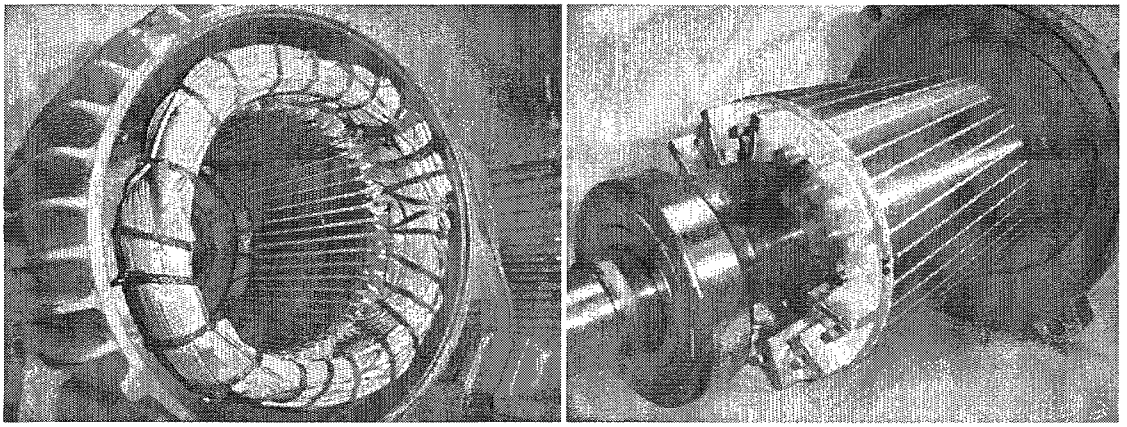

(a) (b)

Fig. 1.4. Cross sectional view of 7.5 hp aluminum-rotor induction machine. (a) Stator. (b) Rotor

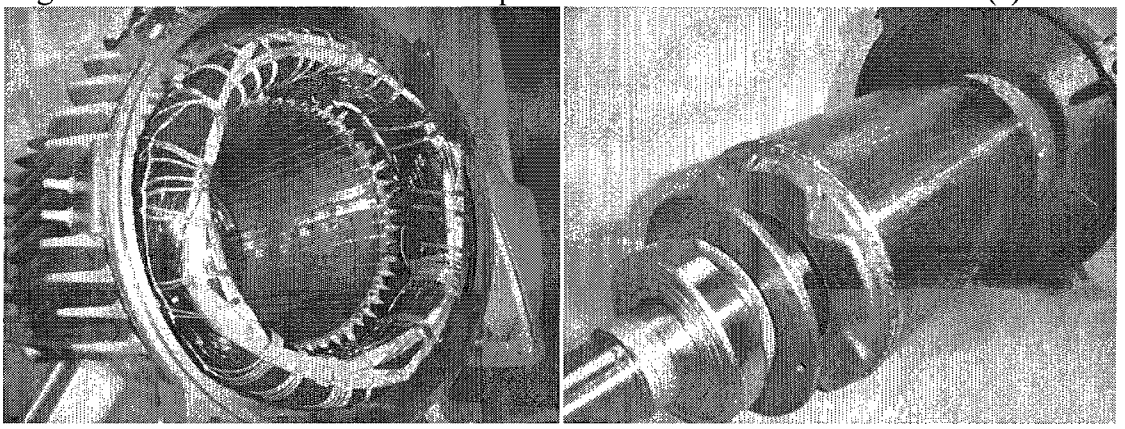

(a) (b)

Fig. 1.5. Cross sectional view of 7.5 hp copper-rotor induction machine. (a) Stator. (b) Rotor.

1.6 Objectives of This Research Work

Investigations on the induction generators have been performed where saturation of the main flux was considered and the machines studied were either wound-rotor or aluminum bar squirrel-cage rotor type. However, studies on the performance analysis of a squirrel-cage aluminum-rotor and copper-rotor SEIG considering both saturation and thermal effect have not yet been carried out extensively. Moreover, this research work gives a detailed description of machine behaviour and the effect of temperature on both aluminum and copper rotor machines. Also, comparative results have been presented between experimental and theoretical results.

Therefore, this research work presented in this thesis broadly covers the following objectives.

1. Consideration of saturation and effects of temperature in the machine modeling.
2. Comparison between experimental and theoretical results.
3. Performance analysis of aluminum-rotor and copper-rotor SEIG.

1.7 References

[1] T. S. Jayadev, "Windmills stage a comeback," *IEEE Spectrum.*, vol. 13, no. 11, pp. 45-49, Nov. 1976.

[2] L. Quazene and G. McPherson Jr., "Analysis of an isolated induction generator," *IEEE Trans. Power App. Syst.*, vol. 102, no. PAS-8, pp. 2793–2798, Aug. 1983.

[3] A. M. Osheiba and M. A. Rehman, "Performance analysis of self-excited induction and reluctance generators," *Elect. Mach. Power Syst.*, vol. 19, pp. 477–499, 1991.

[4] B. Singh, "Induction generator-A prospective," *Elect. Mach. Power Systems*, vol. 23, pp. 163–177, 1995.

[5] N. P. A. Smith, "Induction generator for stand-alone micro-hydro systems," in *Proc. IEEE Int. Conf. Power Electronics Drives and Energy System for Industrial Growth*, vol. 2, Jan. 1996, pp. 669–712.

[6] G. A. Smith and D. M. Donegani, "A variable-speed constant-frequency induction generator for sub and super synchronous operation," in *Proc. Eur. Wind Energy Assoc. Conf.*, Rome, Italy, 1986.

[7] N. Elsonbaty, P. G. Holmes, M. Salama, N. P. A. Smith, and A. A.Williams, "VSCF induction generation in stand-alone micro-hydro generating systems," in *Proc. Int. Conf. Renewable Energy-Clean Power-2001*, 1993, pp. 89–94.

[8] F. C. Dezza, A. D. Geriando, and R. Perini, "Performance comparison among different converters fed by self-excited wind driven induction generators," in *Proc. 7th Int. Conf. on Electric machines Drives*, 1995, pp.438–443.

[9] S. Wekhande and V. Agarwal, "A new variable speed constant voltage controller for self-excited induction generator," *Electr. Power Syst. Res.*,vol. 59, no. 3, pp. 157–164, 2001.

[10] D. W. Novotony, D. J. Gritter, and G. H. Studtmann, "Self-excitation in inverter driven induction machines," *IEEE Trans. Power App. Syst.*, vol. PAS-96, no. 4, pp. 1117–1125, Apr. 1977.

[11] E. Bim, J. Szajner, andY. Burian, "Voltage compensation of an induction generator with long-shunt connections," *IEEE Trans. Energy Conversion.*, vol. 4, no. 3, pp. 526–530, Sep. 1989

[12] P. C. Krause and C. H. Thomas, "Simulation of symmetrical induction machinery," *IEEE Trans. Power App. Syst.*, vol. PAS-84, no.11, pp.1038–1053, Nov. 1965.

[13] D. W. Novotony, D. J. Gritter, and G. H. Studtmann, "Self-excitation in inverter driven induction machines," *IEEE Trans. Power App Syst.*, vol.PAS-96, no. 4, pp. 1117– 1125, Apr. 1977.

[14] S. S. Y. Narayanan and V. J. Johnny, "Contribution to the steady state analysis of wind-turbine driver self-excited induction generator," *IEEE Trans. Energy Conversion.*, vol. EC-1, no. 1, pp. 169–176, Mar. 1986.

[15] G. Raina and O. P. Malik, "Wind energy conversion using a self-excited induction generator," *IEEE Trans. Power App. Syst.*, vol. PAS -102, no.12, pp. 3933–3936, Dec. 1983.

[16] S. P. Singh, B. Singh, and M. P. Jain, "Steady state analysis of self-excited pole changing induction generator," *J. Inst. Eng.*, vol. 73, pp.137–144, Aug. 1992.

[17] E. Bim, J. Szajner, andY. Burian, "Voltage compensation of an induction generator with long-shunt connections," *IEEE Trans. Energy Conversion.*, vol. 4, no. 3, pp. 526–530, Sep. 1989.

[18] E. D. Besant and F. M. Potter, "Capacitor excitation for induction motors,"*AIEE Trans.*, vol. 54, pp. 540–545, May 1935.

[19] S. Rajakaruna and R. Bonert, "A technique for the steady state analysis of a induction generator with variable speed," *IEEE Trans. Energy Conversion.* vol. 8, no. 4, pp. 757–761, Dec. 1993.

[20] L. Quazene and G. McPherson Jr., "Analysis of an isolated induction generator," *IEEE Trans. Power App. Syst.*, vol. 102, no. PAS-8, pp. 2793–2798, Aug. 1983.

[21] N. Ammasaigounden, M. Subbiah, and M. R. Krishnamurthy,"Wind-driven self- excited pole changing induction generators," *Proc. Inst. Elect. Eng. B*, vol. 133, no. 5, pp. 315–321, 1986.

[22] S. S. Murthy, O. P. Malik, and A. K. Tandon, "Analysis of self excited induction generator," *Proc. Inst. Elect. Eng. C*, vol. 129, no. 6, pp.260–265, Nov. 1982.

[23] D. K. Jain, A. P. Mittal, and B. Singh, "An efficient iterative technique for the analysis of self-excited induction generator," *J. Inst. Eng. (India)*,vol. 79, no. 1, pp. 172–177, 1999.

[24] Y. H. A. Rahim, "Excitation of isolated three-phase induction generator by a single capacitor," *Proc. Inst. Elect. Eng., Elect. Power Appl.*, vol.140, no. 1, pp. 44–50, 1993.

[25] T. F. Chan, "Analysis of self-excited induction generators using an iterative method," *IEEE Trans. Energy Convers.*, vol. 10, no. 3, pp. 502–507,Sep. 1995

[26] S. Rajakaruna and R. Bonert, "A technique for the steady state analysis of a induction generator with variable speed," *IEEE Trans. Energy Conversion.*,vol. 8, no. 4, pp. 757–761, Dec. 1993.

[27] S. C. Agarwal and M. Singh, "An analysis of self-excited pole changing induction generators," in *Proc. 8th National Power System Conf.*, Delhi, India, Dec. 14–17, 1994, pp. 888–892.

[28] J. K. Chatterjee and P. K. S. Khan, "Excitation capacitor requirement and performance of pole-changing self-excited induction generator operating with unregulated prime mover," in *Proc. 9th Nat. Power System Conf.*, Kanpur, India, Dec. 19–21, 1996, pp. 83– 87.

[29] K. S. Sandhu and S. K. Jain, "Operational aspects of self-excited induction generator using a novel model," *Elect. Mach. Power Syst.*, vol. 27,pp. 169–180, 1998.

[30] L. Wang and C. H. Lee, "A novel analysis of the performance of an isolated self-excited induction generator," *IEEE Trans. Energy Conversion.*,vol. 12, no. 2, pp. 109–115, Jun. 1997.

[31] L. Wang and C. H. Lee, "Long-shunt and short shunt connections on a dynamic performance of a SEIG feeding an induction motor load," *IEEE Trans. Energy Conversion.*, vol. 15, no. 1, pp. 1–7, Mar. 2000.

[32] T. F. Chan, "Self-excited induction generators driven by regulated and unregulated turbines," *IEEE Trans. Energy Convers.*, vol. 11, no. 2, pp.338–343, Jun. 1996.

[33] S. M. Alghuwainem, "Steady-state analysis of an isolated self-excited induction generator driven by regulated and unregulated turbine," *IEEE Trans. Energy Convers.*, vol. 14, no. 3, pp. 718–723, Sep. 1999.

[34] N. Kumarasen and M. Subiah, "Analysis and control of wind driven selfexcited induction generators with load matching," in *Proc. 11th National Power System Conf.*, Bangalore, India, Dec. 20–22, 2000, pp. 21–26.

[35] A. L. Alolah and M. A. Alkanthal, "Optimization based steady state analysis of three phase SEIG," *IEEE Trans. Energy Conversion.*, vol. 15, no. 1, pp. 61–65, Mar. 2000.

[36] L. Shridhar, B. Singh, and C. S. Jha, "Transient performance of the self regulated short-shunt self-excited induction generator," *IEEE Trans. Energy Conversion.*, vol. 10, no. 2, pp. 261–267, Jun. 1995.

[37] A. K. Tandon, S. S. Murthy, and G. J. Berg, "Steady state analysis of capacitor self-excited induction generators," *IEEE Trans. Power App. Syst.*, vol. PAS-103, no. 3, pp. 612–618, Mar. 1984.

[38] B. Singh, L. Shridhar, and C. S. Jha, "Transient analysis of self-excited induction generator supplying dynamic load," *Elect. Mach. Power Syst.*,vol. 27, pp. 941–954, 1999.

[39] L. Wang and R. Y. Deng, "Transient performance of an isolated induction generator under unbalanced excitation capacitors," *IEEE Trans. Energy Conversion.*, vol. 14, no. 4, pp. 887–893, Dec. 1999.

[40] D. Levy, "Stand alone induction generators," *Elect. Power Syst. Res.*,vol. 41, pp. 191–201, 1997.

[41] S. K. Jain, J. D. Sharma, and S. P. Singh, "Transient performance of three-phase self-excited induction generator during balanced and unbalanced faults," in *Proc. Inst. Elect. Eng., Gen., Transm. Distrib.*, vol. 149, Jan. 2002, pp. 50–57.

[42] N. H. Malik and A. A. Mazi, "Capacitive requirements for isolated self-excited induction generators," *IEEE Trans. Energy Conversion.*, vol. EC-2, no. 1, pp. 62–69, Mar. 1987.

[43] L. Shridhar, B. Singh, C. S. Jha, B. P. Singh, and S. S. Murthy, "Selection of capacitors for the self regulated short shunt self-excited generator," *IEEE Trans. Energy Conversion.*, vol. 10, no. 1, pp. 10–17, Mar. 1995.

[44] A. H. Al-Bahrani and N. H. Malik, "Steady state analysis of parallel operated self-excited induction generators," *Proc. Inst. Elect. Eng. C*, vol. 40, no. 1, pp. 49–55, 1993.

[45] M. A. Elsharkawi, S. S. Venkata, T. J. Williams, and N. G. Butlar, "An adaptive power factor controller for three-phase induction generators," *IEEE Trans. Power App. Syst.*, vol. PAS-104, no. 7, pp. 1825–1831, Jul. 1985.

[46] H. Moghbelli, G. E. Adams and R.G. Hoft, "Performance of a 10-Hp Switched Reluctance motor and comparison with induction motors", *IEEE Trans. on Industry Applications*, vol. 27, no.3, pp. 531-538, May/June 1991.

[47] G Pascoli, F Pirker, H Kapeller and C Kral, "Comparison of two rotor temperature estimation models of a surface cooled squirrel cage induction machine," *IEEE International conference on electric machines and drives*, Vol.1, pp. 207-211, May 2005.

[48] M Maximini and H. J. Koglin, "Determination of the absolute rotor temperature of squirrel cage induction machines using measurable variables", *IEEE Transaction on Energy Conversion*, Vol. 19, No.10, March 2004.

[49] M.S. Rajagopal and K.N. Seetharamu, "Transient thermal analysis of induction motors", *IEEE Transaction on Energy Conservation*, Vol 13, No.1, March 1998.

[50] A.Boglietti, A. Cavagnino, L. Ferraris and M.Lazzari, "Energetic Considerations about the Use of Cast Copper Squirrel Cage Induction Motors," in *Proc. 33rd Annual Conference of the IEEE Industrial Electronics Society*, pp. 157-162, Taipei, 2007.

[51] K. L. Kirtley Jr., J. G. Cowie, E. F. Brush Jr., D. T. Peters and R. Kimmich, "Improving Induction Motor Efficiency with Die-Cast Copper Rotor Cages," in *Proc. IEEE Power Engineering Society General Meeting*, pp. 1- 6, 2007.

[52] D. T. Peters, J. G. Cowie, E. F. Brush Jr., and D. J. Van Son, "Copper in the Squirrel Cage for Improved Motor Performance," in *Proc. IEEE International Electric Machines and Drives Conference*, Vol. 2, pp. 1265-1271, 2003.

CHAPTER 2

INDUCTION GENERATORS

2.1 Self-Excitation

Self-excitation phenomenon in induction machines although known for more than a half century is still a subject of considerable attention [1]-[8]. The interest in this topic is primarily due to the application of SEIG in isolated power systems. Physical background of the self-excitation process has been described in [9]. When an induction machine is driven at a speed greater than the synchronous speed (negative slip) by means of an external prime mover [10], the direction of induced torque is reversed and theoretically it starts working as an induction generator. In the negative slip region, it is seen that the machine draws a current, which lags the voltage by more than 90. This means that real power flows out of the machine but the machine needs the reactive power. To build up voltage across the generator terminals, excitations must be provided by some means.

Therefore, the induction machine can work in two modes:

1) Grid connected mode
2) Isolated mode

In case of a grid-connected mode, the induction generator can draw reactive power either from the grid but it will place a burden on the grid or by connecting a capacitor bank across the generator terminals. For an isolated mode, there must be a suitable capacitor bank connected across the generator terminals. This phenomenon is known as capacitor self-excitation and the induction generator is called a "SEIG".

An induction generator without any external source, using capacitors can self-excite if there is a remnant magnetic flux in the machine core or residual charge across the capacitor terminals. The residual magnetism in the field circuit produces a small voltage. That voltage produces a small capacitive current flow. This boosts up the voltage which further increases the capacitive current until the voltage reaches the steady-state value. Thus a three phase induction machine can be made to work as a self-excited induction generator provided the capacitance

connected across the stator terminals have sufficient charge to provide necessary initial magnetizing current.

It is well known that when capacitors are connected across the stator terminals of an induction machine, driven by an external prime mover, voltage will be induced at its terminals. The induced emf and current in the stator windings will continue to rise until steady state is attained, influenced by the magnetic saturation of the machine. At this operating point the voltage and current will continue to oscillate at a given peak value and frequency. In order for self-excitation to occur, for a particular capacitance value there is a corresponding minimum speed.

When an induction machine is driven by a prime mover, and if the capacitor is charged, that capacitor provides the exciting current required by the induction generator to produce a magnetic flux. The magnetic flux in the induction generator charges the capacitor to increase the terminal voltage. An increase in the capacitor voltage boosts up the excitation current to the generator to increase the flux which in turn increases the terminal voltage. In this way the voltage and current build up continues until the magnetizing inductance decreases to its saturated value and an equilibrium point is attained. The process will continue until steady-state is reached.

Self-excited induction generators are good candidates for wind powered electric generation application especially in remote areas, because they do not need external power supply to produce the magnetic field. Permanent magnet generators can also be used for wind energy applications but they suffer from uncontrollable magnetic field, which decays over a period due to weakening of the magnets, and the generated voltage tends to fall steeply with load. The SEIG has a self-protection mechanism because the voltage collapses when there is a short circuit at its terminals. Further, As compared to conventional synchronous generators, the SEIGs have more advantages such as cost, reduced maintenance, rugged and simple construction, brush-less rotor (squirrel cage), etc. But, on the other hand they also suffer from some inherent disadvantages such as reactive power consumption, poor voltage regulation under varying speeds and low power factor. The following Fig. 2.1 shows the basic operation principal of a SEIG.

The process of self-excitation can also be explained by the following points.

1. A three phase induction machine can be operated as a SEIG if its rotor is driven at a suitable speed and a capacitor bank of sufficient value is connected across its stator terminals.
2. To build up voltage across the generator terminals, excitation must be provided.
3. The residual flux in the rotor iron or initial charge on the excitation capacitor will induce a small emf in the stator winding.
4. This induced voltage will continue to increase until a steady state is reached influenced by the magnetic saturation of the machine.
5. This phenomena is known as capacitor self excitation, and the induction motor is called SEIG.

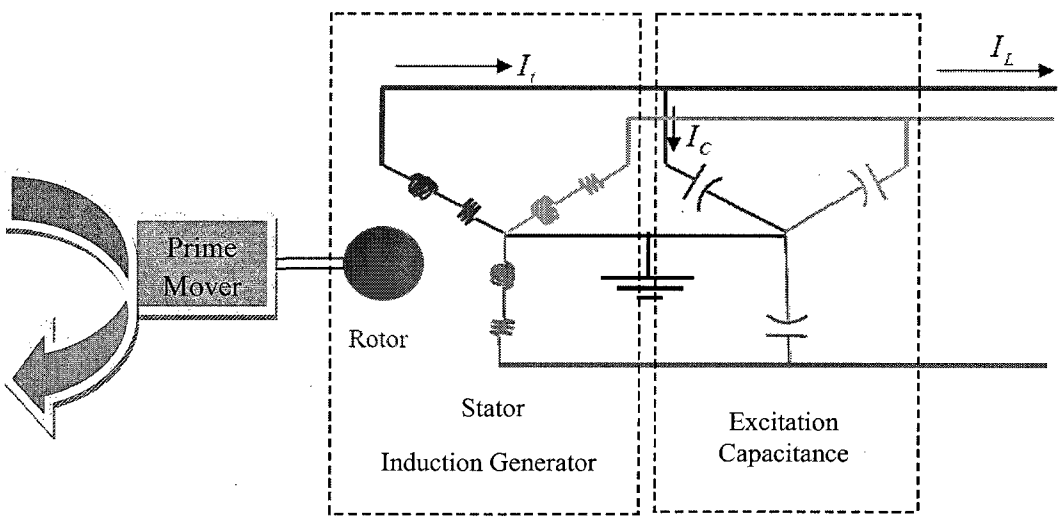

Fig. 2.1. Basic operating principle of a self-excited induction generator.

The process of voltage build-up in an induction generator is very much similar to that of a dc generator. There must be a suitable value of residual magnetism present in the rotor. In the absence of a proper value of residual magnetism, the voltage will not build up. So it is desirable to maintain a high level of residual magnetism, as it does ease the process of machine excitation.

When an induction generator first starts to run, the residual magnetism in the rotor circuit produces a small voltage. This small voltage produces a capacitor current flow, which increases the voltage and so forth until the voltage is fully built up. The no-load terminal voltage of the induction generator is the intersection of the generator's magnetization curve with capacitor load line. The magnetization curve of the induction generator can be obtained by running the machine as a motor at no load and measuring the armature current as a function of terminal voltage.

2.2 Determination of Minimum Capacitance Required for Self-Excitation

There must be an initial charge on the capacitor or residual magnetism in the rotor iron to initiate the voltage and current to build up. When the machine is driven by an external prime-mover, the remnant flux in the rotating rotor induces a small voltage in stator windings, which carries a leading current if suitable terminal capacitors are connected. The steady-state performance characteristics of an isolated self-excited induction generator are influenced by the magnitude of the excitation capacitor and rotor speed. The terminal capacitor must have its value within a certain range to sustain self-excitation. If the value of the excitation capacitor is outside this range, self-excitation will not be possible. The capacitor in such a machine must have a minimum value, C_{min} for self-excitation to take place. On the other hand in order to sustain operation, the terminal capacitor must also be below a certain maximum value C_{max}.

Since core losses do not have a significant effect in the C_{min} estimation, they can be ignored. A SEIG must be in the saturated region at starting, it means that X_m is a saturated reactance. Higher saturation can reduce X_m, and its value is normally chosen the minimum saturated reactance X_{msat}.

The following flowchart as shown in Fig. 2.2 shows the basic steps to determine the minimum capacitance as well as minimum speed.

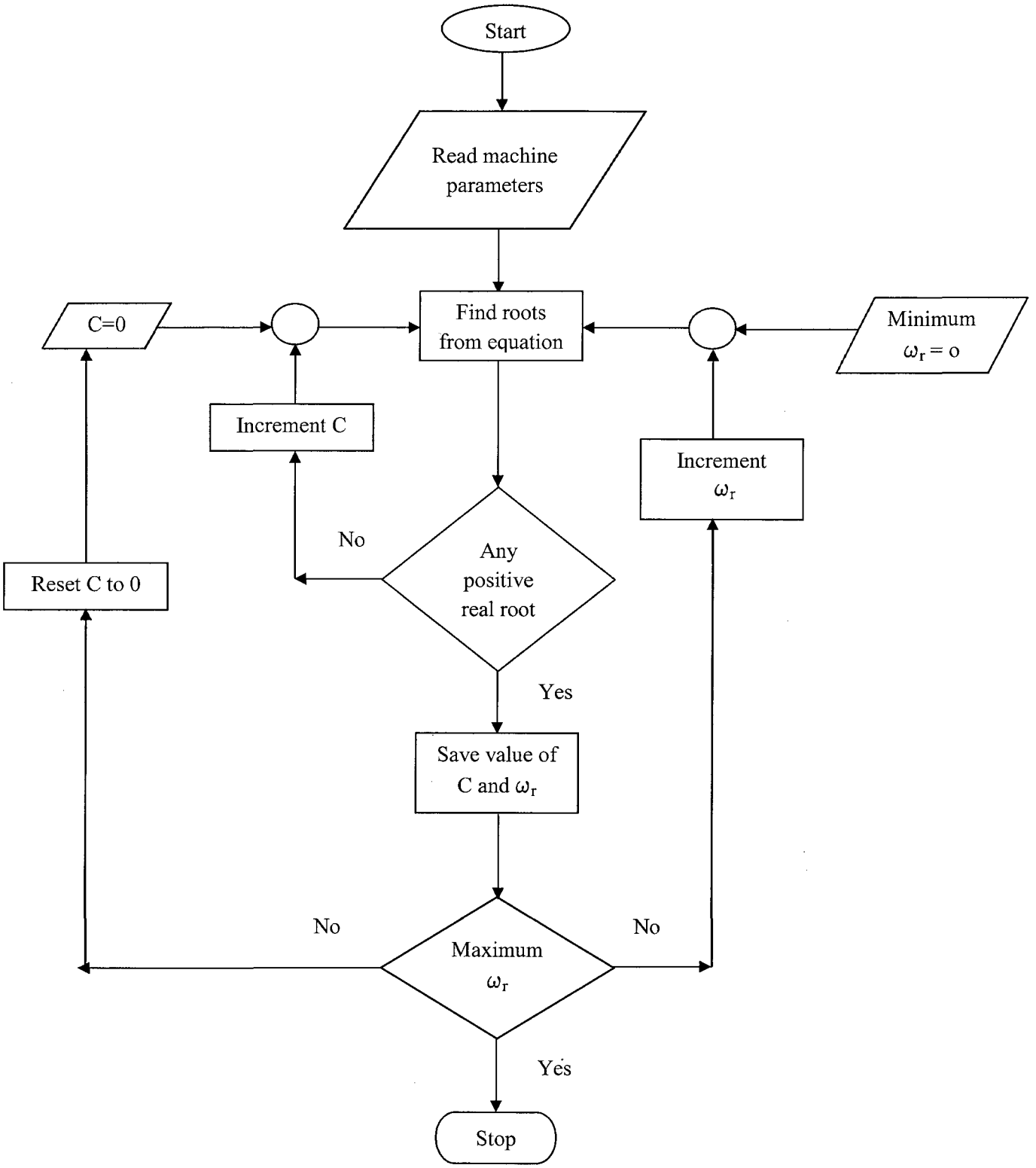

Fig. 2.2. Flowchart to determine the minimum speed and minimum capacitance for SEIG at no load.

Initially, experiments were conducted on a 1/3 hp laboratory induction machine with the following machine parameters to obtain the required values.

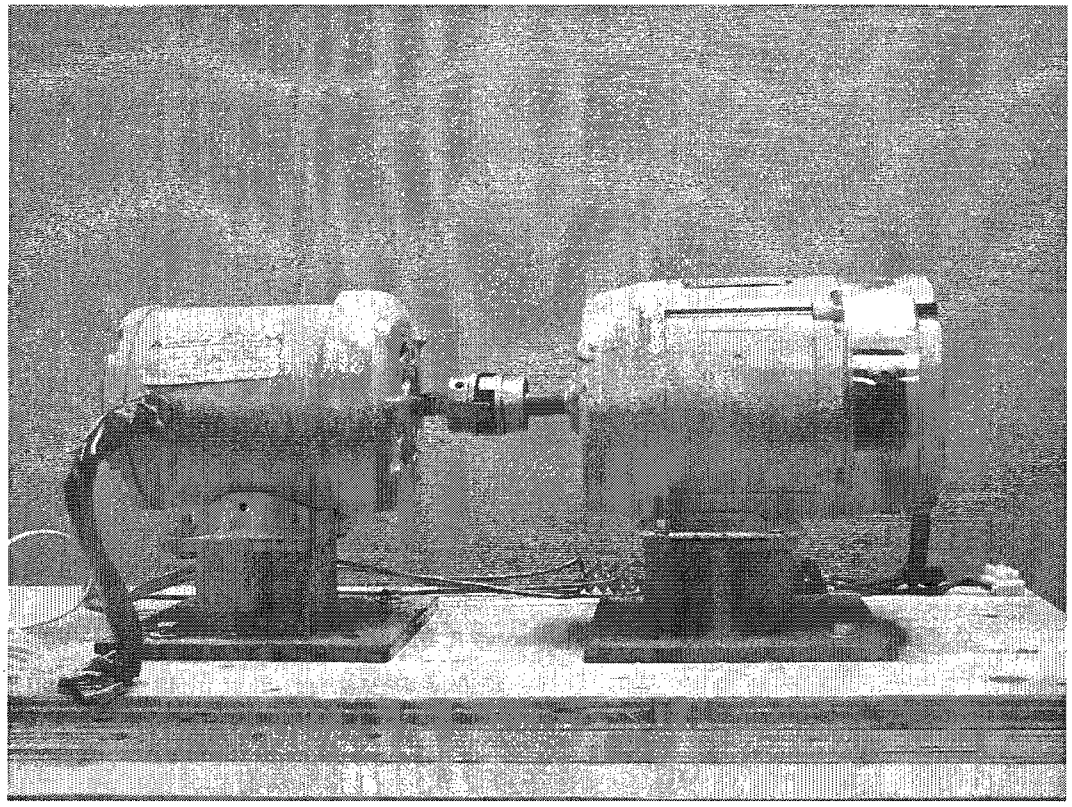

Fig. 2.3. 1/3 hp Laboratory induction machine on which experiments were conducted.

Table 2.1 Rating of 1/3 hp IM

Machine used for investigation	
Rated Voltage	230 V
Rated Current	1.6 A
Rated power	1/3 HP
Rated frequency	60 Hz
RPM	1,725
Poles	4

Table 2.2 Parameters of 1/3 hp IM

Machine parameters	
R_s	5.8433 Ω
R_r	3.2535 Ω
X_s	6.2048 Ω
X_r	6.2048 Ω
X_m	80.5604 Ω
R_m	200.54 Ω

The following figures show the various results for minimum capacitance of the induction machine, both experimental as well as mathematical.

1) Comparison of experimental and calculated values of C_{min}
2) Experimental and calculated values of C_{min} based on different values of X_m
3) Variation of Frequency with Speed (No load & C=52.8 μF)
4) Fig 2.8 Variation of Frequency with Speed (No load & C=61.6 μF)

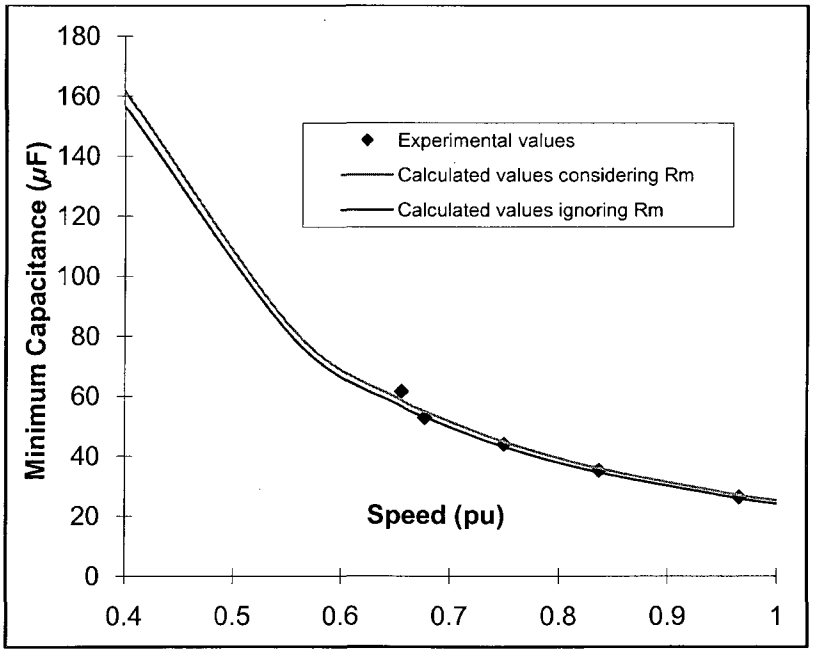

Fig. 2.4. Comparison of experimental and calculated values of C_{min}.

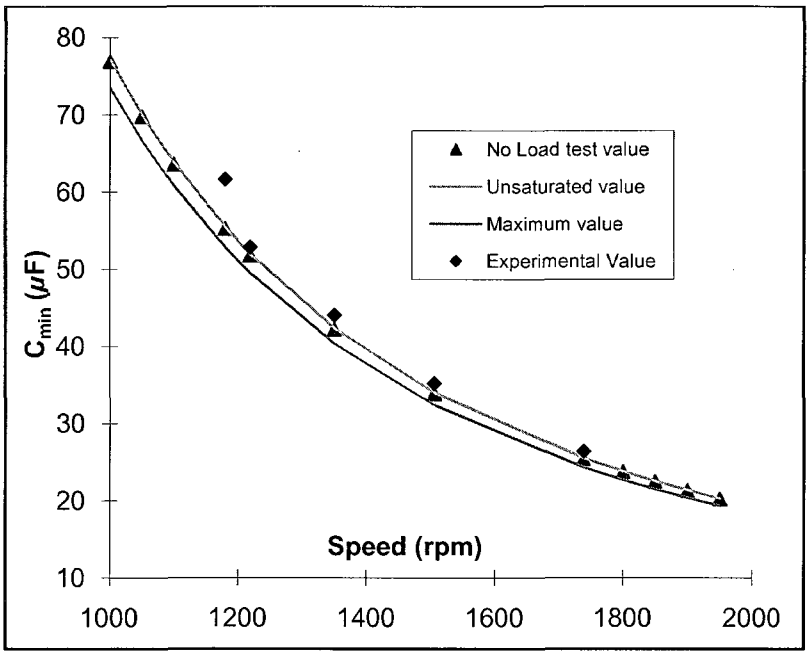

Fig. 2.5. Experimental and calculated values of C_{min} based on different values of X_m.

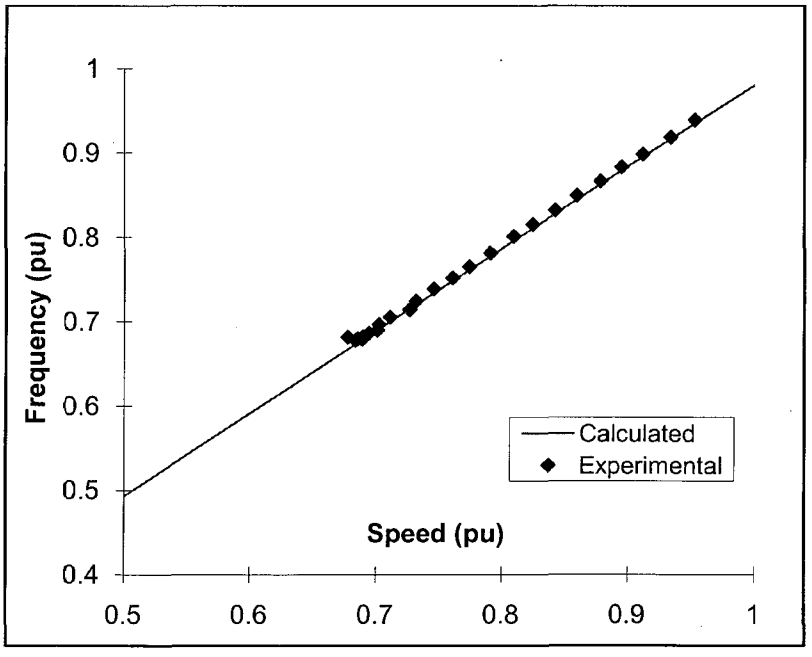

Fig. 2.6. Variation of Frequency with Speed (No load & C=52.8 μF).

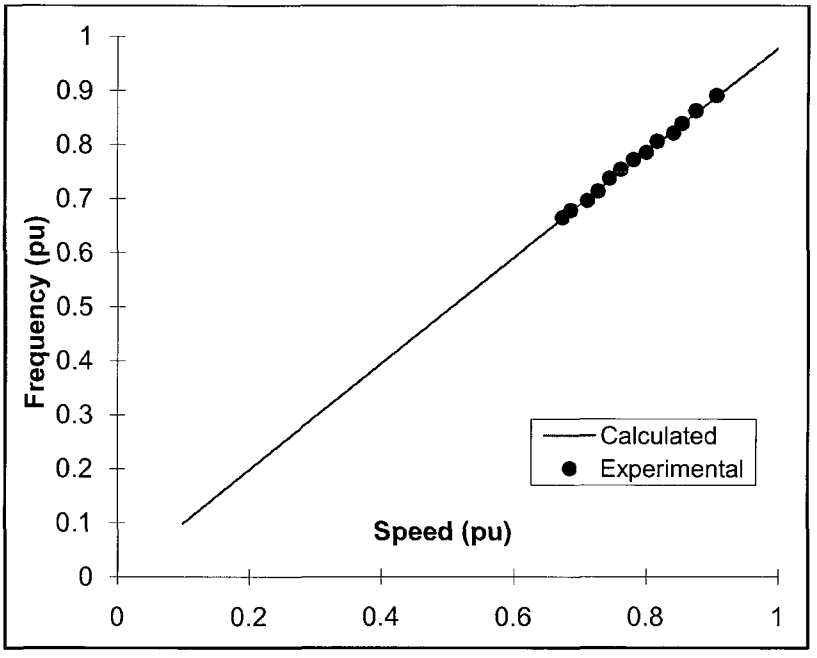

Fig. 2.7. Variation of Frequency with Speed (No load & C=61.6 μF).

Therefore, we can deduce the following inferences

a) Value of minimum capacitance and mutual inductance varies inversely with speed.

b) At any speed below the cut-off speed the machine will not build up terminal voltage

2.3 References

[1] E. D. Besant and F. M. Potter, "Capacitor excitation for induction motors," *AIEE Trans.*, vol. 54, pp. 540–545, May 1935.

[2] C. F. Wanger, "Self-excitation of induction motors," *AIEE Trans.*, vol.58, pp. 47–51, 1939.

[3] J. E. Barkle and R.W. Ferguson, "Induction generator theory and application," *AIEE Trans.*, pt. III A, vol. 73, pp. 12–19, Feb. 1954.

[4] B. C. Doxy, "Theory and application of the capacitor-excited induction generator," *The Eng.*, vol. 216, pp. 893–897, 1963.

[5] D. W. Novotony, D. J. Gritter, and G. H. Studtmann, "Self-excitation in inverter driven induction machines," *IEEE Trans. Power App.Syst.*, vol. PAS-96, no. 4, pp. 1117–1125, Apr. 1977.

[6] J. M. Elder, J. T. Boys, and J. L. Woodward, "The process of self excitation in induction generators," *Proc. Inst. Elect. Eng. B*, vol. 1 30, no. 2, pp. 103–108, Mar. 1983.

[7] J. L. Bhattacharya and J. L. Woodward, "Excitation balancing of self-excited induction generator for maximum output," *Proc. Inst. Elect. Eng.C*, vol. 135, no. 2, pp. 88–97, Mar. 1988.

[8] E. Levy and Y. W. Liao, "An experimental investigation of self-excitation in capacitor excited induction generators," *Elect. Power Syst. Res.*,vol. 53, pp. 59–65, 2000.

[9] D. Levy, "Stand alone induction generators," *Elect. Power Syst. Res.*,vol. 41, pp. 191–201, 1997.

[10] I. J. Nagrath and D. P. Kothari, *Electrical Machines*, 2nd ed. New York: Tata McGraw-Hill, 1997.

CHAPTER 3

INDUCTION GENERATOR MODELING

3.1 General Background

The main aspect which distinguishes the induction machine from other types of electric machines is that the secondary currents are created solely by induction, as in a transformer, instead of being supplied by a DC exciter or other external power source, through slip rings or a commutator, as in synchronous and DC machines. Depending on the condition of operation, the induction machine can be used as a motor or generator. The steady state model of an SEIG is developed as per-phase equivalent circuit. In this circuit the slip and angular frequency are expressed in per unit quantities. When the stator is excited from a balanced three-phase supply, the three phases together create a constant magnitude, synchronously revolving mmf or field in the air gap with a crest value 3/2 times the peak value of the alternating field due to one phase alone [1].

This field rotates around the air-gap at synchronous speed N_s which can be calculated as

$$N_s = \frac{120f}{p} \tag{3.1}$$

Where,

f is the frequency of the source

p is the number of poles

N_s is the synchronous speed

The slip of a motor, s, which is defined as the slip of the rotor with respect to the stator magnetic field, can be given as

$$s = \frac{N_s - N_r}{N_s}, \tag{3.2}$$

Where N_r is the rotational speed of the rotor

Now, if the speeds are expressed in radians per second the slip is given by

$$s = \frac{\omega_b - \omega_r}{\omega_b} \tag{3.3}$$

Where,

ω_b is the synchronous speed in radians per second

ω_r is the speed of the rotor.

The relative speed between the synchronous speed and the rotor speed is expressed in its equivalent electrical speed where the electrical rotor speed is the product of the mechanical speed and the number of pole pairs. Rotation of the rotor changes the relationships between stator and rotor emfs. However, it does not directly change the inductance and resistance parameters. The angular frequency of the induced current in the rotor is $s\omega_b$ and the induced voltage in the rotor will be sE_r, where E_r is the induced voltage in the rotor when the rotor is stationary.

3.2 Conventional Induction Machine Model

Earlier authors [2]-[7] have used the nodal admittance or the loop impedance method to analyze the machine performance. In nodal admittance method, the overall admittance of the induction generator with respect to a single node is taken as zero. For loop analysis technique, the total loop impedance including the capacitance is taken as zero.

3.2.1 Nodal Admittance

The nodal admittance method is used to determine the value of minimum capacitance and frequency. Based on the steady-state equivalent circuit model, and considering the circuit conductance a higher order polynomial in the per-unit frequency is obtained.

The sum of the currents at node 'a' is

$$I_a + I_b + I_c = 0 \tag{3.4}$$

We can rewrite this equation as

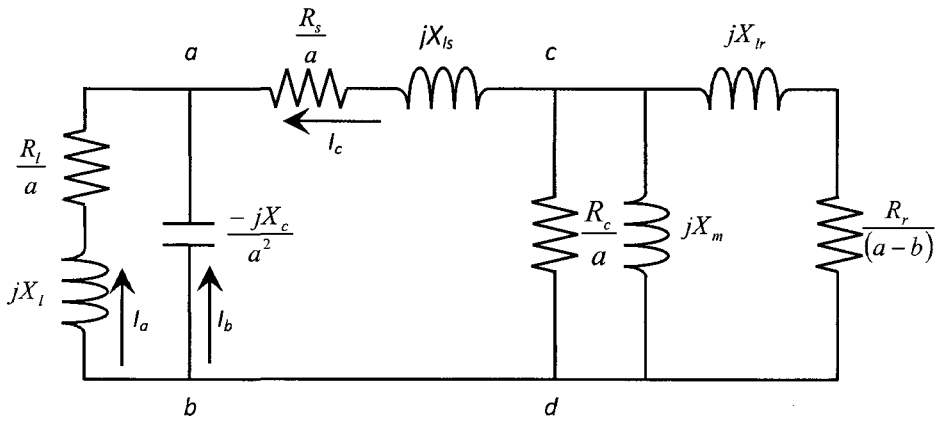

Fig. 3.1. Per phase model of an induction machine for nodal analysis.

$$V_1(Y_t) = 0 \tag{3.5}$$

Where V_1 is the node voltage at 'a' and

$$Y_t = Y_l + Y_c + Y_{ad} \tag{3.6}$$

The admittance between point c and d can be written as

$$Y_{cd} = \frac{a}{R_c} + \frac{1}{jX_m} + \frac{1}{\frac{R_r}{(a-b)} + jX_{lr}} \tag{3.7}$$

$$Z_{cd} = \frac{1}{Y_{cd}} = R_{cd} + jX_{cd} \tag{3.8}$$

$$Y_l = \frac{aR_l}{(R_l^2 + a^2 X_l^2)} - \frac{ja^2 X_l^2}{(R_l^2 + a^2 X_l^2)} \tag{3.9}$$

$$Y_c = \left[-\frac{jX_c}{a^2}\right]^{-1} \tag{3.10}$$

$$Y_{ad} = \left[\left(\frac{R_s}{a^2} + jX_{ls}\right) + (R_{cd} + jX_{cd})\right]^{-1} \tag{3.11}$$

Replacing the equivalent impedance between c and d by $R_{cd} + jX_{cd}$.

Now, since at steady state condition $V_1 \neq 0$, then

$$Y_t = Y_l + Y_c + Y_{ad} = 0 \tag{3.12}$$

$$Y_t = \frac{1}{R} - \frac{1}{jX} = 0 \tag{3.13}$$

Therefore,

Real(Y_t) = 0

and Imag(Y_t) =0

Equating real and imaginary terms separately to zero, we get

$$\frac{a^2}{X_c} - \frac{a^2 X_l}{R_l^{\,2} + a^2 X_l^{\,2}} - \frac{X_{ad}}{R_{ad}^{\,2} + X_{ad}^{\,2}} = 0 \tag{3.14}$$

and

$$\frac{aR_l}{R_l^{\,2} + a^2 X_l^{\,2}} + \frac{R_{ad}}{R_{ad}^{\,2} + X_{ad}^{\,2}} = 0 \tag{3.15}$$

This polynomial can now be solved for finding the roots.

3.2.2 Loop Impedance

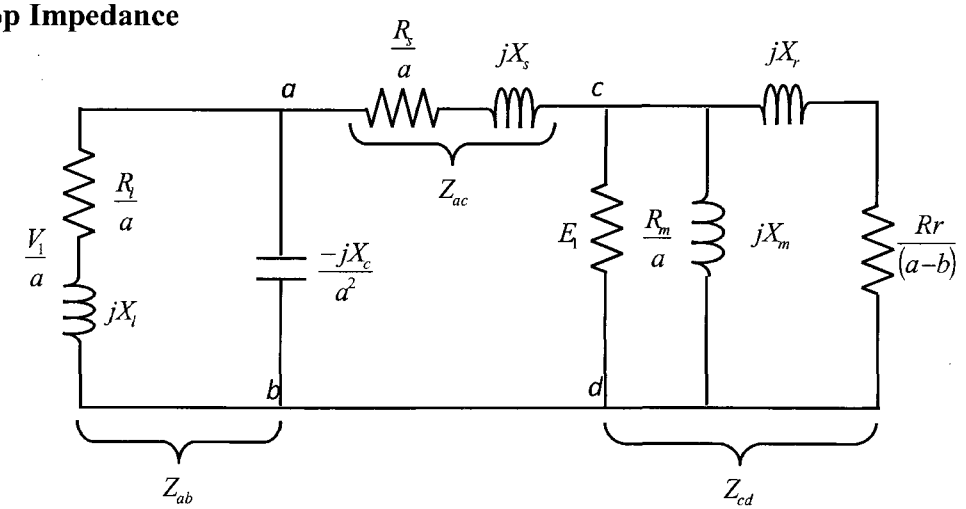

Fig. 3.2. Per phase model of an induction machine for loop analysis.

The loop equation in Fig. 3.2 may be written as

$$I_s Z_t = 0 \tag{3.16}$$

where I_s is the loop current in the loop 'abcd' and

$$Z_t = Z_{ab} + Z_{ac} + Z_{cd} \quad \text{is the total loop impedance.} \tag{3.17}$$

$$\frac{1}{Z_{ab}} = \frac{1}{\frac{R_l}{a} + jX_l} - j\frac{a^2}{X_c} \tag{3.18}$$

$$Z_{ac} = \frac{R_s}{a} + jX_{ls} \tag{3.19}$$

$$\frac{1}{Z_{cd}} = \frac{a}{R_c} + \frac{1}{jX_m} + \frac{1}{\frac{R_r}{(a-b)} + jX_{lr}} \tag{3.20}$$

Since in steady state conditions $I_s \neq 0$, then $Z_t = 0$, therefore

Real $(Z_t) = 0$ and Imag $(Z_t) = 0$.

By equating real and imaginary components, two non-linear equations can be formed. These can be solved simultaneously for finding out the unknown values.

3.3 Induction Machine Thermal Model and Dynamic Model

Using the d-q representation, the induction machine can be modeled as shown in Fig. 3.3. This representation is a general model based on the assumption that the supply voltage can be applied to both the stator and/or rotor terminals. In squirrel cage induction machines voltage is supplied only to the stator terminals. In general power can be supplied to the induction machine (induction motor) or power can be extracted from the induction machine (induction generator). It all depends on the precise operation of the induction machine. If electrical power is applied to the stator of the induction machine then the machine will convert electrical power to mechanical power.

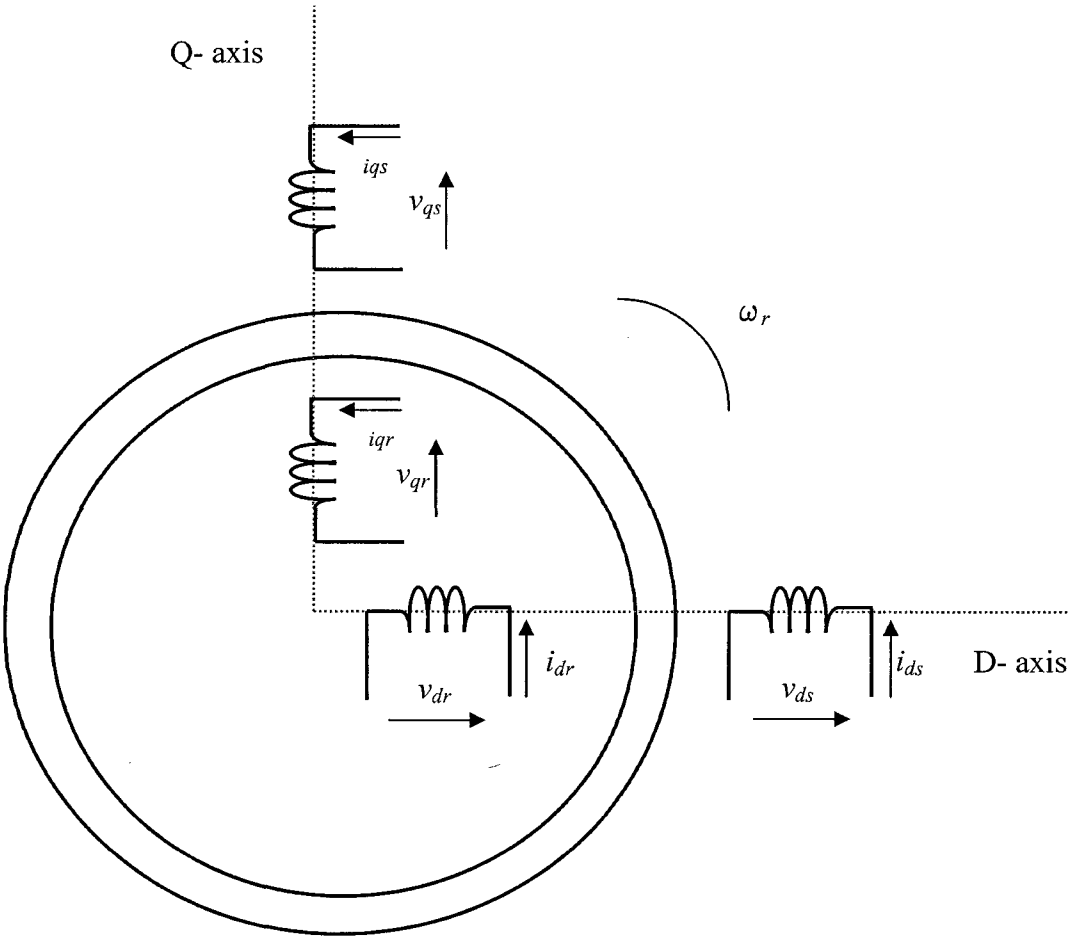

Fig. 3.3. D-Q axis representation of induction machine.

As a result the rotor will start to rotate and the machine is operating as a motor. On the other hand, if mechanical power is applied to the rotor of the induction machine then the machine will convert mechanical power to electrical power. In this case the machine is operating as an induction generator. When the induction machine operating as a generator is connected to the grid or supplying an isolated load, driven by an external prime mover, then the rotor should be driven above synchronous speed. When the machine is operated as a motor, power flows from the stator to the rotor crossing the air gap. However, in the generating mode of operation, power flows from the rotor to the stator.

The conventional model and the d-q axes model are the same for steady state analysis. The advantage of the d-q axes model is that it is powerful for analyzing the transient and steady state conditions, giving the complete solution of any dynamics.

Fig. 3.4 and Fig. 3.5 show the direct and quadrature axes representation of a squirrel-cage induction machine.

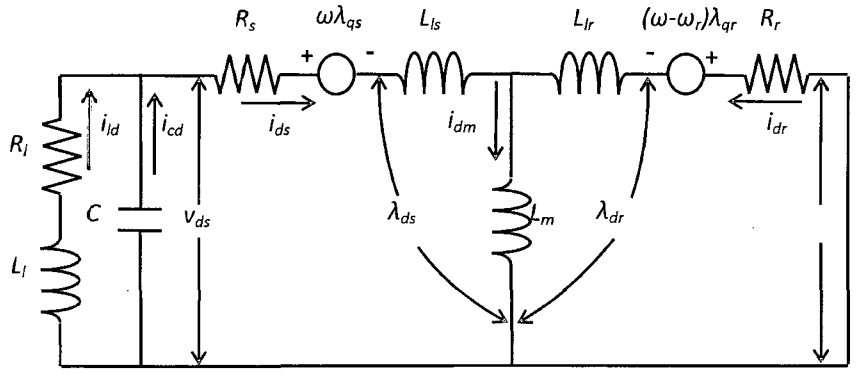

Fig. 3.4. Equivalent circuit of an SEIG in d-axis.

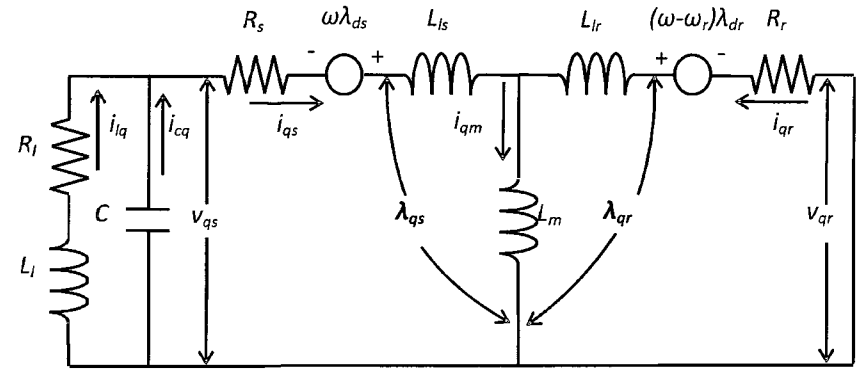

Fig. 3.5. Equivalent circuit of an SEIG in q-axis.

The d-q axis stator and rotor voltages of an induction machine can be expressed in matrix form as

$$\begin{bmatrix} v_{qs} \\ v_{ds} \\ v_{qr} \\ v_{dr} \end{bmatrix} = \begin{bmatrix} R_s + pL_s & \omega L_s & pL_m & \omega L_m \\ -\omega L_s & R_s + pL_s & -\omega L_m & pL_m \\ pL_m & (\omega-\omega_r)L_m & R_r + pL_r & (\omega-\omega_r)L_r \\ -(\omega-\omega_r)L_m & pL_m & -(\omega-\omega_r)L_r & R_r + pL_r \end{bmatrix} \cdot \begin{bmatrix} i_{qs} \\ i_{ds} \\ i_{qr} \\ i_{dr} \end{bmatrix} \tag{3.21}$$

Where,

R_s stator winding resistance, Ω.

R_r rotor winding resistance, Ω.

L_m magnetizing inductance, H.

L_s stator leakage inductance, H.

L_r rotor leakage inductance, H.

ω_r electrical rotor angular speed in rad/sec.

p d/dt (differential operator)

Equation can be written in a first order differential equation form in an arbitrary rotating reference frame

$$\begin{aligned} L_s &= L_{ls} + L_m \\ L_r &= L_{lr} + L_m \end{aligned} \tag{3.22}$$

These four first order differential equations are solved with the well known fourth order Runge-Kutta method to obtain the d- and q- axis leakage fluxes. These fluxes are related to the machine currents by the following equations

$$\begin{aligned} \lambda_{qs} &= L_s i_{qs} + L_m i_{qr} \\ \lambda_{ds} &= L_s i_{ds} + L_m i_{dr} \\ \lambda_{qr} &= L_r i_{qr} + L_m i_{qs} \\ \lambda_{dr} &= L_r i_{dr} + L_m i_{ds} \end{aligned} \tag{3.23}$$

Equation may be written as

$$[v_{dq}] = [RL_{dq}]\,[i_{dq}] + [L_{dq}]\,p[i_{dq}] \tag{3.24}$$

where

$$[v_{dq}] = [v_{qs}\ v_{ds}\ v_{qr}\ v_{dr}]^T \tag{3.25}$$

$$[i_{dq}] = [i_{qs}\ i_{ds}\ i_{qr}\ i_{dr}]^T \tag{3.26}$$

$$[RL_{dq}]=\begin{bmatrix} R_s & \omega(L_m+L_{ls}) & 0 & \omega L_m \\ -\omega(L_m+L_{ls}) & R_s & -\omega L_m & 0 \\ 0 & (\omega-\omega_r)L_m & R_r & (\omega-\omega_r)(L_m+L_{lr}) \\ -(\omega-\omega_r)L_m & 0 & -(\omega-\omega_r)(L_m+L_{lr}) & R_r \end{bmatrix} \tag{3.27}$$

$$[L_{dq}]=\begin{bmatrix} L_m+L_{ls} & 0 & L_m & 0 \\ 0 & L_m+L_{ls} & 0 & L_m \\ L_m & 0 & L_m+L_{lr} & 0 \\ 0 & L_m & 0 & L_m+L_{lr} \end{bmatrix} \tag{3.28}$$

Rearranging

$$p[i_{dq}] = [L_{dq}]^{-1}\,[v_{dq}] - [L_{dq}]^{-1}\,[RL_{dq}]\,[i_{dq}] \tag{3.29}$$

Since the rotor is squirrel-cage one, v_{qr} and v_{dr} are both equal to zero.

The differential equations representing the capacitor circuit is given by

$$\begin{bmatrix} i_{cq} \\ i_{cd} \end{bmatrix} = C\begin{bmatrix} p & \omega \\ -\omega & p \end{bmatrix}\cdot\begin{bmatrix} v_{qs} \\ v_{ds} \end{bmatrix} \tag{3.30}$$

where the voltage across the capacitor is v_{qs} and v_{ds} and the currents are i_{cq} and i_{cd} respectively. Equation can be re-arranged to give

$$p\begin{bmatrix} v_{qs} \\ v_{ds} \end{bmatrix}=\begin{bmatrix} 1/C & 0 \\ 0 & 1/C \end{bmatrix}\begin{bmatrix} i_{qs} \\ i_{ds} \end{bmatrix}+\begin{bmatrix} 0 & -\omega \\ \omega & 0 \end{bmatrix}\begin{bmatrix} v_{qs} \\ v_{ds} \end{bmatrix} \tag{3.31}$$

For open circuit conditions, (3.29) and (3.31) form the set of differential equations to represent the system.

For a resistive load connected across the terminals of the SEIG and noting that

$$i_{qs} = i_{cq} + i_{lq} \tag{3.32}$$

and

$$i_{ds} = i_{cd} + i_{ld} \tag{3.33}$$

the load currents may be expressed as

$$R_l \begin{bmatrix} i_{lq} \\ i_{ld} \end{bmatrix} = \begin{bmatrix} v_{qs} \\ v_{ds} \end{bmatrix} \tag{3.34}$$

In order to take the *RL* load impedance into account

$$\begin{bmatrix} v_{qs} \\ v_{ds} \end{bmatrix} = (R_l + pL_l) \begin{bmatrix} i_{lq} \\ i_{ld} \end{bmatrix} \tag{3.35}$$

or

$$p \begin{bmatrix} i_{lq} \\ i_{ld} \end{bmatrix} = L_l^{-1} \begin{bmatrix} v_{qs} \\ v_{ds} \end{bmatrix} - L_l^{-1} R \begin{bmatrix} i_{lq} \\ i_{ld} \end{bmatrix} \tag{3.36}$$

Effective supervisory systems have two positive effects: the lifetime of the machine can be prolonged and the operating range of the machine and of the following process can be expanded. Still, a critical variable for induction machines, in particular for those of high power, is the rotor temperature. The increasing demands on the reliability of motors, especially during switching operations with frequent reversing starts or run ups in automatic processes, require exact investigation of the thermal behaviour of a motor during transient conditions [8]-[11].

Now, from the previous equations we know that

$$\begin{bmatrix} v_{qs} \\ v_{ds} \\ v_{qr} \\ v_{dr} \end{bmatrix} = \begin{bmatrix} R_s + pL_s & \omega L_s & pL_m & \omega L_m \\ -\omega L_s & R_s + pL_s & -\omega L_m & pL_m \\ pL_m & (\omega - \omega_r)L_m & R_r + pL_r & (\omega - \omega_r)L_r \\ -(\omega - \omega_r)L_m & pL_m & -(\omega - \omega_r)L_r & R_r + pL_r \end{bmatrix} \cdot \begin{bmatrix} i_{qs} \\ i_{ds} \\ i_{qr} \\ i_{dr} \end{bmatrix}$$

and also that

$$\begin{bmatrix} i_{cq} \\ i_{cd} \end{bmatrix} = C \begin{bmatrix} p & \omega \\ -\omega & p \end{bmatrix} \cdot \begin{bmatrix} v_{qs} \\ v_{ds} \end{bmatrix}$$

and

$$\begin{bmatrix} i_{lq} \\ i_{ld} \end{bmatrix} = \begin{bmatrix} v_{qs} \\ v_{ds} \end{bmatrix} \left(R_l + pL_l\right)^{-1}$$

Therefore, substituting the following four equations

$$R_1 = \alpha_1 R_{10} + \beta_1 \tag{3.37}$$

$$R_2 = \alpha_2 R_{20} + \beta_2 \tag{3.38}$$

$$X_{ls} = \alpha_3 X_{ls0} + \beta_3 \tag{3.39}$$

$$X_{lr} = \alpha_4 X_{lr0} + \beta_4 \tag{3.40}$$

Where, R_1, R_{10}, R_2 *and* R_{20} are the initial and final values of the rotor and stator resistance.

α and β are the temperature co-efficient and the initial value of the temperature respectively.

All the values that are obtained for the parameters are obtained from the experimental data and these values are then used to further calculate the new set of parameters. These parameters then give us a clear indication of the effect of temperature on the machine parameters and subsequently give us an overall improved idea of the performance and behaviour of any particular induction machine. The MATLAB code used for these investigations is given in Appendix A.

3.4 References

[1] P. L. Alger, The nature of induction machines, Gordon and Breach Inc., New York, 1965.

[2] M. B. Brennen and A. Abbondanti, "Static exciters for induction generator," *IEEE Transactions, IA-13*, pp. 422-428, 1977.

[3] N. H. Malik and A. H. Al-Bahrani, "Influence of the terminal capacitor on the performance characteristics of a self excited induction generator," *IEE Proceedings*, Vol. 137, Pt. C, No. 2, pp. 168-173, March 1990.

[4] N.H. Malik and S. E. Haque, "Steady state analysis and performance of an isolated self-excited induction generator," *IEEE Transactions on Energy Conversion*, Vol. EC-1, No. 3, pp. 134-139, 1986.

[5] T. F. Chan, "Analysis of self-excited induction generators using and iterative method," *IEEE Transactions on Energy Conversion*, Vol. 10, No. 3, pp. 502-507, Sep 1995.

[6] R. J. Harrington and F. M. M. Bassiouny, "New approach to determine the critical capacitance for self-excited induction generators," *IEEE Transactions on Energy Conversion*, Vol. 13, No. 3, pp. 244-249, Sep 1998.

[7] A. K. Tandon, S. S. Murthy and G. J. Berg, "Steady-state analysis of capacitor self-excited induction generator," *IEEE Transactions, PAS-103*, pp. 612-618, 1984.

[8] G Pascoli, F Pirker, H Kapeller and C Kral, "Comparison of two rotor temperature estimation models of a surface cooled squirrel cage induction machine," *IEEE International conference on electric machines and drives*, Vol.1, pp. 207-211, May 2005.

[9] M Maximini and H. J. Koglin, "Determination of the absolute rotor temperature of squirrel cage induction machines using measurable variables", *IEEE Transaction on Energy Conversion*, Vol. 19, No.10, March 2004.

[10] A.Boglietti, A. Cavagnino, L. Ferraris and M.Lazzari, "Energetic Considerations about the Use of Cast Copper Squirrel Cage Induction Motors," in *Proc. 33rd Annual Conference of the IEEE Industrial Electronics Society*, pp. 157-162, Taipei, 2007.

[11] M.S. Rajagopal and K.N. Seetharamu, "Transient thermal analysis of induction motors", *IEEE Transaction on Energy Conservation*, Vol 13, No.1, March 1998.

CHAPTER 4

EXPERIMENTAL SET UP OF INDUCTION GENERATOR

4.1 Aluminum- and Copper-Rotor Induction Generator

Most induction motors in the fractional and integral horsepower range of sizes are made with die-cast alum rotor cages. With the present day push for higher efficiency of energy usage, the possibility of improving efficiency in such motors has become enough of a priority to cause renewed interest in the use of copper in the squirrel cage because of its substantially higher electrical conductivity. Induction motors have been made with fabricated copper rotors since there were induction motors. However, the high melting point of copper leads to difficulties in casting. Short die life resulting from high temperature has, in the past, made cast copper rotors uneconomical. Because of higher energy costs and improvements to the metallurgy of casting apparatus, the economics of the situation appear to have changed and a number of manufacturers of induction machines are taking a look at die-cast copper rotors. For a given speed the IM with copper rotor develops higher torque and also efficiency of a Cu-rotor IM is higher than a conventional Al-rotor IM. Copper has higher electrical conductivity and higher thermal capacity per unit volume than aluminum leading to lower copper losses and lower temperature rise. Also, the tensile strength and melting point of copper are more than that of aluminum.

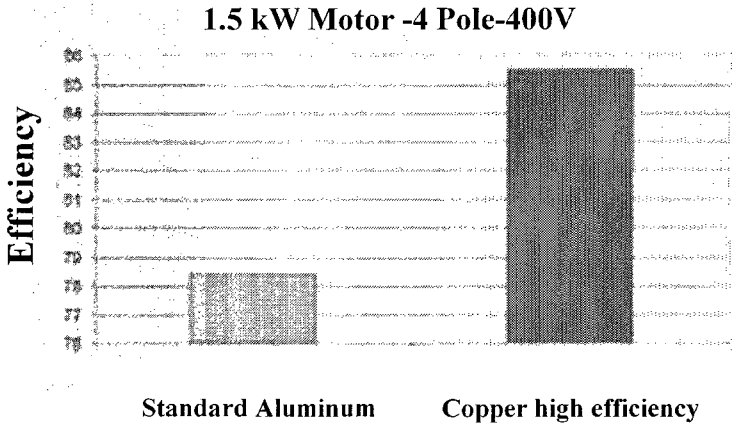

Fig. 4.1. Comparison of efficiency between copper and aluminum.

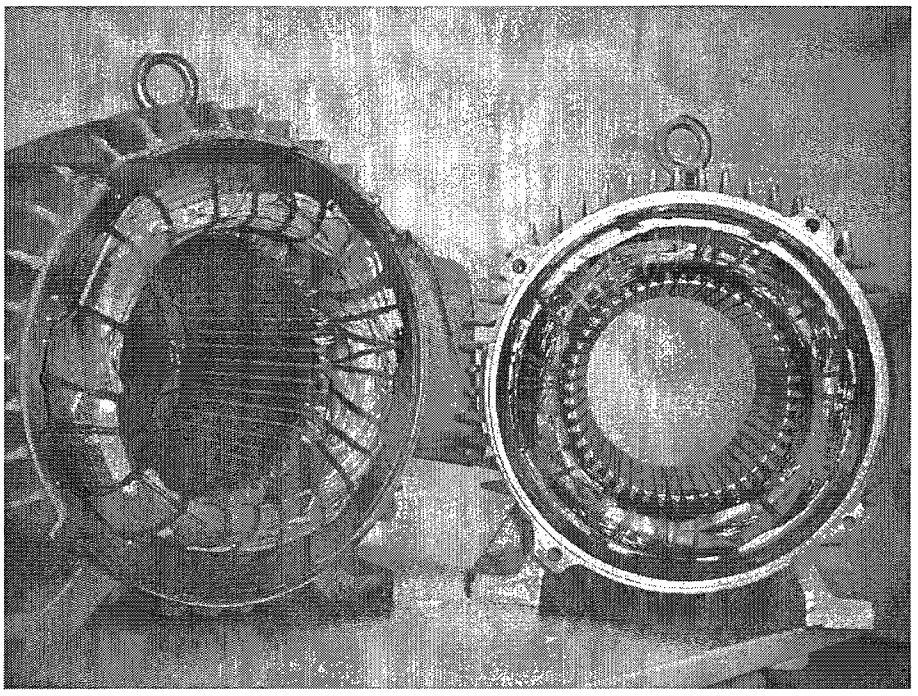

Fig. 4.2 Stators of Al-and Cu-rotor Induction Machine.

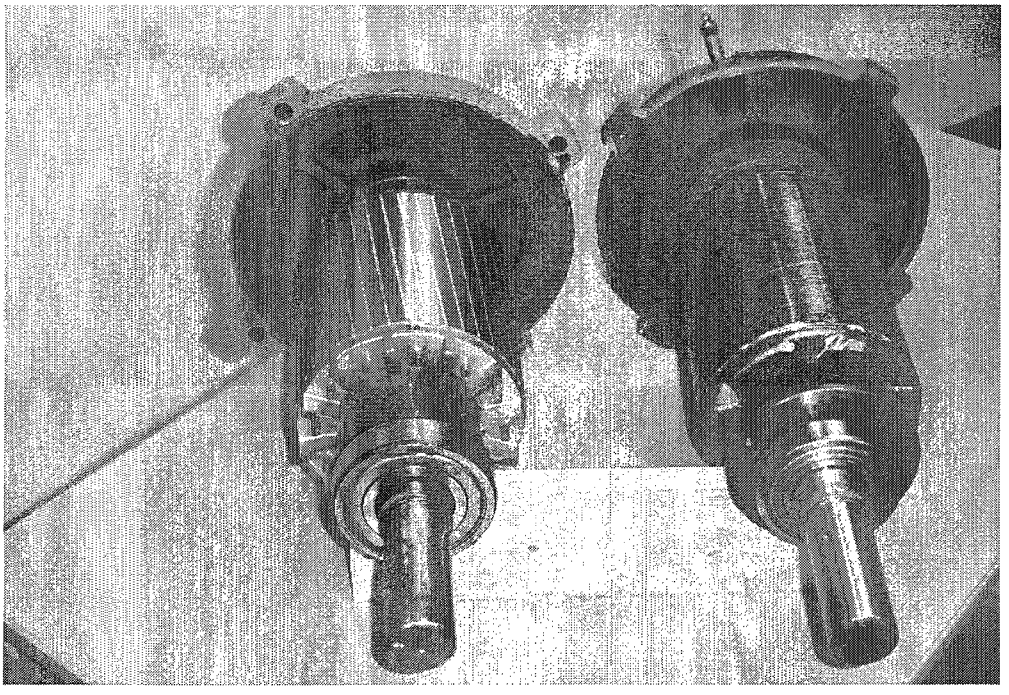

Fig. 4.3 Rotors of Al-and Cu-rotor Induction Machine.

Figs. 4.2 and 4.3 show the stators and rotors of the two machines used in investigation.

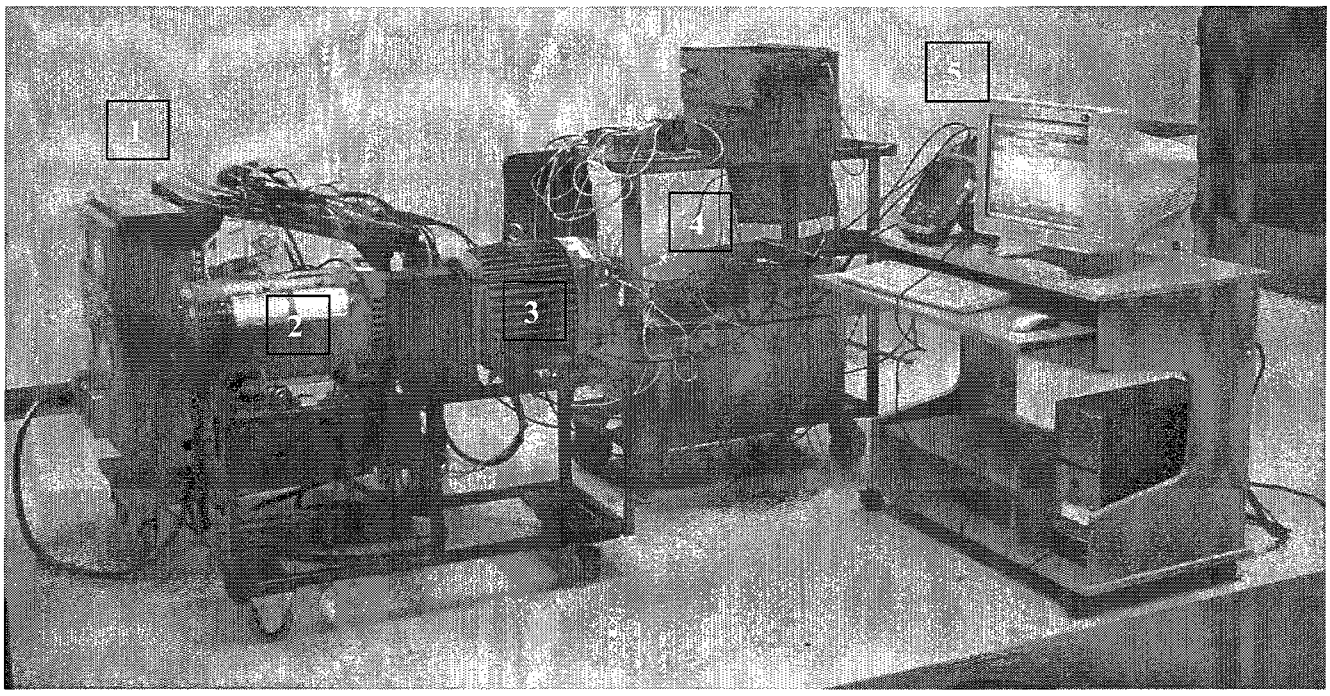

Fig 4.4 Experimental set-up used for the investigations.

Fig. 4.4 shows the experimental set-up in the laboratory which is used for conduction all the experimental investigations. The set-up consists of five different components namely

1) Power Supply
2) DC Motor
3) Induction Motor
4) Capacitor Bank
5) Measurement & Recording Instrument

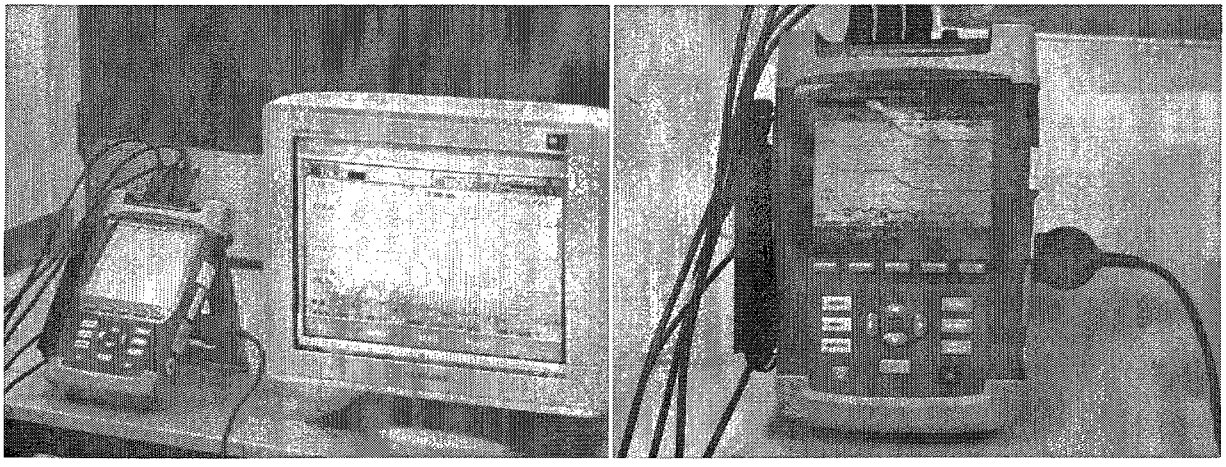

Fig. 4.5 Fluke Power Analyzer connected to the induction generator recording real-time data .

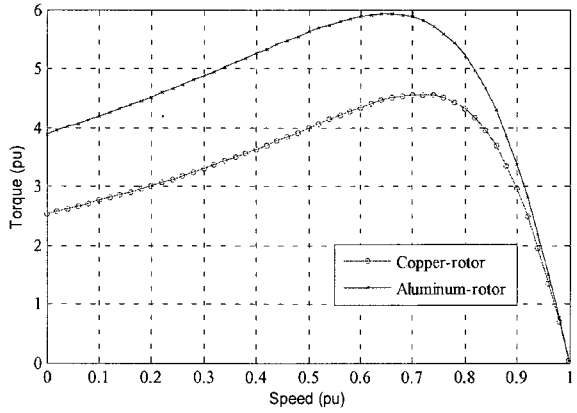

Fig. 4.6. Calculated torque-speed characteristics for the copper- and aluminum-rotor induction machines used in the investigations.

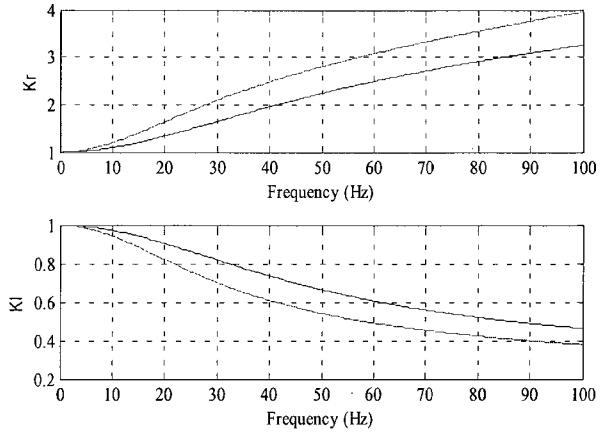

Fig. 4.7. Variation of rotor resistance coefficient and inductance coefficient with stator frequency.

It can be seen from figure 4.6 that the starting and pull-out torques of the copper-rotor machine are relatively lower than the aluminum-rotor machine for rated condition.

4.2 Determination of Machine Parameters

In order to determine the performance of the induction machine precisely, the machine equivalent circuit parameters need to be determined accurately. The tests required to determine the machine parameters are based on the standardized experimental methods. The typical three tests that are conducted to find the machine parameters for an induction machine are:

1) DC Test: The dc resistance test is carried out by passing a dc current through the phase winding of the stator and measuring the voltage drop across it. Several measurements are

made and the dc resistance of the stator winding is taken to be the mean of all the calculated values of resistance.

2) Open Circuit Test: Open-circuit test is conducted by driving the induction machine at its rated synchronous speed using an external prime mover which in this case is a dc motor. The stator terminals are supplied with rated voltage. When the machine is running at synchronous speed, the rotor slip is zero and hence the rotor circuit becomes open.
3) Locked-Rotor Test: The locked-rotor or short-circuit test is conducted by blocking the rotor by some means to prevent it from moving. Since under this condition the slip s is equal to one the equivalent circuit is modified. At standstill condition of the rotor, the rated current is supplied to the stator terminals.

Two 7.5 hp industrial type induction machines one with conventional aluminum-rotor and the other with copper-rotor. Table 4.1 shows the physical features of the two machines. It should be noted that these two machines are manufactured by two different companies. Even though the designs are consistent with NEMA guidelines, there are subtle dissimilarities in many areas. Table 4.2 Equivalent Circuit Parameters of the Machines Used in the Investigations. As can be seen, the aluminum cage rotor is skewed with the fan blades integrally cast on the end rings while the copper cage rotor is plain and without such blades attached to the end rings. The copper-rotor motor has comparatively longer core that lowers flux density while increasing cooling capacity and reducing magnetic and stray losses. Despite such subtle dissimilarities between these machines, a detailed qualitative analysis has been carried out.

Table 4.1 Induction Machine Data.

	Aluminum-rotor	Copper-rotor
Manufacturer	General Electric	Siemens
NEMA Design	B	B
NEMA efficiency	89.5 %	92.4 %
Rated voltage	346 V	460 V
Rated current	12 A	9.5 A
Output power	7.5 hp	7.5 hp
Connections	Wye	Wye
Number of poles	4	4
Rated speed	1755 rpm	1775 rpm
Rated frequency	60 Hz	60 Hz
Weight	75.9 kg	90 kg
Diameter of rotor	134.9 mm	129.9 mm
Length of rotor core	35.7 mm	165.8 mm
Length of stator core	135 mm	166 mm
Inside diameter of stator core	144.96 mm	139.86 mm
Number of stator slots	48	48
Height of rotor bar	25.79 mm	26.6 mm
Width of rotor bar	5.62 mm	5.6 mm
Length of rotor bar	136.8 mm	165.8 mm
Number of conductors	40	40
Conductivity of rotor bar	37.71 μS/mm	59.61 μS/mm

Table 4.2 Equivalent Circuit Parameters of the Machines Used in the Investigations.

	Parameters of Al-rotor IM (pu)	Parameters of Cu-rotor IM (pu)
R_s	0.0232	0.0234
R_r	0.0491	0.0530
X_{ls}	0.0556	0.0745
X_{lr}	0.0834	0.1117
X_m	2.4440	2.4668
R_c	33.915	36.8881
I_{nl}	0.4000	0.3929
$P_{rotation}$	0.029	0.0270
$P_{core(stator)}$	0.026	0.024
$P_{cu(stator)}$	0.0273	0.0245
$P_{cu(rotor)}$	0.0456	0.0414
τ_{st}	3.89	2.53
τ_{max}	5.91	4.55

4.3 Saturation Characteristics

It is well known that saturation takes place in almost all electrical machines and induction machines are no exception. In order to achieve a better representation of the induction machines, saturation should be included in the machine model. The performance of saturated induction machines and the accurate calculation of the stator and rotor parameters depend significantly on the saturation conditions of their main flux and leakage flux paths. It has been found that the inclusion of the saturation effects gives more accurate and realistic results [1]-[5].

Figs. 4.8 and 4.9 show the saturation characteristics and the magnetizing inductances of the two copper-rotor and aluminum-rotor induction machines. The saturation characteristics in Fig 4.8 show that the relationship between the two is non-linear.

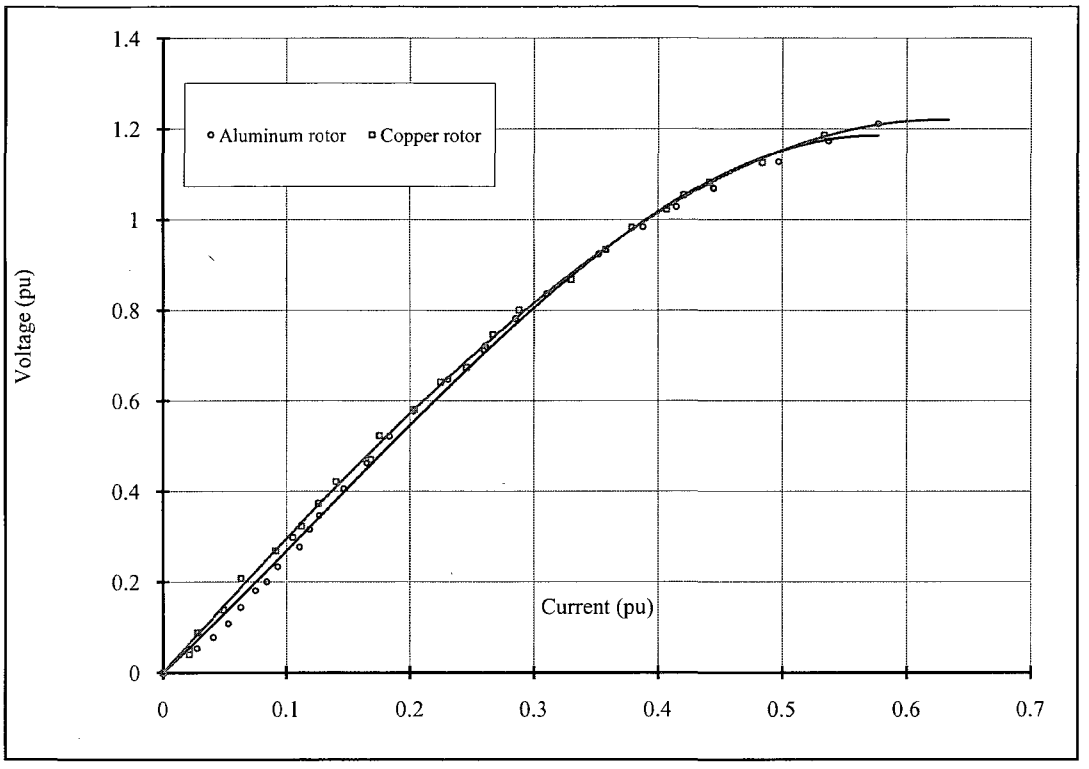

Fig. 4.8. Measured saturation characteristics of the two SEIGs.

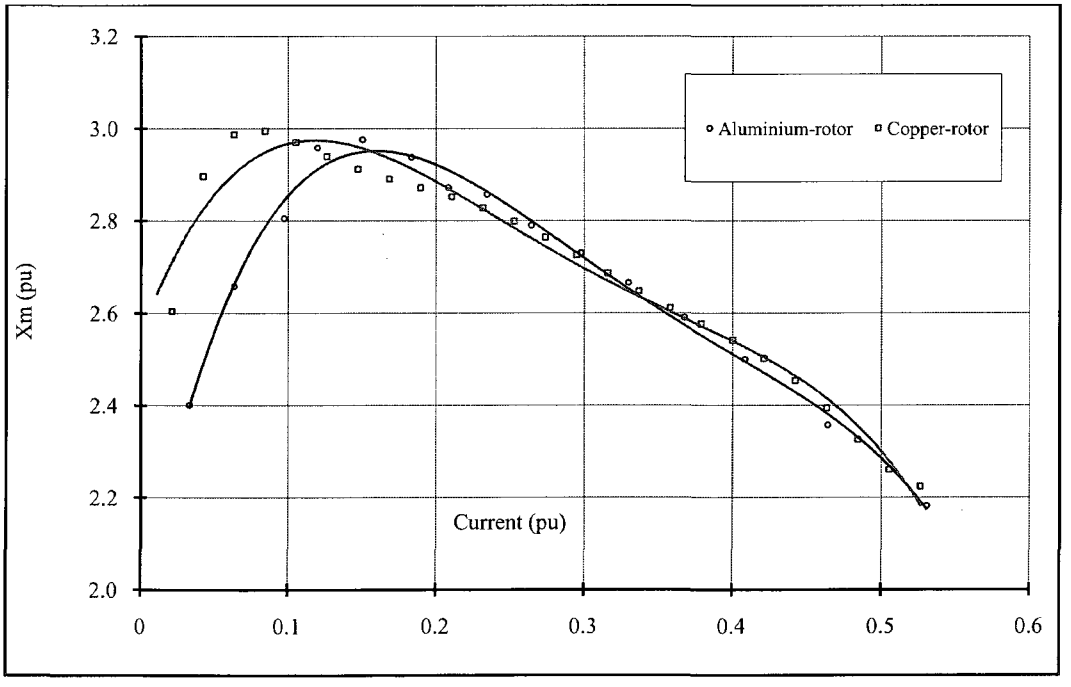

Fig. 4.9. Magnetizing inductances as a function of stator current of the two SEIGs calculated from the measured saturation characteristics.

4.4 References

[1] P. Vas, "Generalized transient analysis of saturated a.c. machines," *Archiv Für Elektrotechnik*, vol. 63, pp. 57-62, 1981.

[2] J. Robert, "On the transient performance of saturated electrical machines with cylindrical rotor," *Proceedings of the International Conference on Electrical Machines*, pp. 469-471, 1986.

[3] J. M. F. de Jesus, "A model for saturation in induction machines," *IEETransactions on Energy Conversion*, vol. 3, pp. 682-688, 1988.

[4] K. E. Hallenius, "On the theory of main flux saturation in smooth-air-gap electrical machines," *Archiv Für Elektrotechnik*, vol. 69, pp. 137-142, 1986.

[5] E. Levi, "A unified approach to main flux saturation modelling in D-Q axis models of induction machines," *IEEE Transactions on Energy Conversion*, vol.10, pp. 455-461, 1995.

CHAPTER 5

RESULTS

5.1 Build-up Time Variation with Temperature

The following Figs 5.1-5.14 show the various build up time at different intervals of temperature for aluminum-rotor and copper-rotor machine. The Value $T_{initial}$ and T_{final} represent the starting temperature and the final temperature. The simulation time in all the simulations conducted varies from 18 to 20 seconds.

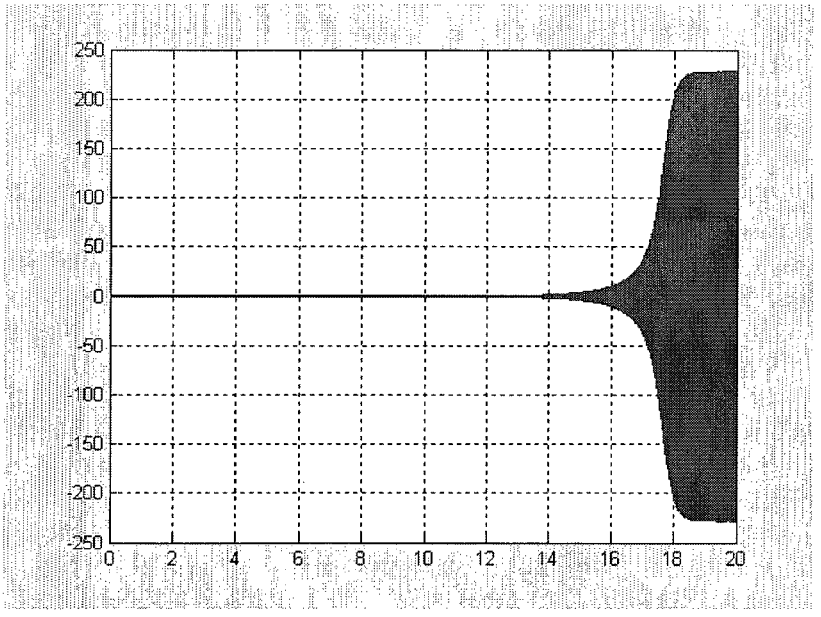

Fig. 5.1. Al-rotor machine; T_{final} = 23 °C.

Fig 5.1 represents the voltage build-up time for the aluminum-rotor induction machine. In this case the starting temperature $T_{initial}$ and the final temperature T_{final} are both equal. For this condition, $T_{initial}$ = 23°C; T_{final} = 23 °C.

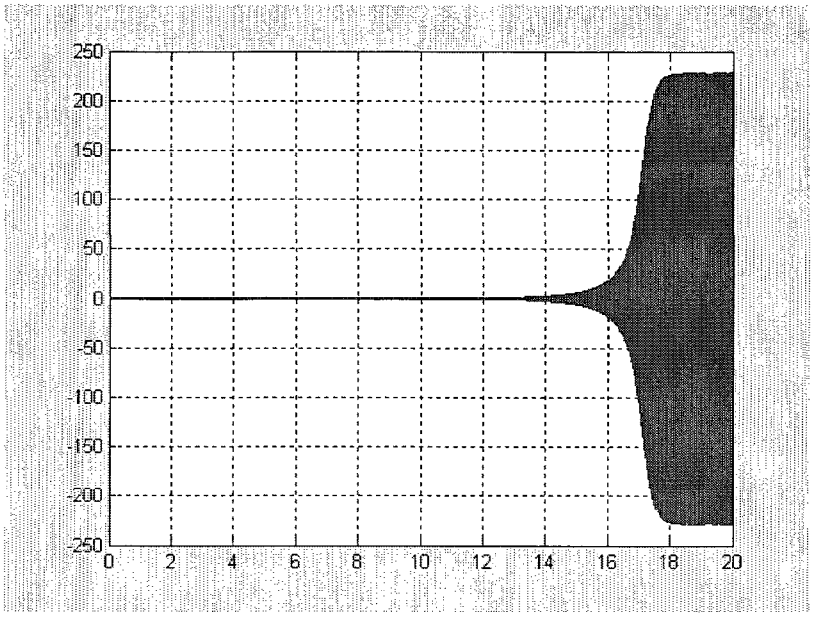

Fig. 5.2. Al-rotor machine; $T_{final} = 30\,^{\circ}C$.

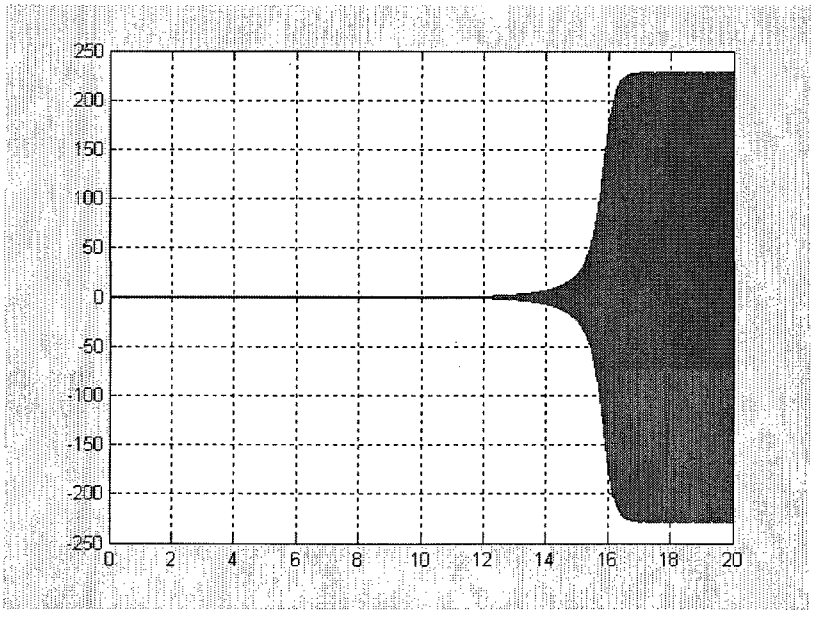

Fig. 5.3. Al-rotor machine; $T_{final} = 50\,^{\circ}C$.

Figs. 5.2 and 5.3 represents the voltage build-up time for the aluminum-rotor induction machine. In this case the starting temperature $T_{initial}$ and the final temperature T_{final} are given as $T_{initial} = 23\,^{\circ}C$; $T_{final} = 30\,^{\circ}C$ for Fig 5.1 and $T_{initial} = 23\,^{\circ}C$; $T_{final} = 50\,^{\circ}C$ for the second Fig.

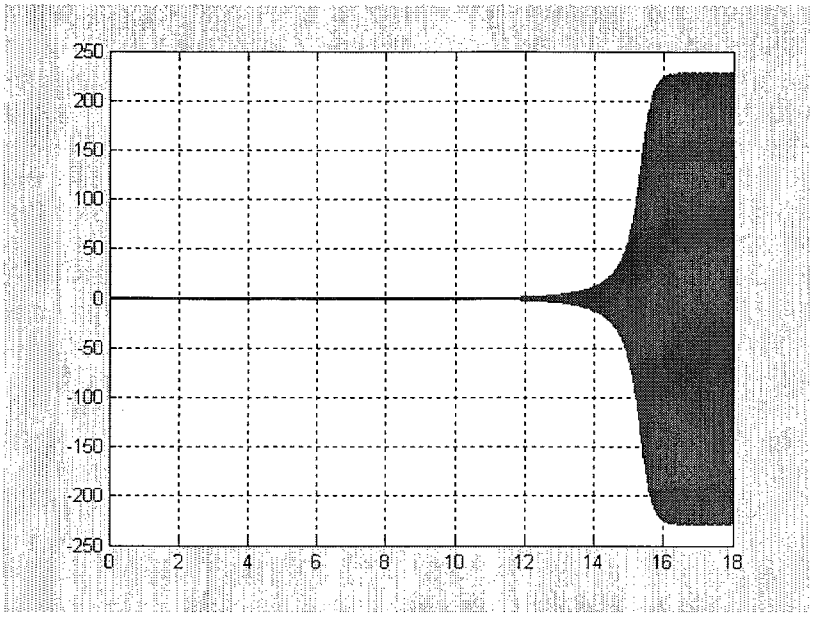

Fig. 5.4. Al-rotor machine; T_{final} = 60 °C.

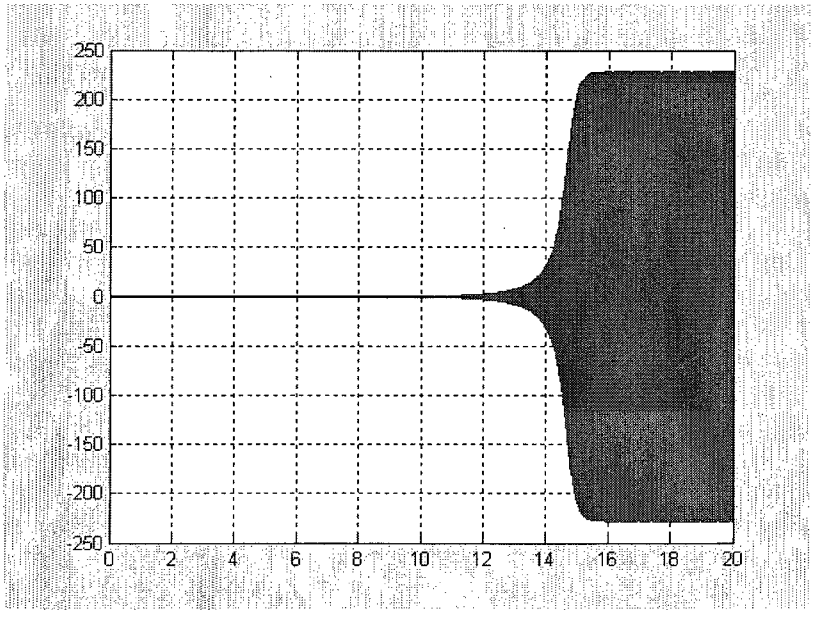

Fig. 5.5. Al-rotor machine; T_{final} = 75 °C.

Figs. 5.4 and 5.5 represents the voltage build-up time for the aluminum-rotor induction machine. In this case the starting temperature $T_{initial}$ and the final temperature T_{final} are given as $T_{initial}$ = 23 °C; T_{final} = 60 °C for Fig 5.4 and $T_{initial}$ = 23 °C; T_{final} = 75 °C for the second case.

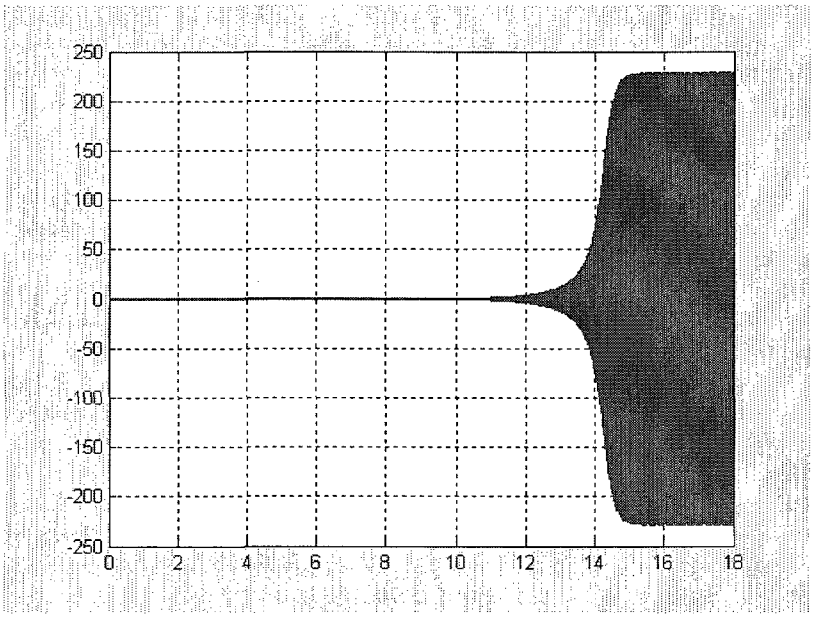

Fig. 5.6. Al-rotor machine; T_{final} = 85 °C.

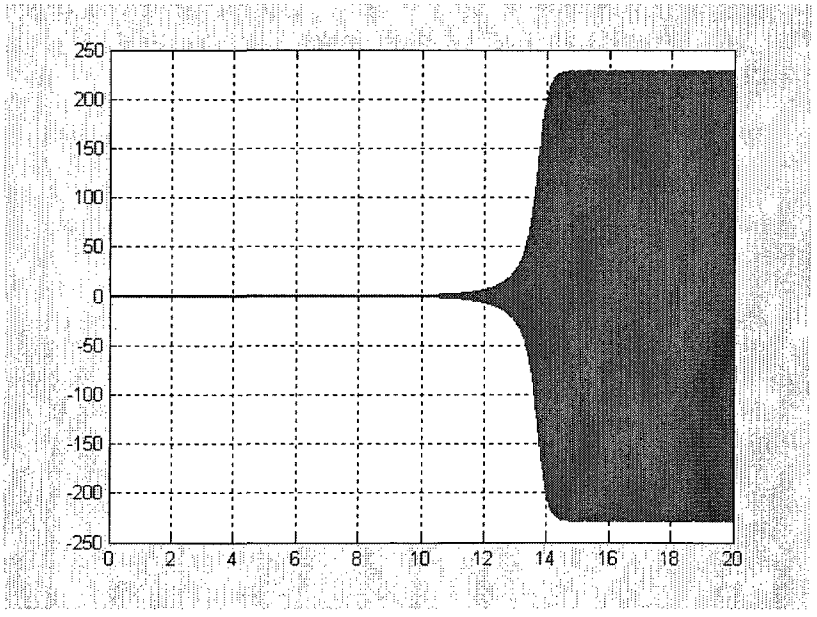

Fig. 5.7. Al-rotor machine; T_{final} = 100 °C.

Figs. 5.6 and 5.7 represents the voltage build-up time for the aluminum-rotor induction machine. In this case the starting temperature $T_{initial}$ and the final temperature T_{final} are given as $T_{initial}$ = 23 °C; T_{final} = 85 °C for Fig 5.6 and $T_{initial}$ = 23 °C; T_{final} = 100 °C for Fig. 5.7.

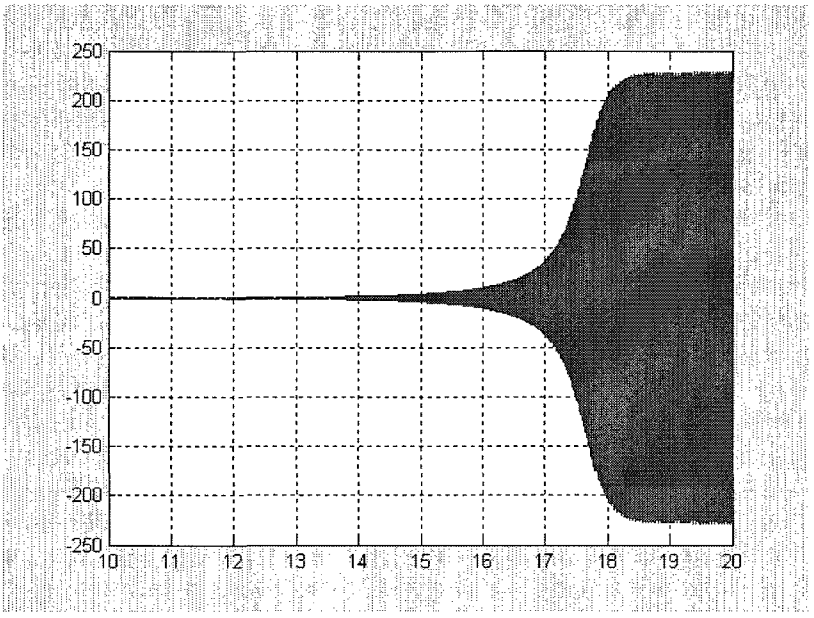

Fig. 5.8. Cu-rotor machine; T_{final} = 23 °C.

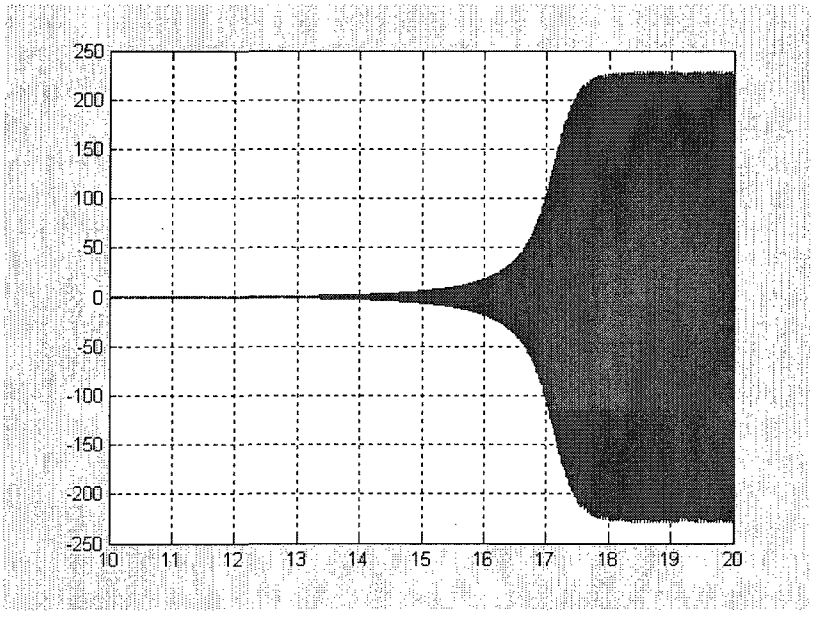

Fig. 5.9. Cu-rotor machine; T_{final} = 30 °C.

Figs. 5.8 and 5.9 represents the voltage build-up time for the copper-rotor induction machine. In this case the starting temperature $T_{initial}$ and the final temperature T_{final} are given as $T_{initial}$ = 23 °C; T_{final} = 23 °C for Fig 5.8 and $T_{initial}$ = 23 °C; T_{final} = 30 °C for Fig. 5.9.

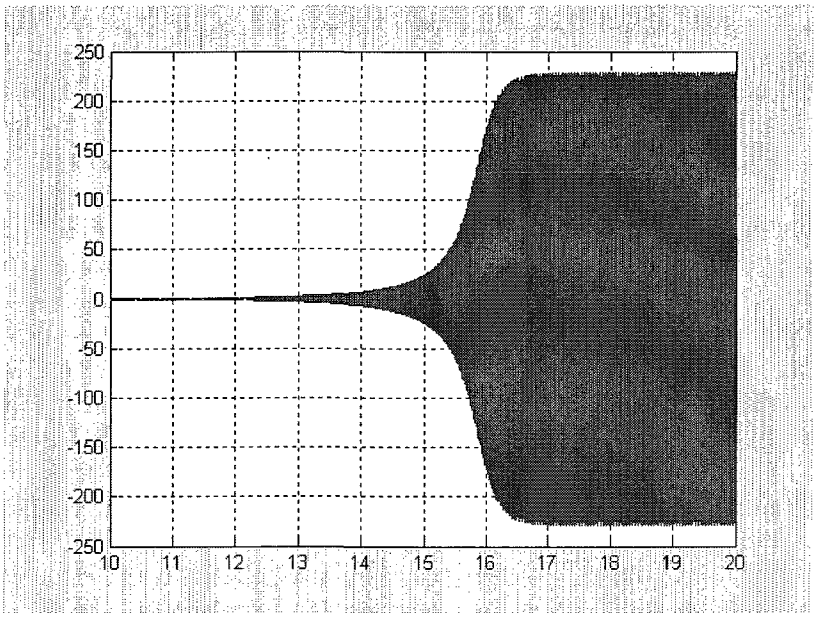

Fig. 5.10. Cu-rotor machine; T_{final} = 50 °C.

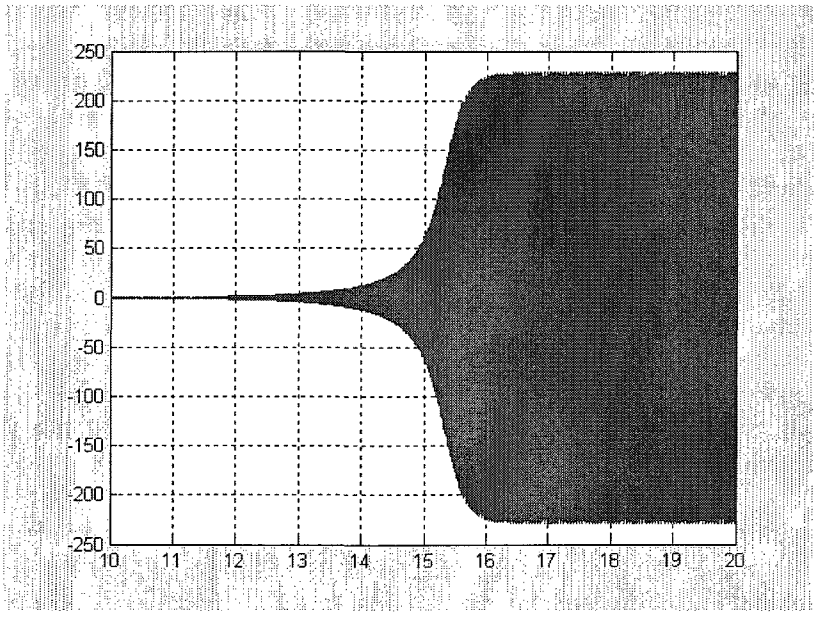

Fig. 5.11. Cu-rotor machine; T_{final} = 60 °C.

Figs. 5.10 and 5.11 represents the voltage build-up time for the copper-rotor induction machine. In this case the starting temperature $T_{initial}$ and the final temperature T_{final} are given as $T_{initial}$ = 23 °C; T_{final} = 50 °C for Fig 5.10 and $T_{initial}$ = 23 °C; T_{final} = 60 °C for Fig. 5.11.

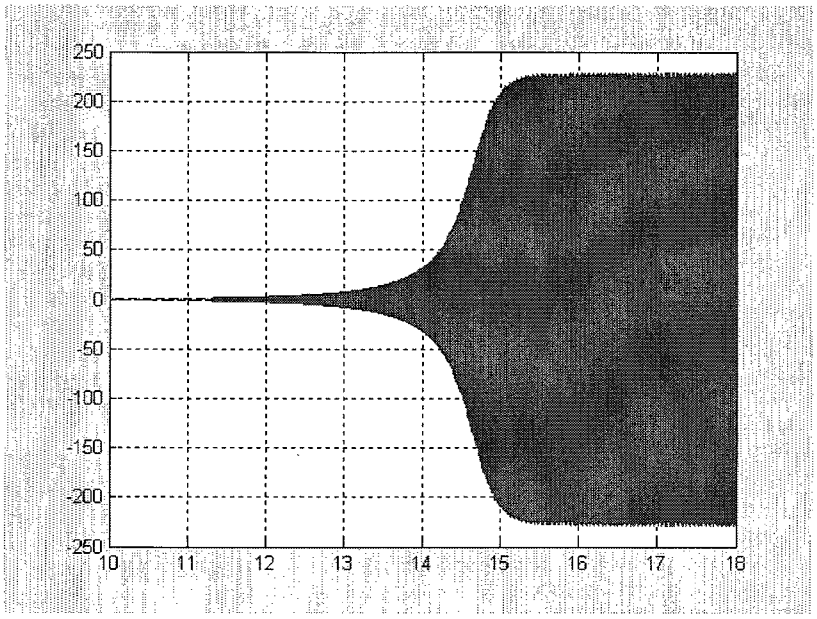

Fig. 5.12. Cu-rotor machine; T_{final} = 75 °C.

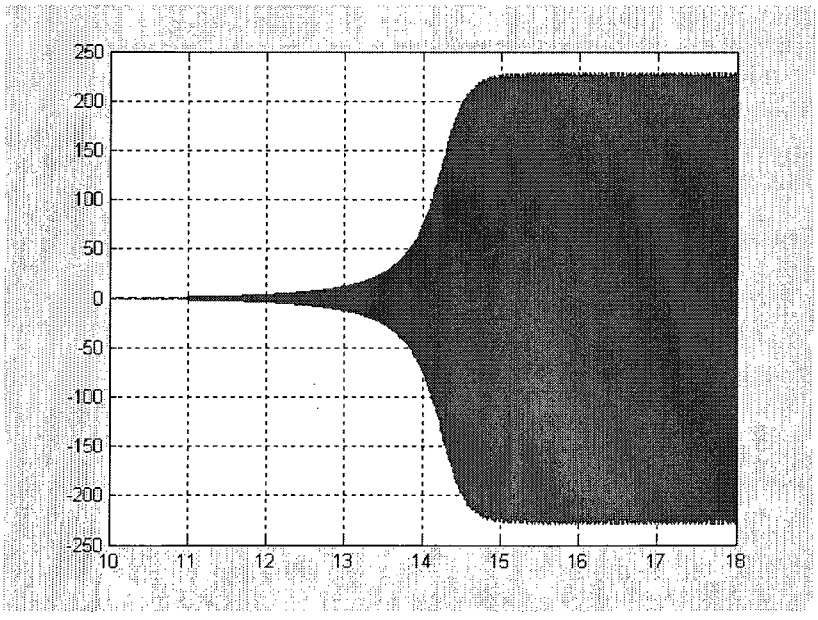

Fig. 5.13. Cu-rotor machine; T_{final} = 85 °C.

Figs. 5.12, 5.13 and 5.14 represents the voltage build-up time for the copper-rotor induction machine. In this case the starting temperature $T_{initial}$ and the final temperature T_{final} are given as $T_{initial}$ = 23 °C; T_{final} = 75 °C for Fig 5.12, $T_{initial}$ = 23 °C; T_{final} = 85 °C for Fig. 5.13. and $T_{initial}$ = 23 °C; T_{final} = 100 °C for Fig 5.14.

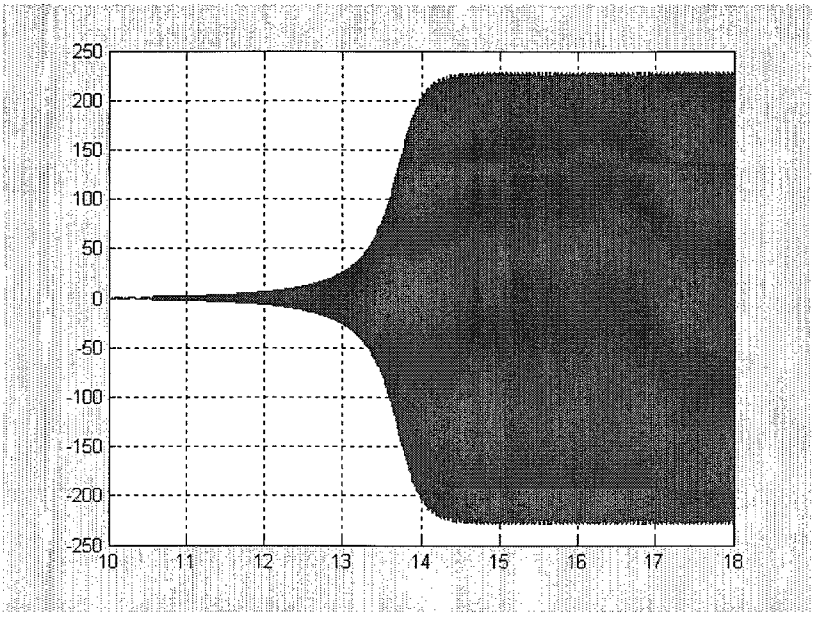

Fig. 5.14. Cu-rotor machine; $T_{final} = 100\,^{\circ}C$.

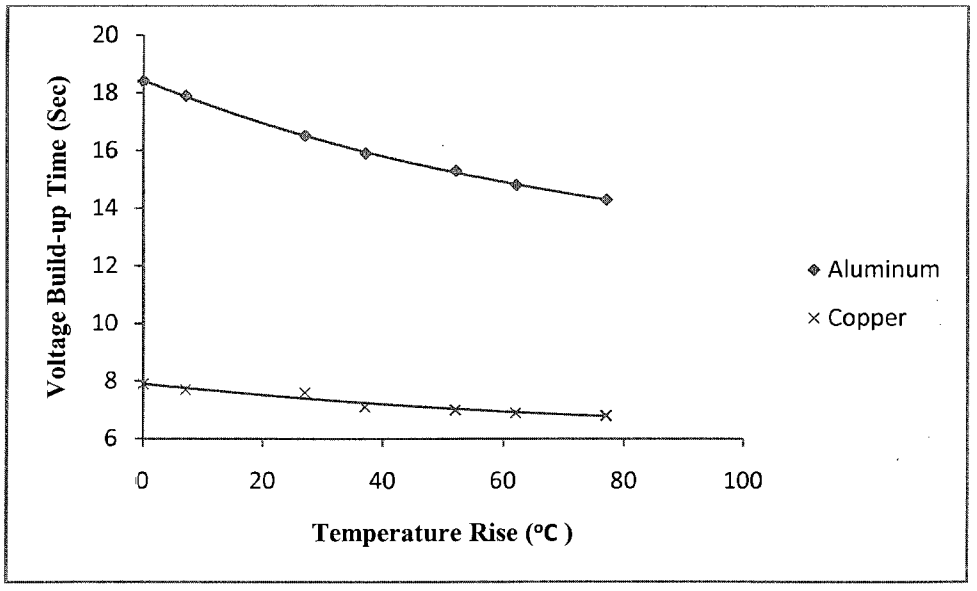

Fig. 5.15. Variation of voltage build-up time with temperature.

Fig 5.15 shows the change in voltage built-up time as a function of temperature, for both aluminum- and copper-rotor induction machines. This graph confirms that gradual change in temperature effects the built-up times in induction machine. In this case, aluminum-rotor induction machine is affected more as compared to the copper-rotor induction machine.

5.2 Machine Parameters with Respect to Temperature

Figs. 5.16-5.18 show the variation of machine parameters with respect to rise in temperature for both aluminum-rotor and copper-rotor machine.

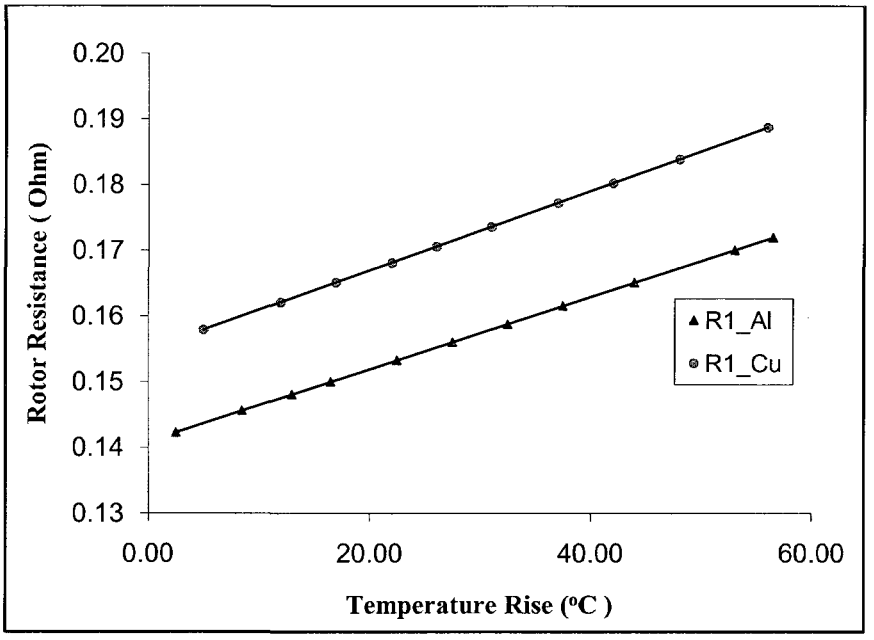

Fig .5.16. Change in rotor resistance R1 for aluminum and copper machine with respect to temperature rise.

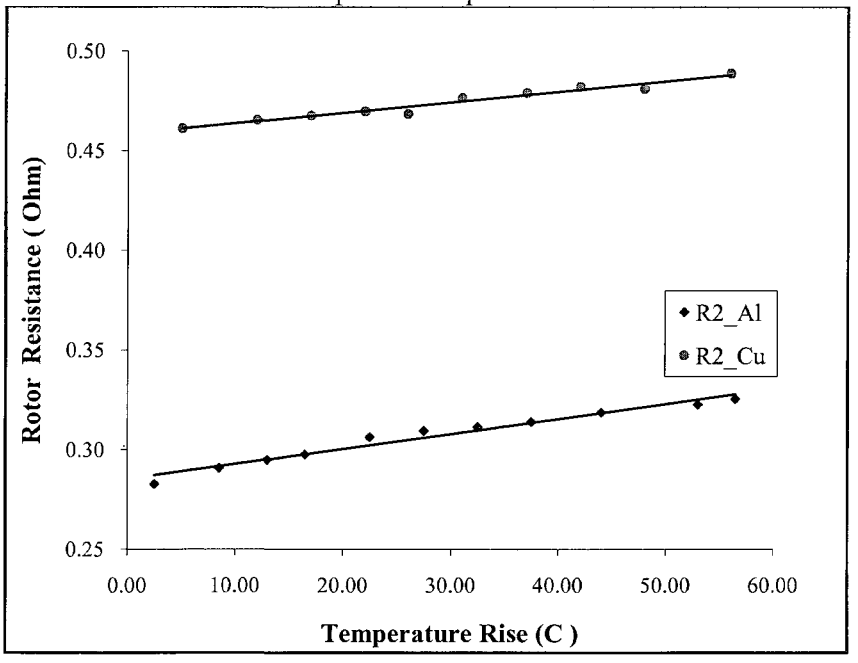

Fig. 5.17. Change in rotor resistance R2 for aluminum and copper machine with respect to temperature rise.

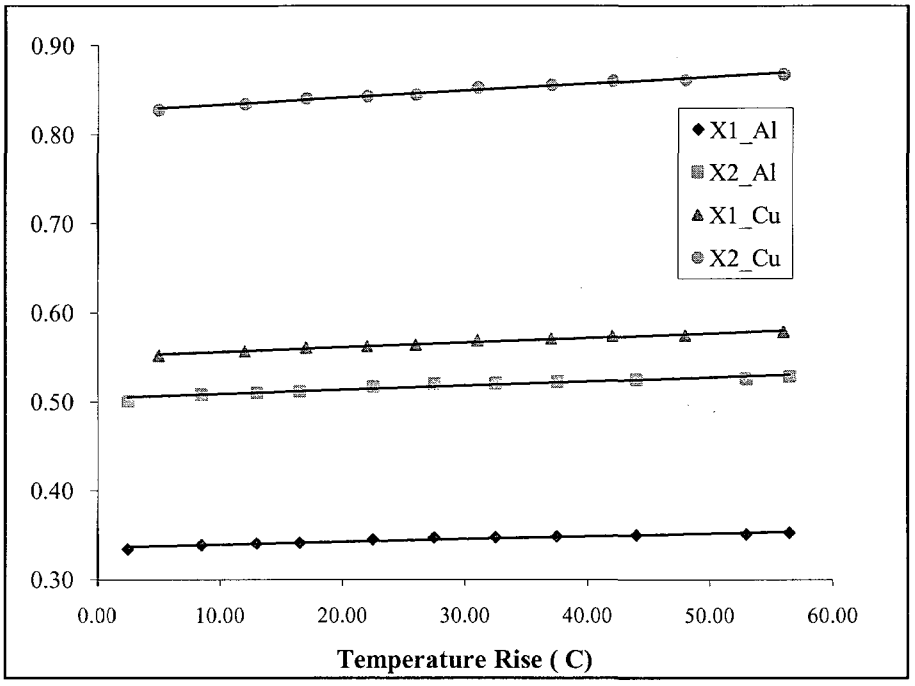

Fig. 5.18. Change in reactances X_1 and X_2, both for aluminum and copper machine with respect to change in temperature.

From the above given figures, it is clearly seen that rise in temperature makes a significant effect on the machine parameters. The change in parameters is more or less equal for both the machines, but the aluminum-rotor induction machine is slightly affected more as compared to the copper one.

The following tables shown in Table 5.1 and 5.2 show the gradual change in the machine parameters with continuous rise in the temperature.

Table 5.1 Change in machine parameters w.r.t. temperature rise for aluminum-rotor induction machine

Temp rise (°C)	R_1(ohm)	R_2(ohm)	X_1(ohm)	X_2(ohm)
2.50	0.1423	0.2825	0.3338	0.5007
8.50	0.1456	0.2907	0.3386	0.5079
13.00	0.1481	0.2949	0.3403	0.5104
16.50	0.1500	0.2976	0.3411	0.5117
22.50	0.1533	0.3062	0.3447	0.5171
27.50	0.1560	0.3094	0.3466	0.5199
32.50	0.1588	0.3114	0.3471	0.5206
37.50	0.1615	0.3139	0.3482	0.5224
44.00	0.1651	0.3186	0.3499	0.5249
53.00	0.1701	0.3226	0.3507	0.5260
56.50	0.1720	0.3254	0.3524	0.5286

Table 5.2 Change in machine parameters w.r.t. temperature rise for copper-rotor induction machine

Temp rise (°C)	R_1(ohm)	R_2(ohm)	X_1(ohm)	X_2(ohm)
5	0.157924	0.461274	0.551596	0.827394
12	0.162152	0.465351	0.556413	0.834619
17	0.165174	0.467792	0.560379	0.840568
22	0.168169	0.469887	0.562005	0.843008
26	0.170611	0.46861	0.563252	0.844878
31	0.173631	0.476664	0.568527	0.852791
37	0.177256	0.479056	0.570453	0.855679
42	0.180277	0.482118	0.573858	0.860787
48	0.183901	0.481065	0.574587	0.86188
56	0.188734	0.488845	0.578293	0.867439

5.3 Variation of Rotor Resistance and Temperature

The following table shows real time experimental values obtained through continuous running of the induction machine.

Table 5.3 Variation of temperature and rotor resistance w.r.t. time

Time(Min)	Temp (° C)	R_r(Ohm)
0	30	0.905
5	52.5	0.94
10	60	0.95
15	67.5	0.975
20	71	0.985
25	77.5	1.01
30	82	1.025
37	86	1.042
43	90	1.05
60	102.5	1.093
70	105	1.125
80	110	1.16
90	116	1.17
100	120	1.225
123	127.5	1.23
127	129	1.235
142	130	1.27
174	135	1.275
179	137.5	1.275
190	138	1.28
200	138	1.28
224	139	1.28
232	139	1.285

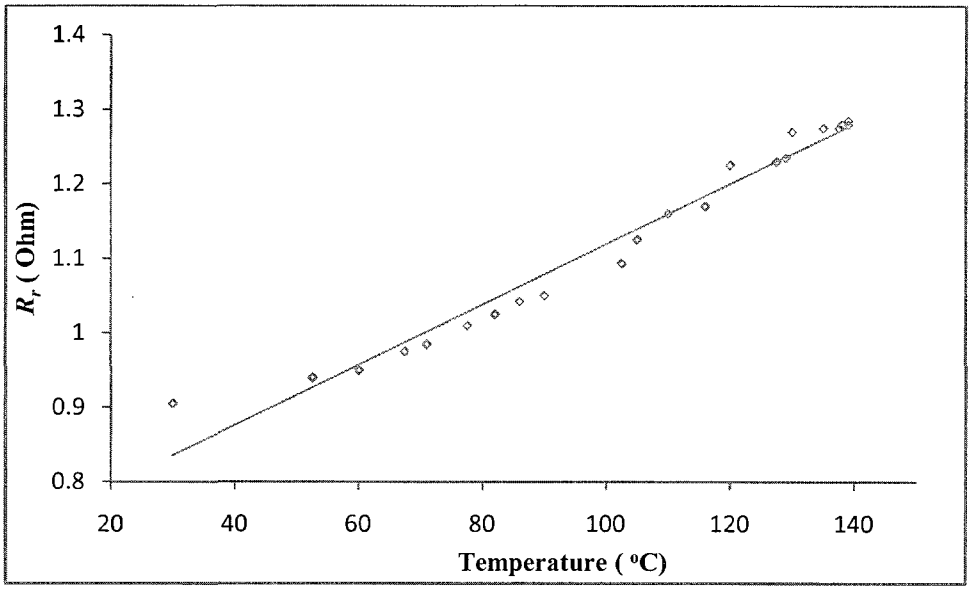

Fig 5.19 Change in rotor resistance as a function of temperature.

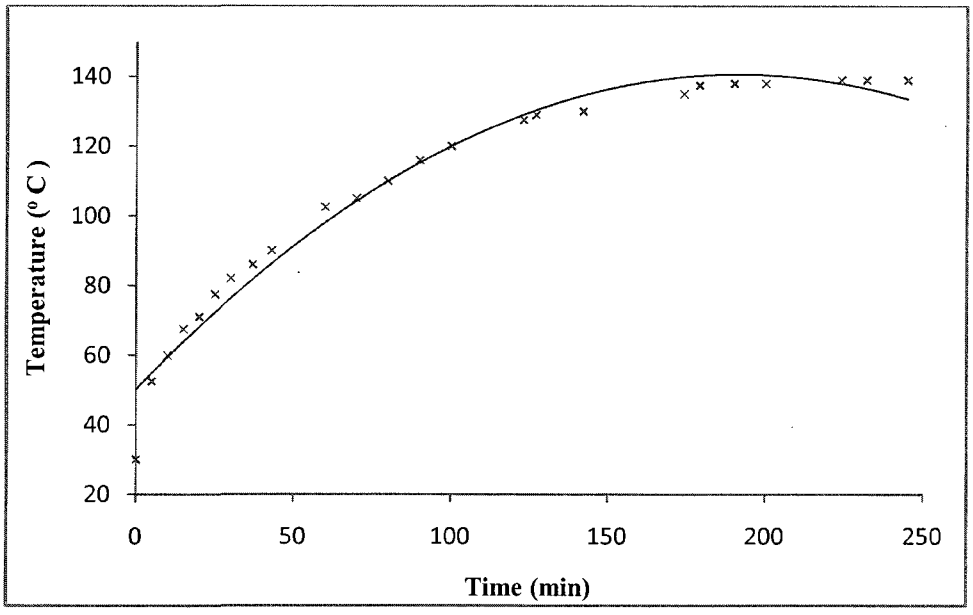

Fig 5.20 Change in Temperature as function of time.

Figs. 5.19, 5.20 and 5.21 show the relationships between time, temperature and the rotor resistance. These curves clearly show that the rotor resistance increases linearly with respect to change in temperature.

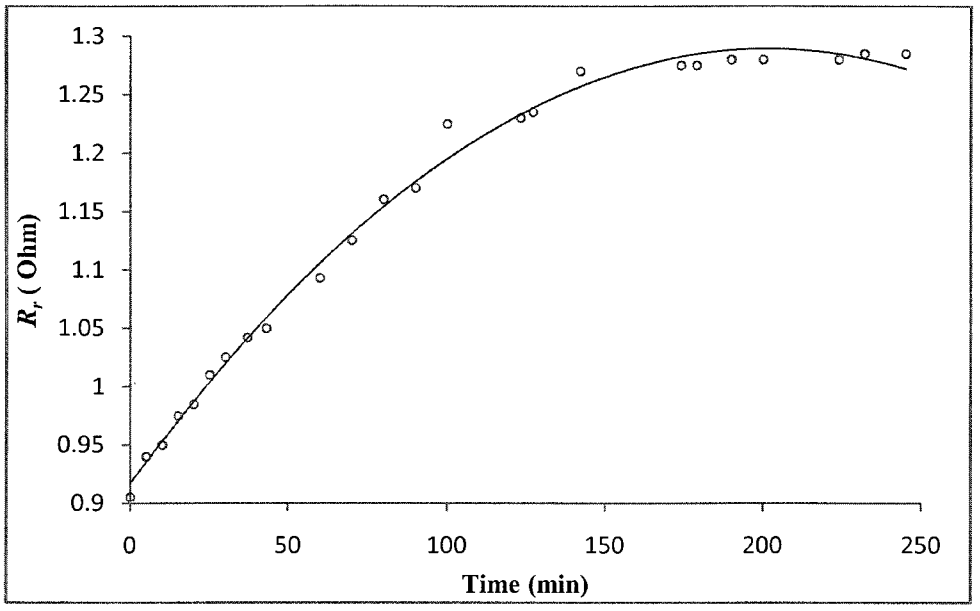

Fig. 5.21. Change in rotor resistance with respect to time.

5.4 Variation of Real and Reactive Power for the Two Induction Machines

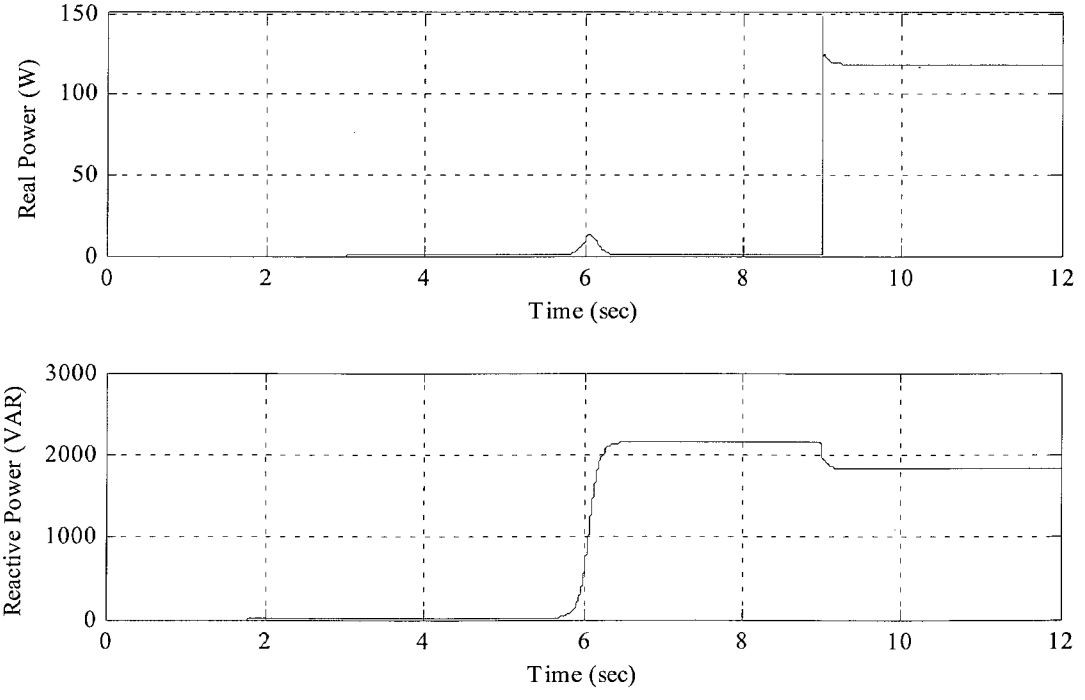

Fig. 5.22. Calculated real and reactive power for aluminum-rotor SEIG under *R-L* loading condition.

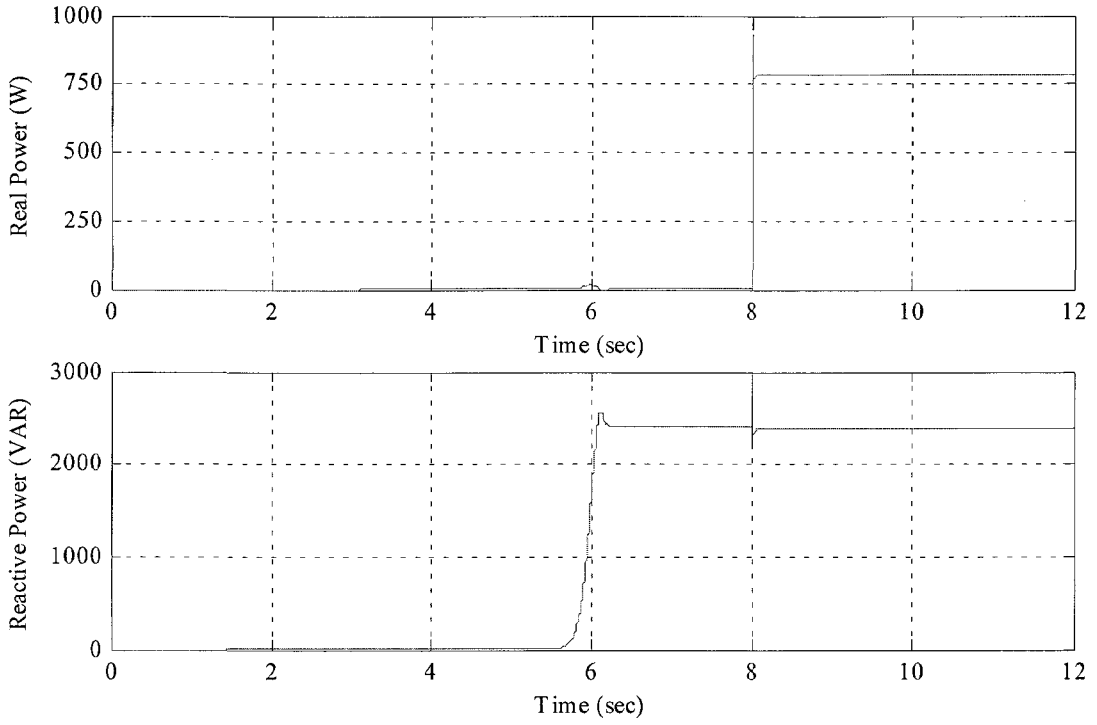

Fig. 5.23. Calculated real and reactive power for copper- rotor SEIG under *R-L* loading condition.

The real and reactive power build-up processes in Figs. 5.22 and 5.23 for aluminum- and copper-rotor machines are similar to the ones under no load condition. It can be seen from these figures that there is a small transient rise in real power during the self-excitation process for both the machines. With the application of the load, reduction in the magnitude and frequency of the terminal voltage has been noticed. For stable operation, the equivalent impedance of the *R-L* load in parallel with the excitation capacitance *C* has to be capacitive. As a result, under loaded condition, the slope of the equivalent capacitive impedance will now be steeper than that for the no load condition. Hence the machine continues to run at steady state condition with a lower frequency and the operating point will shift to a lower point on the magnetizing characteristic curve of the SEIG. The measured values in Figs. 5.24 and 5.25 show closer agreement with the calculated ones.

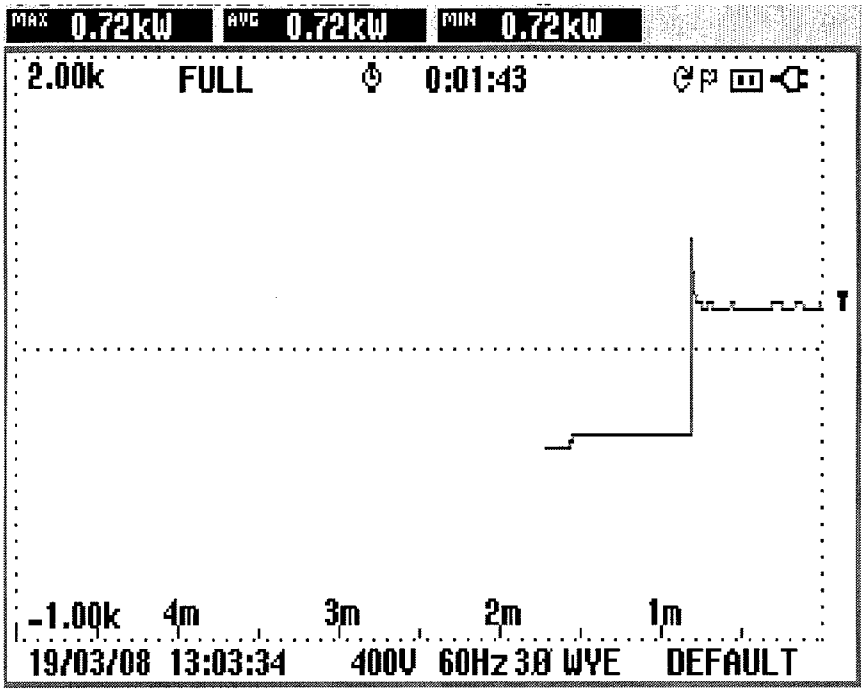

(a)

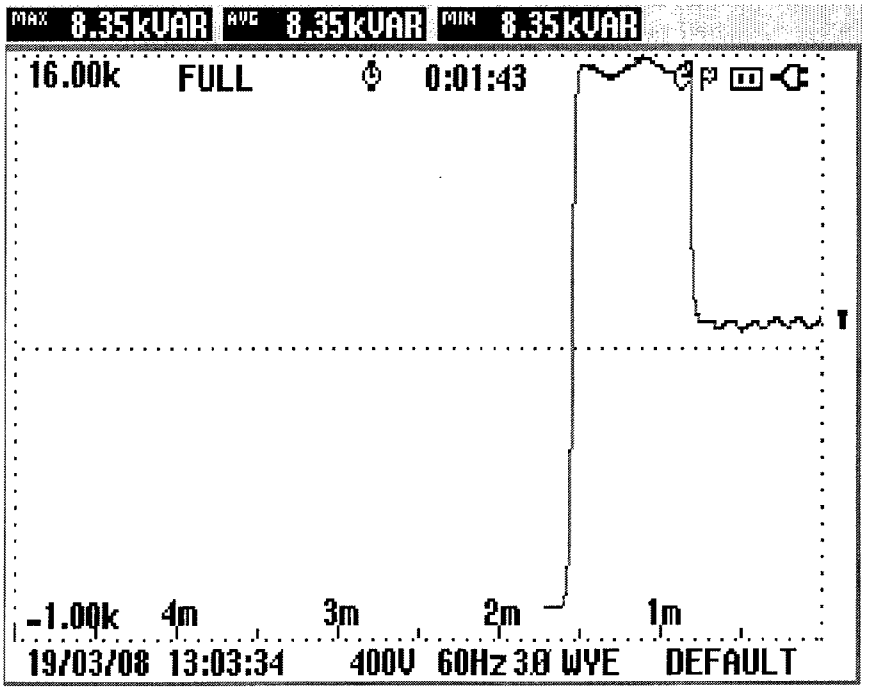

(b)

Fig. 5.24. Measured real and reactive power for aluminum-rotor SEIG under *R-L* load. (a) Real power. (b) Reactive power.

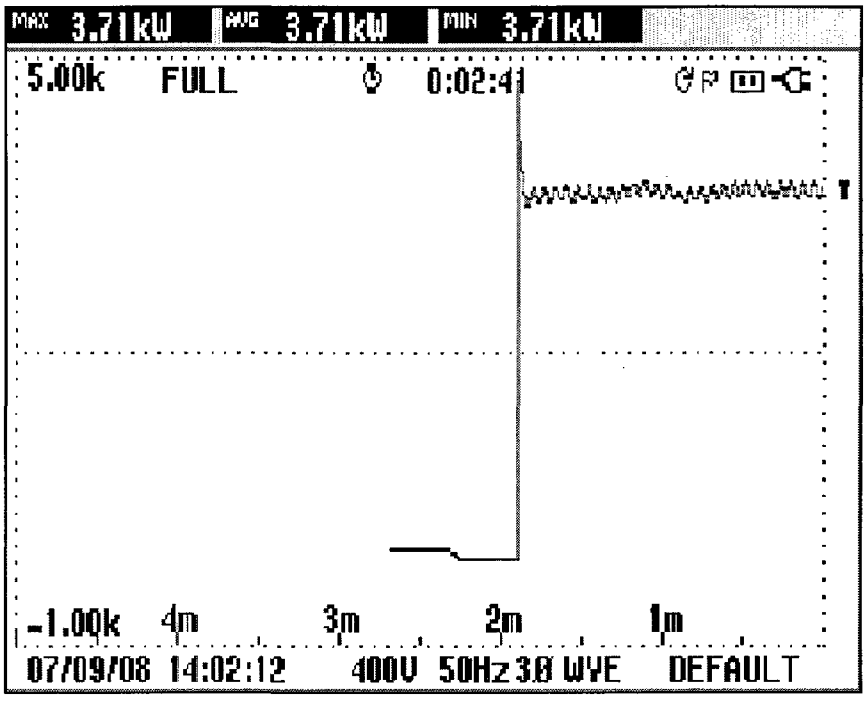

(a)

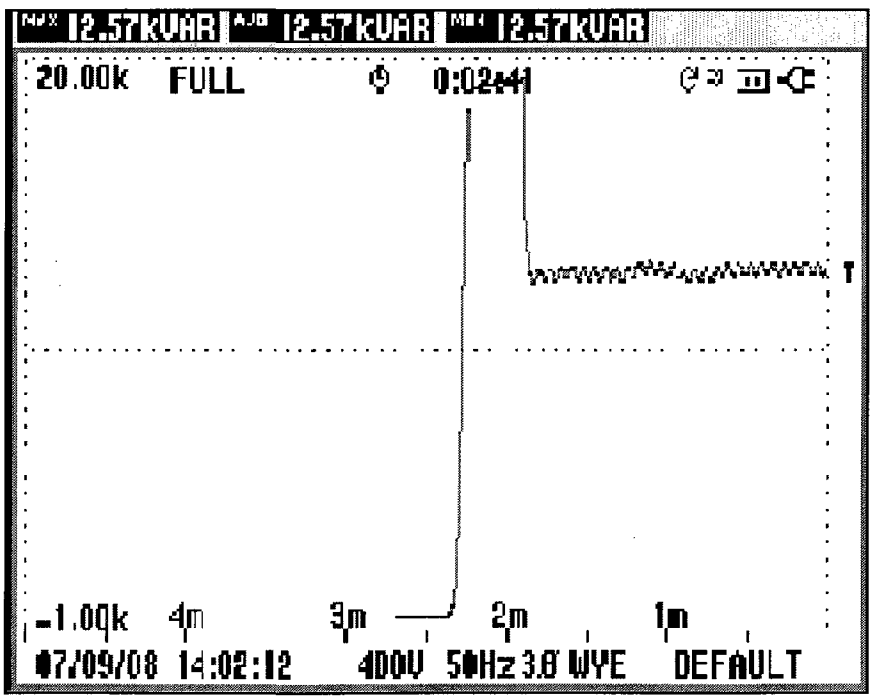

(b)

Fig. 5.25. Measured real and reactive power for copper rotor SEIG under *R-L* load. (a) Real power.

5.5 Experimental Results from Power Quality Analyzer

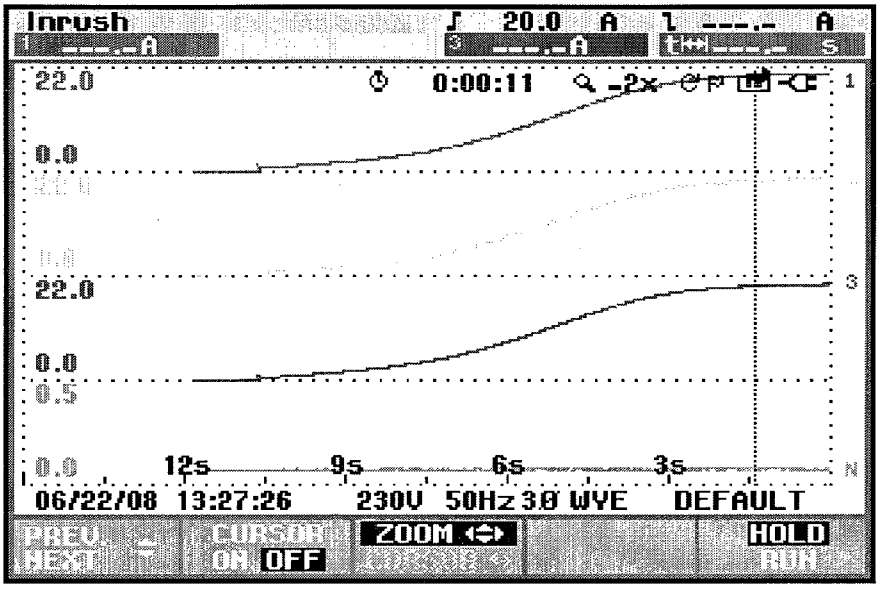

Fig. 5.26. Inrush current for cu-rotor machine for no load condition.

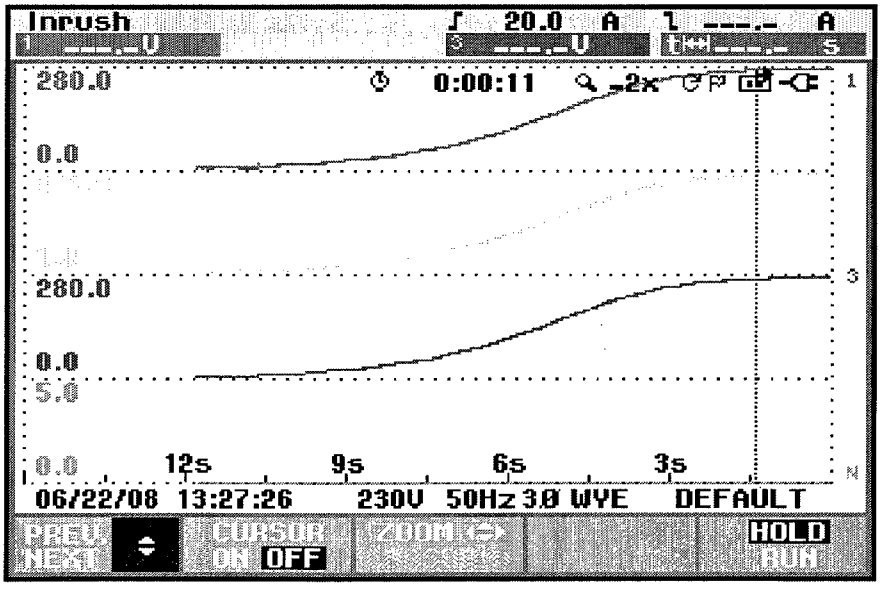

Fig. 5.27. Inrush voltage for cu-rotor machine for no load condition.

Figs. 5.26 and 5.27 show the values for inrush current and inrush voltage for a copper-rotor induction machine operating at no load and running at 1750 rpm.

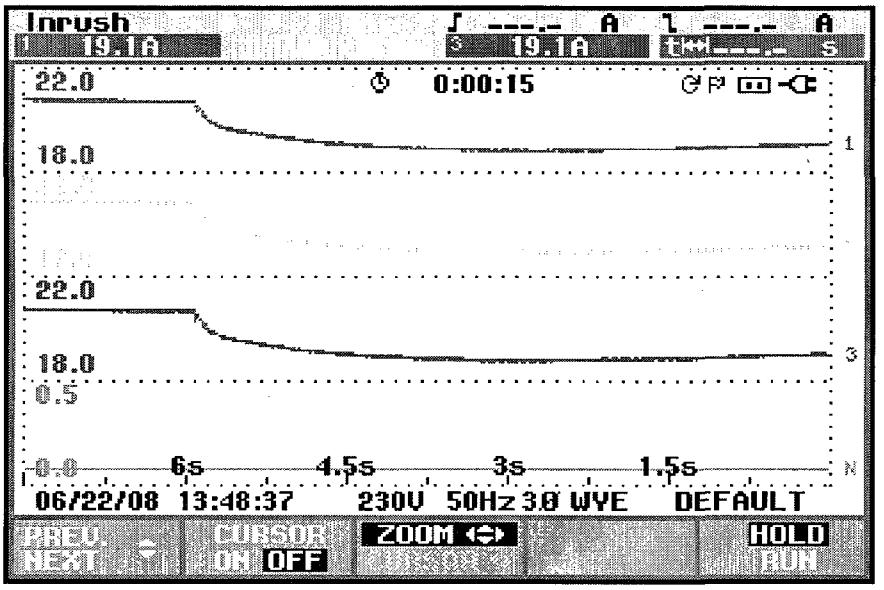

Fig. 5.28. Inrush current for cu-rotor machine for *R* load.

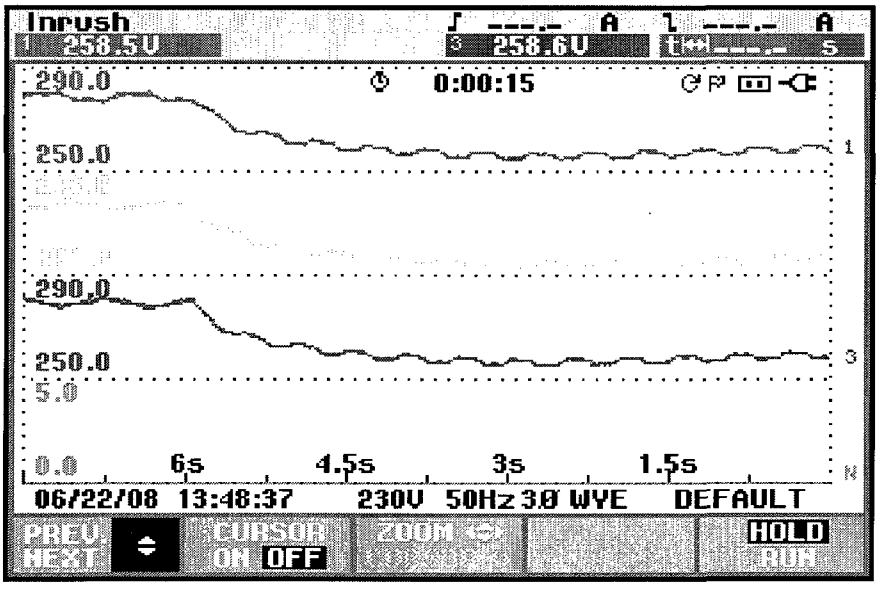

Fig. 5.29. Inrush voltage for cu-rotor machine for *R* load.

Figs. 5.28 and 5.29 show the values for inrush current and inrush voltage for a copper-rotor induction machine operating with a resistive load *R* load and running at 1750 rpm.

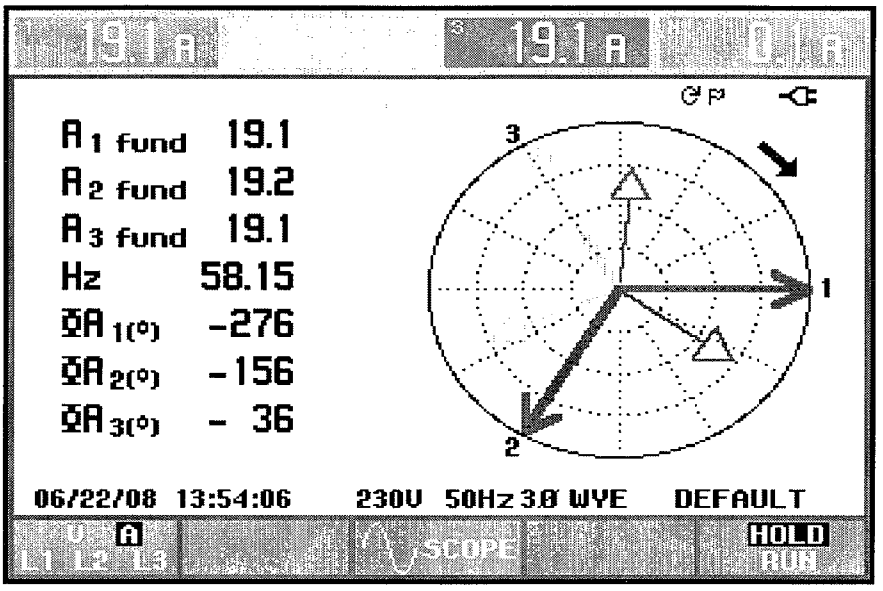

Fig. 5.30. Phasor current for cu-rotor machine for *R* load.

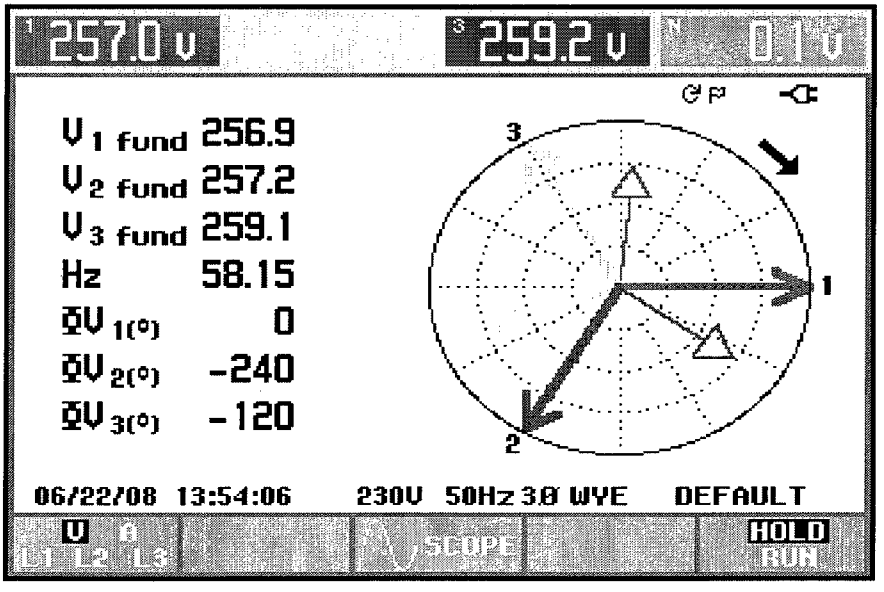

Fig. 5.31. Phasor voltage for cu-rotor machine for *R* load.

Figs. 5.30 and 5.31 depict the phasor diagram showing the position of all the three phases of the system for a copper-rotor induction machine running with *R* load.

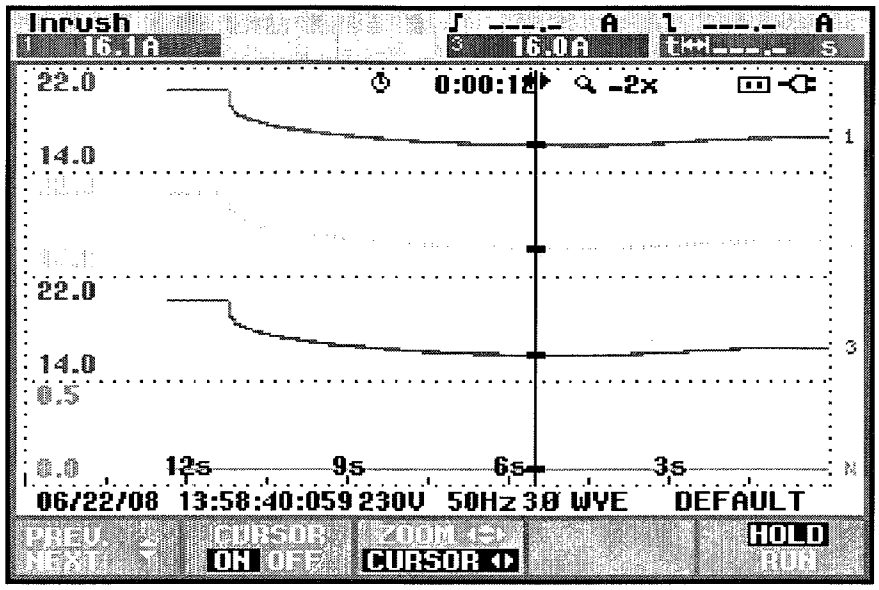

Fig. 5.32. Inrush current for cu-rotor machine for *RL* load.

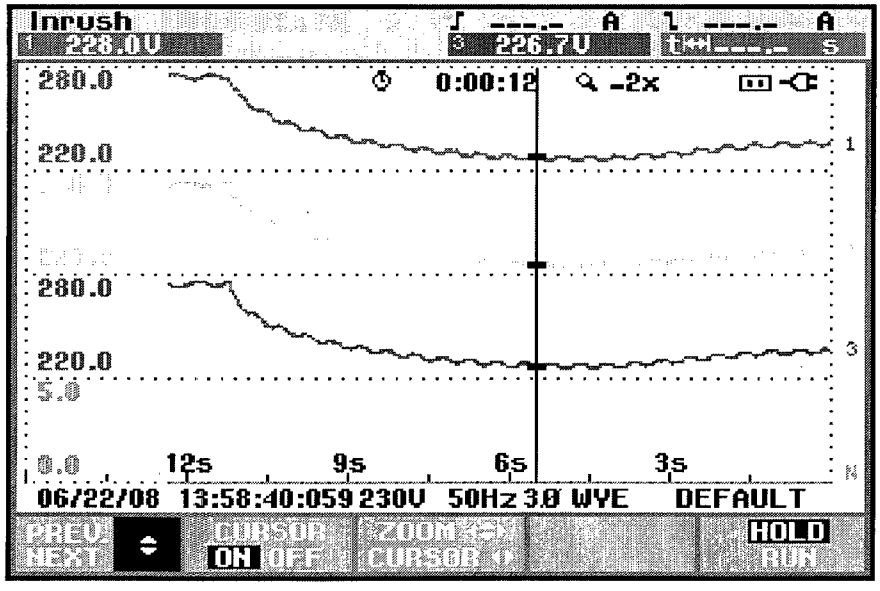

Fig. 5.33. Inrush voltage for cu-rotor machine for *RL* load.

Figs. 5.32 and 5.33 show the values for inrush current and inrush voltage for a copper-rotor induction machine operating with a resistive load *RL* and running at 1750 rpm. The values for both current and voltage go down as compared to the case of the machine running with only *R* load.

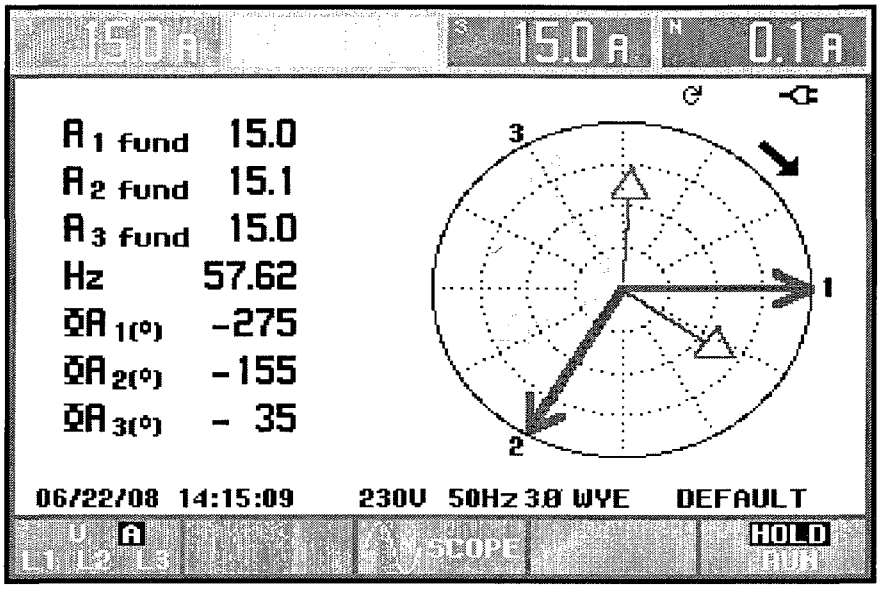

Fig. 5.34. Phasor current for cu-rotor machine for *RL* load.

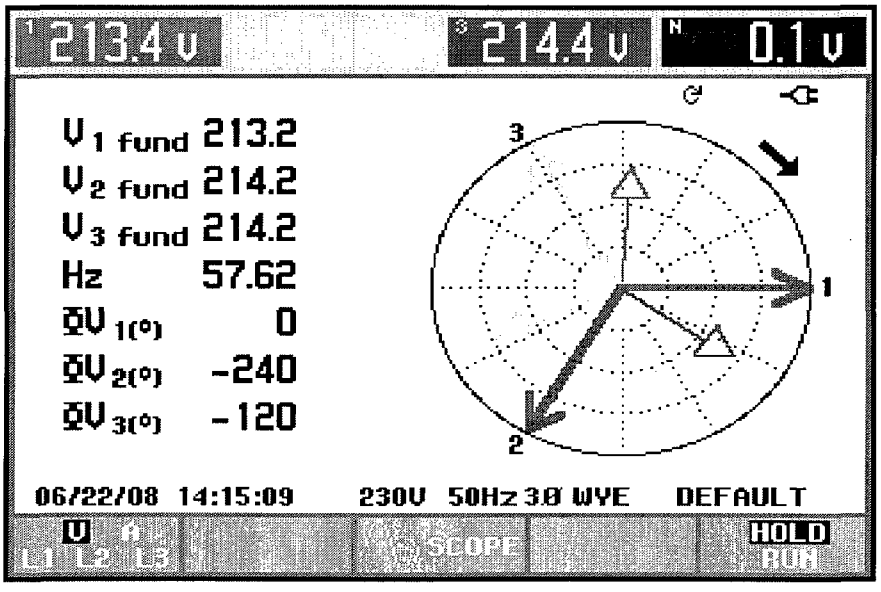

Fig. 5.35. Phasor current for cu-rotor machine for *RL* load.

Figs. 5.34 and 5.35 depict the phasor diagram showing the position of all the three phases of the system for a copper-rotor induction machine running with *RL* load.

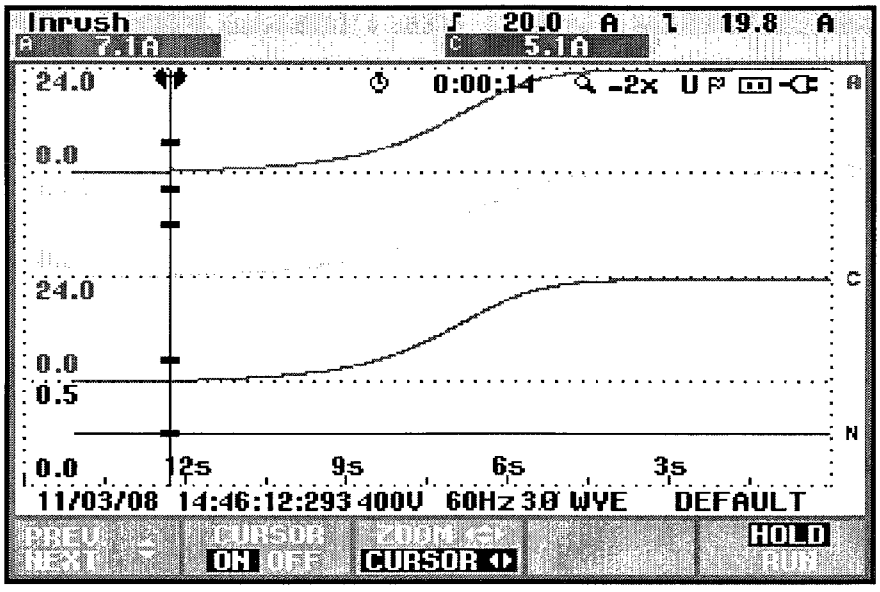

Fig. 5.36. Inrush current for al-rotor machine for no load condition.

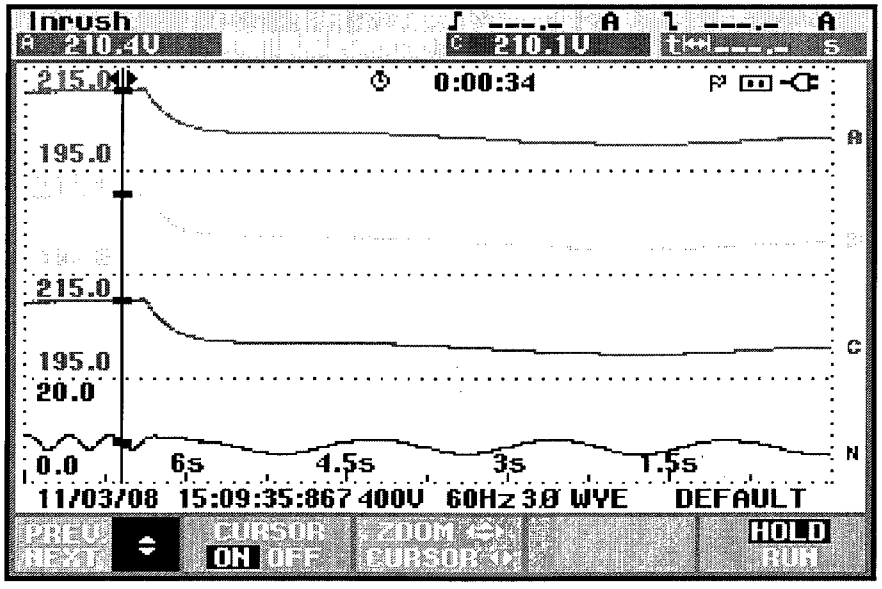

Fig. 5.37. Inrush voltage for al-rotor machine for no load condition.

Figs. 5.36 and 5.37 show the values for inrush current and inrush voltage for an aluminum-rotor induction machine operating at no load and running at 1750 rpm.

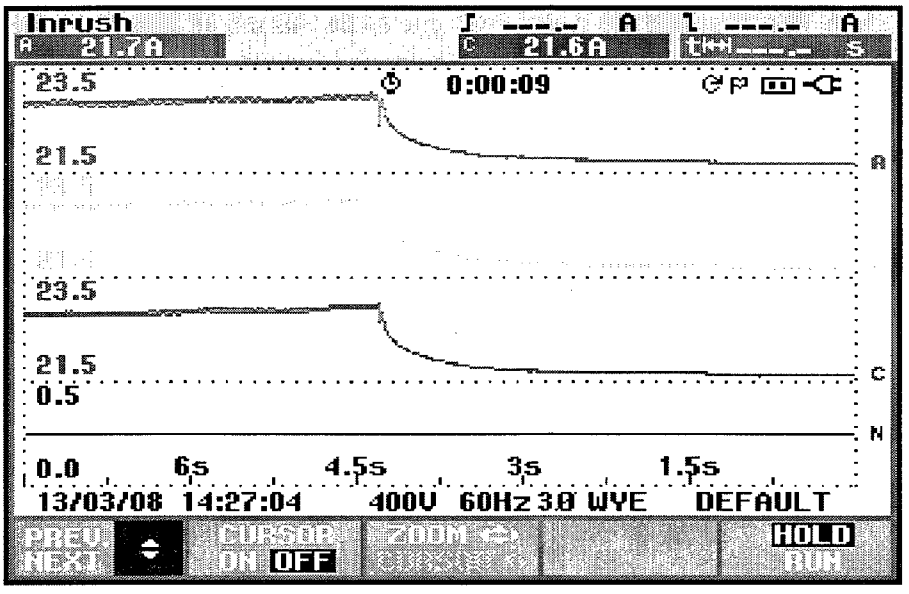

Fig. 5.38. Inrush current for al-rotor machine for *R* load.

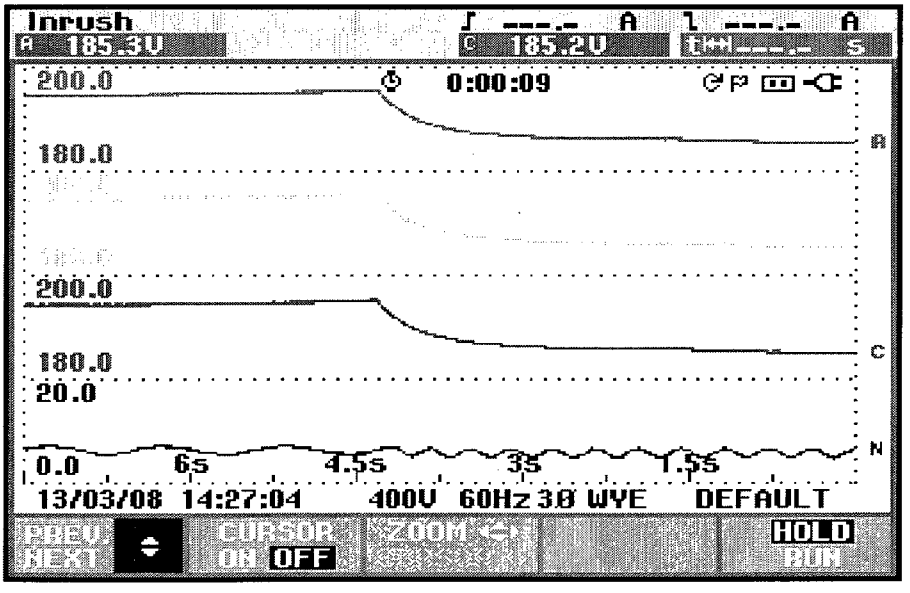

Fig. 5.39. Inrush voltage for al-rotor machine for *R* load.

Figs. 5.38 and 5.39 show the values for inrush current and inrush voltage for an aluminum-rotor induction machine operating with a resistive load *R* load and running at 1750 rpm.

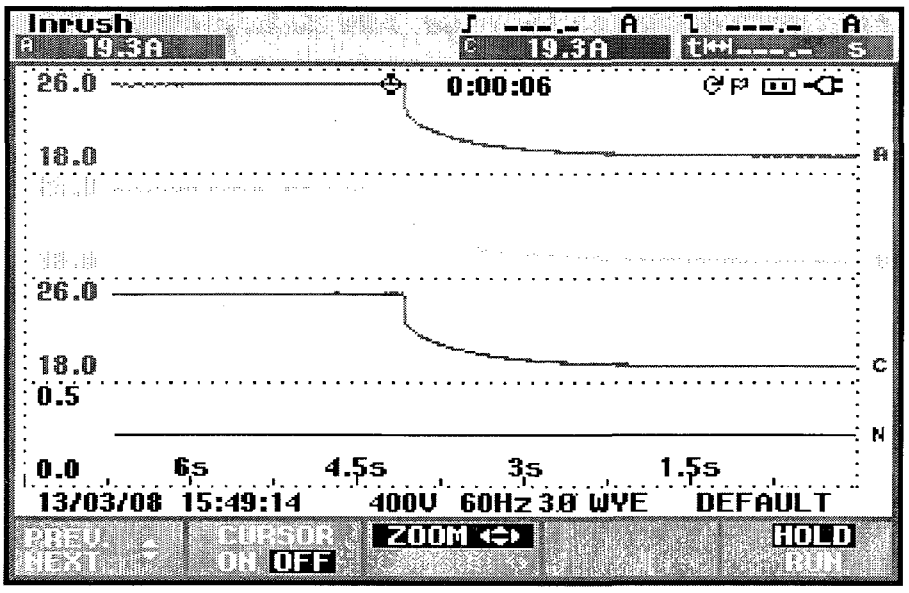

Fig. 5.40. Inrush current for al-rotor machine for *RL* load.

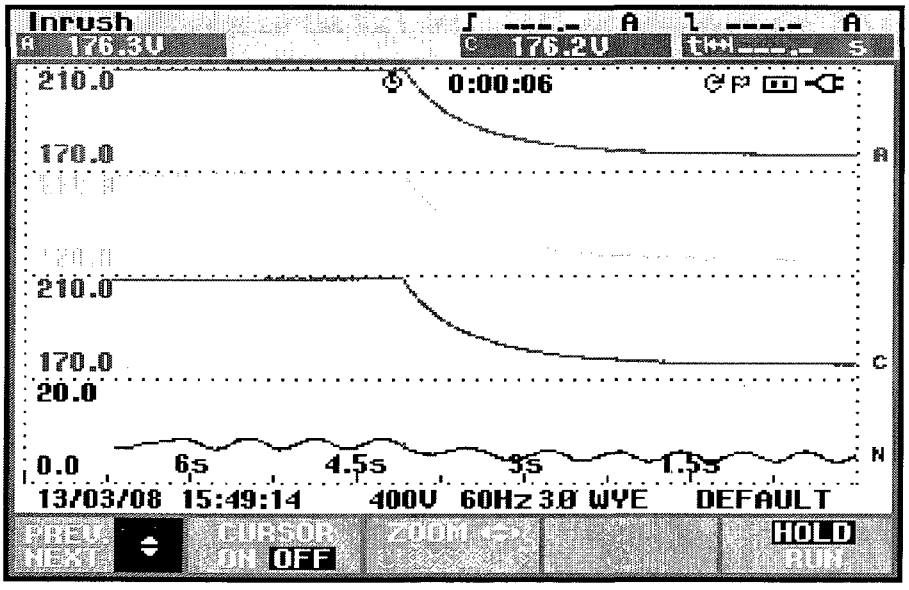

Fig. 5.41. Inrush voltage for al-rotor machine for *RL* load.

Figs. 5.40 and 5.41 show the values for inrush current and inrush voltage for an aluminum-rotor induction machine operating with a resistive load *RL* and running at 1750 rpm. The values for both current and voltage go down as compared to the case of the machine running with only *R* load.

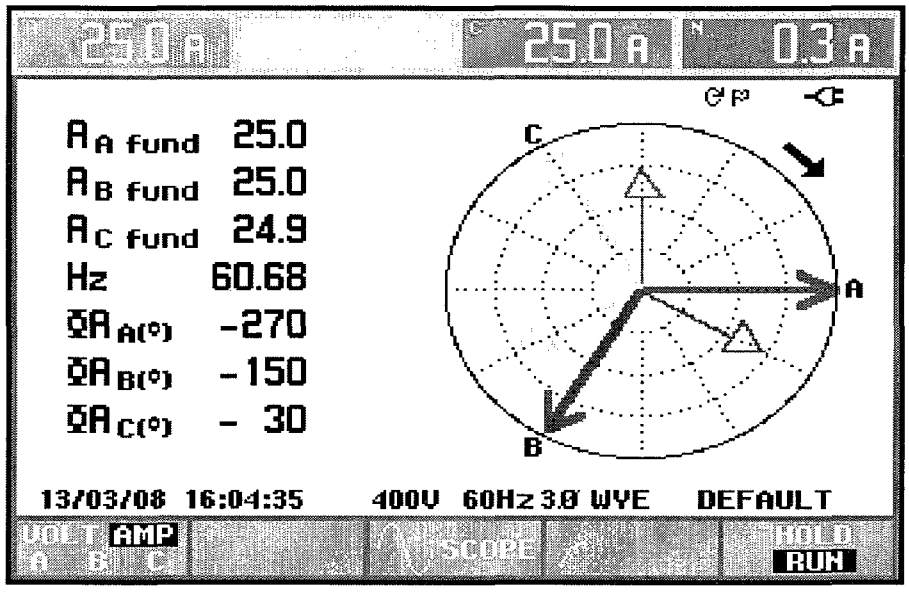

Fig. 5.42. Phasor current for al-rotor machine for *RL* load.

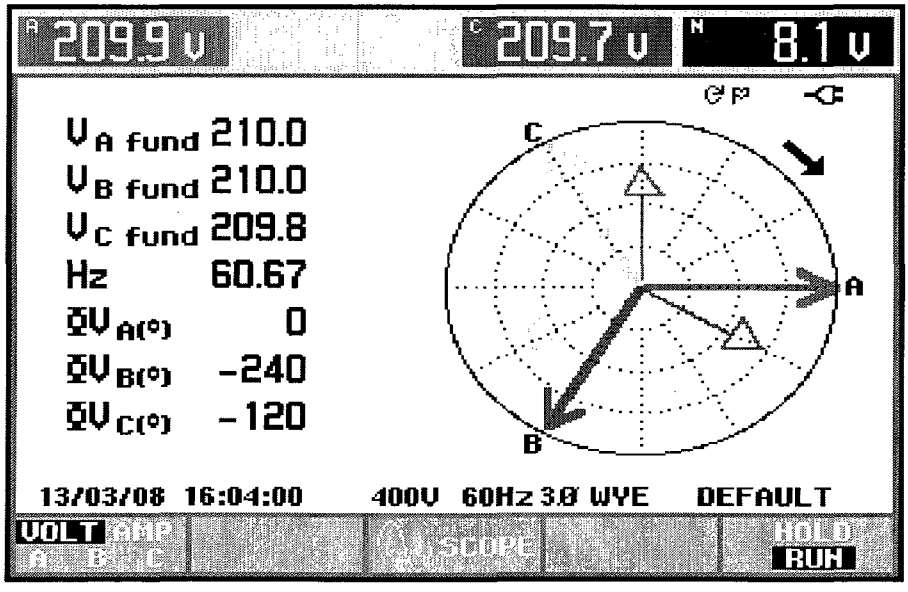

Fig. 5.43. Phasor voltage for al-rotor machine for *RL* load.

Figs. 5.42 and 5.43 depict the phasor diagram showing the position of all the three phases of the system for an aluminum-rotor induction machine running with *RL* load.

CHAPTER 6

CONCLUSIONS AND FUTURE WORK

6.1 Conclusions

This research work encompasses a wide range of topics dealing with induction machines and more specifically induction generators. An effort has been made so that the reader with a background in electrical engineering can easily understand the topics being discussed. The main research topics covered in this work include the theory and development of induction generators, conventional mathematical modeling of induction generators, taking into account the effect of thermal modeling on induction generators and finally a broad discussion and comparative analysis between an aluminum-rotor induction generator and a copper-rotor induction generator.

The main conclusions that can be drawn are

1) Comprehensive background and research literature related to induction generators has been presented.
2) Consideration of saturation in the machine modeling.
3) Temperature as a factor is considered in the machine modeling.
4) Experimental and theoretical results are compared
5) Performance analysis of aluminum-rotor and copper-rotor SEIG under varying conditions has been done.
6) Value of minimum capacitance and mutual inductance varies inversely with speed.
7) At any speed below the cut-off speed the machine will not build up terminal voltage.
8) Starting and pull-out torques of the copper-rotor machine are relatively lower than the aluminum-rotor machine for rated condition.
9) Gradual change in temperature effects the built-up times in induction machines.
10) Rise in temperature makes a significant effect on the machine parameters.

11) Real-time run diagrams from power quality analyzers for aluminum- and copper –rotor induction generators have been presented.

6.2 Future Work

In the current scenario, Wind Energy is one of the most promising areas of research. Not only in academia but in industry also there is a vast amount of research being done. Induction generators form an integral part of wind energy. A few suggested topics of research that can enhance this present work are:

1) Consideration of temperature parameters of induction generators by conduction Finite Element analysis on the machine. This will give a more detailed analysis.
2) Investigating the effect on the machine parameters by including material properties of the different components used in the induction generators.
3) Thermal modeling can be enhanced by considering the machine to be made of different heat zones, while the machine is in operation. Even though this procedure is complex, but this will lead to a much better understanding of the fundamentals of the induction machine.

LIST OF PUBLICATIONS

K Hafiz, G Nanda and Narayan C Kar, "Performance analysis of aluminum rotor and copper rotor SEIG considering thermal effect and skin effect," to be submitted to the *IEEE Transactions on Industrial Electronics*.

K Hafiz, G Nanda and Narayan C Kar, "Comparative performance analysis of aluminum rotor and copper rotor SEIG considering skin effect," in *Proceedings of the 18th International Conference on Electrical Machines* (ICEM 08), Vilamoura, Portugal, Sep 2008.

K Hafiz, G Nanda and Narayan C Kar, "Skin effect modeling of self excited induction generators in wind power applications," in *Proceedings of the IEEE Canadian conference on electrical and computer engineering* (CCECE 08), Niagara Falls, May 2008.

G Nanda and Narayan C Kar, "A survey and comparison of characteristics of motor drives used in electric vehicles", in *Proceedings of the IEEE Canadian conference on electrical and computer engineering* (CCECE 06), Ottawa, May 2006.

APPENDIX A

Matlab code used for calculations

```
% Parameters from Lab 7.5 hp machine
%%%%uses state space matrix to solve the equations.
%%% Im-Xm characteristics using Wang atan()function and piecewise
%%% linearization.
%%% included Vabc Iabc with transform matrix
%%% implemented Find_Freq sub-routine to calculate frequency

clear all
global Rs Rr0 Xls Xlr Xm Rl Xl v
%%% machine parameters

Tinitial = 23;
Tfinal = 100;
DelTemp = Tfinal-Tinitial;
Rs= .0006*DelTemp+.1549;          %7.5 hp motor stator resistance
% Rr0 = 0.9239;          %%% rotor resistance Auminum bars
Rr0 = .0005*DelTemp+.4585;          %%% rotor resistance Copper bars
Lls= (-4*10^-6*DelTemp^2+.0007*DelTemp+.548)/377;          %stator inductance
Llr0 = (-5*10^-6*DelTemp^2+.0011*DelTemp+.822)/377;          %%%rotor inductance
Lm = 13.27/377;                    %magnetizing inductance
fb=60;                 %base frequency
p=4;                   %number of poles
wb=2*pi*fb;            %base speed
we = 0;
wr = 377;
Xls=wb*Lls;            %stator impedance
Xlr=wb*Llr0;           %rotor impedance
Xm = wb*Lm;

C = .5*146.4e-6;
%%%%%%%%%%%%
stop_time = input('Simulation for Open Circuit conditions.\nEnter simulation time in seconds:  ');

Rl =1000000000;
Xl =0;
v  = wr/wb;            % per unit speed

Finit = 1;             %% per unit frequency (assumed)
Xcinit= 43;            %Impedance of exxcitation capacitance (assumed)
Cx =[Finit Xcinit];

[XX] =fminsearch('Find_Freq', [Cx]);
```

```
Fpu = XX(1);          %% calculated per unit frequency
fb_new = fb*Fpu;      %% new calculated frequency

kappa = 5.5/(5.5+0.03); % ratio of bar width to width of slot (mm)
hl  = 27.77; %hieght of rotor bar (mm)
%sigma= 37.71; %% aluminium
sigma = 59.61; %copper
eta = 2*pi*hl*sqrt(kappa*fb_new*(10^-7)*sigma); %%% use updated value of frequence

Kr = eta*(sinh(2*eta)+ sin(2*eta))/(cosh(2*eta)-cos(2*eta));
Ke = (3/(2*eta))*(sinh(2*eta)- sin(2*eta))/(cosh(2*eta)-cos(2*eta));

alpha = 144.5666;
beta = 0.3626;
gamma = 0.5668;
Nu = atan(gamma);

if flag <1 || flag >2
   disp ('Wrong info')
   return;
elseif flag == 1
Rr = Rr0;
Llr = Llr0;
elseif  flag == 2
Rr = Kr*Rr0;
Llr = Ke*Llr0;
end

%%%%%%%%%%%%%%%

theta = 0;
T_matrix = (2/3)*[cos(theta), cos(theta-2*pi/3), cos(theta+2*pi/3);
      sin(theta), sin(theta-2*pi/3), sin(theta+2*pi/3);
      0.5, 0.5, 0.5];

%stop_time = 8;

% impedance and angular speed calculations
IQS=[]; IDS =[]; Ia =[]; Ib =[]; Ic =[];
IQR=[]; IDR=[]; Imag =[];
VQS= []; VDS = []; Va =[]; Vb =[]; Vc =[];
Pwr =[]; Qwr = [];
Telec =[];
Lmag =[];
Tm = .12; Te= 0; J =.05; W =[];
```

```
% initial conditions
Lmatrix =[Lls+Lm 0 Lm 0; 0 Lls+Lm 0 Lm;
        Lm 0 Llr+Lm 0; 0 Lm 0 Llr+Lm];
Rmatrix =[Rs   we*(Lm+Lls)   0   we*Lm;
       we*(Lm+Lls) Rs   we*Lm  0;
       0 (we-wr)*Lm     Rr    (we-wr)*(Lm+Llr);
       -(we-wr)*Lm  0   -(we-wr)*(Lm+Llr)   Rr];
ImatrixOld = [ 0 0 0 0]';
VmatrixOld = [.0015 0 0 0]';
%VmatrixOld = [230 230 0 0]';

Omega = [0 -we 0 0; we 0 0 0; 0 0 0 0; 0 0 0 0]';
%Omega = [ 0 0 0 0; 0 0 0 0; 0 0 0 0; 0 0 0 0]';
Cmatrix =[1/C 0 0 0; 0 1/C 0 0; 0 0 0 0; 0 0 0 0];

h = .001;
t = 0:h:stop_time;
for n = 1:length(t) -1
   X1 = h*(-inv(Lmatrix)*VmatrixOld - (inv(Lmatrix)*Rmatrix)*ImatrixOld);
   Y1 = h*(Cmatrix*ImatrixOld + Omega*VmatrixOld);
   W1 = h*(p/(2*J))*(Tm-Te);

   X2 = h*(-inv(Lmatrix)*(VmatrixOld+Y1/2) - (inv(Lmatrix)*Rmatrix)*(ImatrixOld+X1/2));
   Y2 = h*(Cmatrix*(ImatrixOld+X1/2) + Omega*(VmatrixOld+Y1/2));
   W2 = h*(p/(2*J))*(Tm-Te);

   X3 = h*(-inv(Lmatrix)*(VmatrixOld+Y2/2) - (inv(Lmatrix)*Rmatrix)*(ImatrixOld+X2/2));
   Y3 = h*(Cmatrix*(ImatrixOld+X2/2) + Omega*(VmatrixOld+Y2/2));
   W3 = h*(p/(2*J))*(Tm-Te);

   X4 = h*(-inv(Lmatrix)*(VmatrixOld+Y3) - (inv(Lmatrix)*Rmatrix)*(ImatrixOld+X3));
   Y4 = h*(Cmatrix*(ImatrixOld+X3) + Omega*(VmatrixOld+Y3));
   W4 = h*(p/(2*J))*(Tm-Te);

   ImatrixOld = ImatrixOld+(X1+2*X2+2*X3+X4)/6;
   VmatrixOld = VmatrixOld+(Y1+2*Y2+2*Y3+Y4)/6;
   %wr = wr+(W1+2*W2+2*W3+W4)/6; W =[W wr];

%    ImatrixOld = ImatrixNew;
%    VmatrixOld = VmatrixNew;

   iqs = ImatrixOld(1,1); IQS=[IQS iqs];
   ids = ImatrixOld(2,1); IDS=[IDS ids];
   iqr = ImatrixOld(3,1); IQR=[IQR iqr];
   idr = ImatrixOld(4,1); IDR=[IDR idr];
   im = sqrt((iqs+iqr)^2+(ids+idr)^2); Imag =[Imag im];
```

```
vqs = VmatrixOld(1,1); VQS =[VQS vqs];
vds = VmatrixOld (2,1); VDS = [VDS vds];

Vabc = inv(T_matrix)* [vds, vqs, 0]';  % transform to phase quantities
va = Vabc(1,1); Va =[Va va];
vb = Vabc (2,1); Vb =[Vb vb];
vc = Vabc (3,1); Vc =[Vc vc];
Iabc = inv(T_matrix)* [ids, iqs, 0]';
ia = Iabc(1,1); Ia =[Ia ia];
ib = Iabc(2,1); Ib =[Ib ib];
ic = Iabc(3,1); Ic =[Ic ic];

Pinst = vqs*iqs+vds*ids;  %Pwr =[Pwr Pinst];
Qinst = vqs*ids-vds*iqs;  Qwr =[Qwr Qinst];
% Pabc= va*ia+vb*ib+vc*ic; Pwr=[Pwr Pabc];
Pabc= va*ia+vb*ib+vc*ic; Pwr=[Pwr Pabc];
Lamds = (Lls+Lm)*ids+ Lm*idr;
Lamqs = (Lls+Lm)*iqs + Lm*iqr;

Te = (0.75)*p*Lm*(-iqs*idr+ids*iqr);
%Te = Lamds*iqs-Lamqs*ids;
Telec = [Telec Te];

 if im<10  %%%% Wang atan() function
 Xm = alpha*(atan(beta*im-gamma)+ Nu)/im;
  elseif im>=10
    Xm = 28;
 end

% if im <=1.5
%    Xm = 46.42;
% elseif im >1.5 & im <=4.0
%    Xm = 1035.1/(im+ 19.2);
% elseif im >4.0 & im <= 6.5
%    Xm = 483.1255/(im+ 6.8);
% elseif im >6.5 & im <=9
%    Xm = 343.5826/(im+3.0133);
% elseif im > 9
%    Xm = 254.7902/(im+.0421);
% elseif im > 12
%    Xm = 26;
% end

Lm = Xm/377;
Lmag = [Lmag Lm];
Lmatrix =[Lls+Lm 0 Lm 0; 0 Lls+Lm 0 Lm;
```

```
        Lm 0 Llr+Lm 0; 0 Lm 0 Llr+Lm];
   Rmatrix =[Rs   we*(Lm+Lls)    0   we*Lm;
       we*(Lm+Lls) Rs   we*Lm  0;
       0 (we-wr)*Lm      Rr     (we-wr)*(Lm+Llr);
       -(we-wr)*Lm   0   -(we-wr)*(Lm+Llr)    Rr];

%         if n > 5000   %%% simulation of loss of capacitance
%            C = 50e-6 ;
%         end
       Cmatrix =[1/C 0 0 0; 0 1/C 0 0; 0 0 0 0; 0 0 0 0];
% %            Rmatrix =[Rs   we*(Lm+Lls)    0   we*Lm;
% %         we*(Lm+Lls) Rs   we*Lm  0;
% %         0 (we-wr)*Lm      Rr     (we-wr)*(Lm+Llr);
% %         -(we-wr)*Lm   0   -(we-wr)*(Lm+Llr)    Rr];
% %         end

end

l=1:n;

plot (l/1000,Va);
grid on

%%% saving data in seperate file
% % % A1 =[l',VQS',VDS',IQS',IDS',IQR',IDR',Pwr',Qwr',Telec', Va',Ia'];
% % % varname = input('Name of file to save data: \n ', 's'); %%% input name of file to save
data
% % %   fid = fopen(varname, 'w'); %% create and open file to write
% % %   for k =1:n
% % %   fprintf(fid, '%f %f %f %f %f %f %f %f %f %f %f %f\n', A1(k,:)); % write to file
% % %   end
% % %   fclose(fid); % % % finally close the file
```

VITA AUCTORIS

Gaurav Nanda was born in India in 1980. He graduated from Gulbarga University, India with a degree in Electrical and Electronics Engineering in 2002. Subsequently he worked as a research associate at Indian Institute of Technology, Kanpur till 2005. He is currently a candidate for the Master's degree in Electrical Engineering at the University of Windsor, Ontario, Canada.